

**Modeling Thinning Effects on Ring Width Distribution and Wood
Specific Gravity of Loblolly Pine (*Pinus taeda* L.)**

by

Gudaye Tasissa

Dissertation submitted to the Faculty of the
Virginia Polytechnic Institute and State University
in partial fulfillment of the requirements for the degree of

Doctor of Philosophy

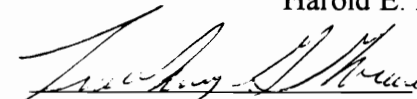
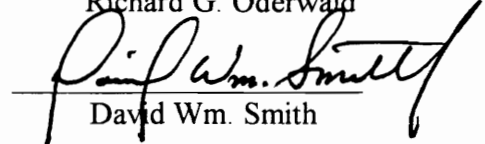
in

Forestry

APPROVED:



Harold E. Burkhart, Chairman


Timothy G. Gregoire
Richard G. Oderwald
Marion R. Reynolds, Jr.
David Wm. Smith

November, 1996.

Blacksburg , Virginia

Keywords: Thinning, Correlation, Specific gravity, Form exponent

LD
5655
V856
1996
T375
c.2

**MODELING THINNING EFFECTS ON RING WIDTH
DISTRIBUTION AND WOOD SPECIFIC GRAVITY
OF LOBLOLLY PINE (*Pinus taeda L.*)**

by

Gudaye Tasissa

Harold E. Burkhart, Chairman

(ABSTRACT)

An appropriate accounting for thinning effects on growth rate and wood quality requires a clear understanding and quantification of these effects. In this regard, four basic interrelated issues were addressed in this study: 1) thinning effects on ring specific gravity 2) thinning effects on ring width distribution 3) thinning effects on stem form, and 4) prediction models for these quantities. The study showed that thinning does not significantly affect ring specific gravity, whereas its effects on ring width distribution and stem form were significant. Thinning increases ring width significantly over most of the tree bole and increases the earlywood and latewood components proportionally maintaining an approximately constant latewood proportion. As a consequence, thinning effects on latewood proportion is not significant; confirming the results obtained in the specific gravity study and further dispelling the concern that thinning may substantially reduce wood specific gravity. Thinning affects stem form by increasing the form exponent especially near the tree base accentuating the neiloid form expected in that area. High up in the stem, the form exponent changes little within a tree and among thinning treatments, with a general tendency towards a paraboloid shape. Differences due to thinning intensities, in general, were not significant indicating the applicability of results within a wide range of densities. Prediction models for ring specific gravity, ring width, latewood proportion and stem profile based on ring, tree, stand and site factors were developed.

Influences of stand level factors, density measures in particular, in prediction models are minor probably because tree level factors such as, stem diameter at breast height, crown ratio, etc. themselves manifest stand conditions. The mixed-effects analysis technique was used in data analysis to account for correlation among observations from the same subject. Direct covariance modeling yielded better fits than accounting for correlation indirectly using random effects covariates in many cases; however, both could not be accommodated simultaneously. Structures which assume decreasing correlation with increasing distance between observations, such as the first-order autoregressive structure, performed better than alternative specifications. Results consistently showed that accounting for correlation among observations substantially improves the fits over ignoring correlation; effectively addressing the issue of bias in the standard errors of estimates.

Acknowledgments

I would like to express my special thanks and heart felt appreciation for my major professor Dr. Harold E. Burkhart. For his insightful comments, direction, consistent support and encouragement he deserves my utmost gratitude. My appreciation and thanks to Drs. Timothy G. Gregoire, Richard G. Oderwald, Marion R. Reynolds, Jr, and David Wm. Smith for taking the time from their demanding schedules to serve on my advisory committee. I would like to especially thank Dr. Tim Gregoire for his help in providing me with additional reference materials and pointing me in the right direction at several junctures.

The Loblolly Pine Growth and Yield Research Cooperative maintained at Virginia Polytechnic and State University provided me with the financial support and data for the research. I highly appreciate their support and commend their commitment to continued research. I would also like to thank the Buruss Fellowship for providing me with the very valuable financial support that paid my school fees.

I am eternally grateful to my wife, Tigist Gessesse, for the support and love she gave me over these years and the sacrifices she endured so that my dream may come true. I love you Tigist.

Table of contents

Chapter 1: Introduction and objectives	1
1.1 Introduction	1
1.2 Objectives	8
1.3 Variable definition and notation	10
Chapter 2 : The analysis of longitudinal data	12
2.1 Introduction	13
2.1.1 Longitudinal vs cross-sectional studies	13
2.1.2 Consequences of ignoring correlations	16
2.2 Alternative approaches	
2.2.1 Maximum likelihood procedure	18
2.2.2 Multi-stage analysis	19
2.2.3 Generalized least squares	20
2.2.4 Mixed-effects modeling	22
2.2.4.1 Alternative models	24
2.2.4.1.1 Linear mixed effects models	24
2.2.4.1.2 Nonlinear mixed effects models	31
2.2.4.1.3 Generalized mixed effects models	34
2.2.4.2 Modeling correlations	38
2.2.4.3 Inference	41
2.2.4.4 Model fitting criteria	42
2.2.4.4.1 The AIC	42
2.2.4.4.2 The LRT	43
2.2.4.5 Model diagnostics	44
Chapter 3: Materials and methods	48
3.1 Data description	48
3.2 Methodology	54
3.2.1 Accounting for correlation.	61
3.2.2 Tests on thinning effects – design considerations	62
3.2.3 Model selection and validation criteria	64

Chapter 4: Thinning effects on ring specific gravity and ring specific gravity prediction model	67
4.1 Introduction and literature review	67
4.1.1 Introduction	67
4.1.2 Literature review	68
4.2 Data and methods	73
4.2.1 Data	73
4.2.2 Methods	74
4.3 Results and analyses	76
4.3.1 Covariance structure	76
4.3.2 Thinning effects on ring specific gravity	78
4.3.3 Specific gravity prediction model	81
4.4 Discussion and conclusions	87
4.4.1 Discussion	87
4.4.2 Conclusions	90
Chapter 5: Thinning effects on ring width distribution and prediction models.	104
5.1 Introduction and literature review	104
5.1.1 Introduction	104
5.1.2 Literature review	105
5.2 Data and methods	110
5.2.1 Data	110
5.2.2 Methods	111
5.3 Results and analyses	113
5.3.1 Covariance structure	113
5.3.2 Thinning effects	114
5.3.2.1 Effects on ring width	114
5.3.2.2 Effects on latewood proportion	121
5.3.3 Prediction models	123
5.3.3.1 Total ring width	123
5.3.3.2 Latewood proportion	128
5.4 Discussion and conclusions	133
5.4.1 Discussion	133
5.4.2 Conclusions	136
Chapter 6: Thinning effects on stem form and stem profile model	152
6.1 Introduction and literature review	152
6.1.1 Introduction	152

6.1.2 Literature review	154
6.2 Data and methods	159
6.2.1 Data	159
6.2.2 Methods	160
6.3 Results and analyses	161
6.3.1 Covariance structure	161
6.3.2 Thinning effects on stem form	162
6.3.3 Stem profile model	165
6.4 Discussion and conclusions	174
6.4.1 Discussion	174
6.4.2 Conclusions	176
Chapter 7: Summary and recommendations	188
7.1 Summary	188
7.2 Recommendations	192
Literature cited	195
Appendix	206
Vita	218

List of figures

Figure 2.1: Scatter plots of DBH, total tree height and height to the base of live crown over remeasurement periods	46
Figure 2.2: Parallel profile plots of DBH, total tree height and height to the base of live crown over remeasurement periods	47
Figure 4.1: Parallel profile plots of ring specific gravity by height and by physiological age for specific tree	93
Figure 4.2: A 3D plot of ring specific gravity by height and physiological age for a specific tree	94
Figure 4.3: A 3D plot of earlywood specific gravity by height and physiological age for a specific tree	95
Figure 4.4: A 3D plot of latewood specific gravity by height and physiological age for a specific tree	96
Figure 4.5: Average ring specific gravity, percent earlywood and percent latewood by height and physiological age	97
Figure 4.6: Average ring, earlywood and latewood specific gravity for groups of rings by height and physiological age	98
Figure 4.7: Relationships between average specific gravity and various tree level factors	99
Figure 4.8: Relationships between average specific gravity and various stand level factors.	100
Figure 4.9: Average ring, earlywood and latewood specific gravity by height and physiological age by thinning treatment	101
Figure 4.10: Average ring, earlywood and latewood specific gravity by height and physiological age by physiographic region	102
Figure 4.11: A normal probability plot for the specific gravity residuals	103

Figure 5.1: Parallel profile plots of ring width by height and by physiological age for a specific tree	139
Figure 5.2: A 3D plot of ring width by height and by physiological age for a specific tree	140
Figure 5.3: A 3D plot of earlywood width by height and by physiological age for a specific tree	141
Figure 5.4: A 3D plot of latewood width by height and by physiological age for a specific tree	142
Figure 5.5: Average ring, earlywood and latewood width by selected height and physiological age by thinning treatment	143
Figure 5.6: Average ring, earlywood, and latewood width by selected heights and physiological age classes	144
Figure 5.7: Relationships between average ring width and height over time by thinning treatment: [a] first, [b] second, [c] third, and [d] fourth remeasurement	145
Figure 5.8: Relationships between average ring, earlywood and latewood width by height and physiological age by physiographic region	146
Figure 5.9: Relationships between average ring width and various tree level factors	147
Figure 5.10: Relationships between average ring width and various stand level factors	148
Figure 5.11: Latewood proportion by height and physiological age by physiographic region	149
Figure 5.12: Latewood proportion by height and physiological age by thinning treatment	150
Figure 5.13: A normal probability plot for ring width residuals	151
Figure 6.1: Parallel profile plots of form exponent by height and time since thinning for a specific tree	178

Figure 6.2: A 3D plot of form exponent by height and time since thinning for a specific tree	179
Figure 6.3: Relationships between average form exponent and height by thinning treatment over time: [a] first, [b] second, [c] third, and [d] fourth remeasurement	180
Figure 6.4: Relationships between average form exponent and remeasurement occasion by thinning treatment at selected heights: [a] 0.5 ft [b] 16.5 ft [c] 32.5 ft [d] 48.5 ft	181
Figure 6.5: Relationships between average form exponent and various tree level factors	182
Figure 6.6: Relationships between average form exponent and various stand level factors	183
Figure 6.7: Absolute tree stem profile over measurement occasions for specific trees from [a] control, [b] light thinned, and [d] heavy thinned stands	184
Figure 6.8: Relative tree stem profile over measurement occasion for specific trees from [a] control, [b] light thinned, and [c] heavy thinned stands	185
Figure 6.9: A vertical profile of individual growth rings for a specific tree	186
Figure 6.10: A vertical profile of cumulative growth for the tree depicted in Figure [6.9]	187

List of tables

Table 2.1: Examples of covariance structures available for modeling within subject correlation	40
Table 4.1: Tree summary statistics for ring specific gravity prediction model fitting and validation data	73
Table 4.2: Ring summary statistics for specific gravity prediction model fitting and prediction fitting and validation data	74
Table 4.3: A Test of thinning effects on ring specific gravity for all data combined	78
Table 4.4: Tests of thinning effects on ring specific gravity by selected heights	79
Table 4.5: Thinning effects on ring specific gravity over measurement periods by selected heights	80
Table 4.6: Quality of fit and prediction statistics double cross-validated on the fitting and validation data	84
Table 4.7: Coefficient estimates and their asymptotic standard errors for the combined data and by physiographic region	84
Table 5.1: Tree summary statistics for ring width and latewood proportion prediction models fitting and validation data	110
Table 5.2: Ring summary statistics for ring width and latewood proportion prediction models fitting and validation data	111
Table 5.3: A test of thinning effects on ring width for all data combined	116
Table 5.4: Tests of thinning effects on ring width by selected heights	117
Table 5.5: Thinning effects on ring width over measurement periods for selected heights	117

Table 5.6: Contrast tests between control vs thinned and heavy vs light thinning treatments	118
Table 5.7: Contrast tests among control vs thinned and heavy vs light thinning treatments for selected heights by measurement periods	119
Table 5.8: Tests of thinning effects on latewood proportion for all data combined	123
Table 5.9: Quality of fit and prediction statistics for the ring width prediction model double cross validated on the fitting and validation data	127
Table 5.10: Coefficient estimates, asymptotic standard errors and associated parameter estimates for the ring width prediction model	128
Table 5.11: Quality of fit and prediction statistics for the latewood proportion model double cross-validated on the fitting and validation data	130
Table 5.12: Coefficient estimates, asymptotic standard errors and associated parameter estimates for the latewood proportion prediction model	131
Table 6.1: Tree summary statistics for stem profile model fitting and validation data	159
Table 6.2: A test of thinning effects on the form exponent for all data combined	163
Table 6.3: A contrast test between control vs thinned and between heavy vs light thinning treatments	163
Table 6.4: Tests of thinning effects on the form exponent, and contrast tests between control vs thinned and between heavy vs light thinning treatments by height classes	164
Table 6.5: Quality of fit and prediction statistics for the stem profile model double cross-validated on the fitting and validation data	170
Table 6.6: Estimates of regression parameters, covariance parameters, standard errors and quality of fit measures for all regions combined	171
Table 6.7: Estimates of regression parameters, covariance parameters, standard errors and quality of fit measures for the Coastal Plain	172
Table 6.8: Estimates of regression parameters, covariance parameters, standard errors and quality of fit measures for the Piedmont	172

Table A4.1: A comparison of the performance of alternative specific gravity prediction models	210
Table A5.1: A comparison of the performance of alternative models for ring width prediction	212
Table A5.2: A comparison of the performance of alternative models for the latewood proportion prediction	213
Table A6.1: A comparison of the performance of alternative stem profile models	215
Table A6.2: A comparison of the performance of the proposed stem profile model with selected existing stem profile models	217

CHAPTER ONE

1.0 Introduction and objectives

1.1 Introduction

Loblolly pine (*Pinus taeda* L.) is the most important commercial tree species in the Southeastern United States and extensive areas of the region have been planted with the species. The USDA Forest Service (1988) reported that plantations comprised about one-third of the pine forest area in the South, but projected that the area would exceed that in natural stands in the near future. Similarly, Alig *et al.* (1986) projected that the timberland area in planted pine will double in the 12 southern states by the year 2030.

Because of the species' high responsiveness to silvicultural practices, loblolly pine plantations are managed intensively for wide ranging product objectives. Accordingly, the demand for management information not only on the quantity, but also the quality of wood expected to be produced given a set of silvicultural prescriptions is increasing. In order to provide detailed information on the quantity of wood produced, growth simulators such as PTAEDA2 (Burkhart *et al.* 1987) have been developed for loblolly pine trees.

These simulators provide quantitative information on stand responses under various silvicultural prescriptions such as site preparation, vegetation control, fertilization and thinning. The next logical step is to further refine growth simulators so that more detailed information on the quantity and quality of wood produced can be obtained for

alternative management prescriptions. Integrating detailed quantitative information with information on wood quality will enable one to make informed management decisions to obtain optimum product mixes.

Some of the major factors affecting wood quality are the size and distribution of knots and wood density. Doruska and Burkhart (1994) developed models that describe diameter and locational distribution of branches within the crown of unthinned loblolly pine trees. Their work can be used to quantify the size and distribution of knots. Among the many measures available for evaluating wood quality, specific gravity or relative density is often preferred as it is a simple index to the suitability of wood for a variety of uses (Koch 1972). Thus the other major wood quality issue, that of wood density, can be addressed via the assessment of wood specific gravity.

Many loblolly pine plantations are routinely thinned to obtain products that meet management objectives. Thinning is a type of partial cutting designed to direct the production of trees along desirable channel by removing surplus trees to concentrate the potential wood production of the stand on a limited number of trees (Smith 1986). It is desirable to quantify thinning effects to make informed management decisions.

While volumes of work exist on efforts to understand and explain thinning effects, results obtained and conclusions drawn are sometimes contradictory particularly on thinning effects on wood specific gravity. The apparent contradictions are largely because of variation in species response to site conditions, methods of stand manipulation and variations in method of measuring response, but also due to various other physical factors that cannot be controlled.

Among studies on thinning effects, many dealt with thinning influences on the rate of growth and pattern of wood deposition. Numerous studies have been conducted to determine thinning effects on wood production and silvicultural literature abounds with

reports on thinning effects – particularly on its effects on volume production (see for instance, Thomson and Barclay 1984; Cutter *et al.* 1991). Studies that have been conducted on thinning effects are commonly based on changes in stem diameter at breast height.

Various studies (Duff and Nolan 1953, 1957; Myers 1963), however, show that the pattern of wood deposition along the stem is not uniform, but varies by position along the stem and over time. It is suggested that for a given tree exposed to intense competition, thinning leads to a temporary shift in the pattern of annual wood deposition with the maximum shifting from the area of the base of live crown to close to the base of the tree. The reason is partly mechanistic, trees responding to forces such as wind when stands are opened up, but response can also be nutritional (Larson 1963).

As stands close when competition level increases, the point of maximum growth shifts back up the stem, and continues to do so until eventually it converges to the vicinity of the base of live crown (Farrar 1961; Myers 1963). Consequently, studies entirely based on the changes in breast height diameter likely give biased estimates of thinning response because they fail to account for growth reallocation that follows changes in stand density.

Wood volume in a tree bole is traditionally estimated from diameter and height measurements. With the increasing demand for more detailed and precise information on the effect of silvicultural inputs on increment, the layer of woody material deposited along the stem annually may be of interest. Because of the expected shift in the wood deposition pattern following thinning, direct prediction of ring width at any point in the tree bole may be more appropriate as it potentially provides a more accurate quantification of increment than those based on breast height diameter alone. Thus, direct prediction of ring width is

a reasonable approach to the quest for refining existing volume estimation systems and methods of determining effects of silvicultural treatments on increment.

Estimation of annual wood increment can also be approached from a different perspective. If tree stem profiles can be modeled accurately, it should be possible to obtain periodic increment along the stem as a shift in profile from one period to the next. Many taper models that have been successfully used to predict upper stem diameters for determining volume to various merchantability limits have been developed. Most existing stem profile models are designed to predict upper stem diameters by explaining the vertical variation in profile at one point in time. If changes in stand density occur, such as by thinning, because of the stipulated shift in wood deposition pattern changes in stem profile pattern also are expected. One expects a stem profile model that does not account for such change to have its performance deteriorate with time.

The primary purpose of this study was to determine thinning effects on ring specific gravity, ring width distribution, and stem form variation along the stem over time. The study aims at explaining how thinning intensity and associated stand and tree factors (such as site quality, density, age and size) affect ring specific gravity and ring width and hence stem profile variation over time. In addition, the study aims at developing models that predict ring specific gravity and ring width. Also, a stem profile model that accounts for possible changes in form over time will be developed.

Detailed data on ring by ring specific gravity, ring width as well as tree remeasurement data were obtained from the Loblolly Pine Growth and Yield Research Cooperative Thinning Study. The thinning study was established in 1981-82 and consisted of two thinning treatments and a control. The data used in this study partly came from measurements conducted on the permanent sample plots over the life of the thinning study

and partly from stem analysis on trees removed in the second thinning in a subset of the plots.

In investigating thinning effects on the various attributes of tree rings considered in this study, in model development as well as in evaluation of model performance, extensive use of statistics is inevitable. It is necessary that the conclusions drawn are based on valid theoretical principles and practices. Studies in experimental design for example show that, unless the procedures in which data are collected are clearly understood and the analyses techniques are appropriately tailored to the methods of data collection, it is possible to reach erroneous conclusions. In this study problems of similar nature, but of different dimension, exist and need to be addressed.

Classical analyses techniques such as the Ordinary Least Squares (OLS) assume independence among observations. If the OLS technique is used where observations are correlated, provided that the models are correctly specified, one obtains unbiased parameter estimates. However, the standard errors of the estimated parameters will be biased and associated hypothesis tests operate at unknown levels of significance. As a consequence, erroneous conclusions regarding the parameters may be drawn (West *et al.* 1984). The magnitude and direction of the bias incurred depends on the incorrectly specified but unknown covariance structure making it impossible to determine and take corrective measures (Gregoire 1992).

Researchers have dealt with correlation among observations in different ways-from using transformations to break down correlation to using estimation techniques robust to correlation. The need for accounting for correlation in growth and yield data has been long appreciated in forestry. Sullivan and Clutter (1972), Ferguson and Leech (1978, also see Davis and West 1981) and others recognized the problem and suggested ways in which to account for correlation among observations. More recently, Gregoire *et al.*

(1995) introduced mixed-effects modeling techniques into the forestry literature. The mixed-effects modeling approach has wide appeal in its theoretical basis, generality and interpretability. The technique enables modeling the covariance structure directly or accounting for correlation indirectly.

Observations obtained in repeated measures, in which individuals are repeatedly measured or observed over time, tend to be correlated. Repeated measure studies fall in the general category of longitudinal data analysis in which modeling only the usual mean response is inadequate, but some accounting for the expected correlation among observations within a unit is needed to obtain unbiased estimates of standard errors of estimated coefficients and to perform valid hypothesis testing.

The data used in this study in general fall into repeated measures category. The ring width and specific gravity data are ring-by-ring observations from disks taken at selected heights along the stem. One can plausibly argue that observations from the same disk are likely to be correlated since biological effects are seldom abrupt, but tend to carry over to subsequent years. Also, measurements on different disks on the same tree, at least measurements on growth rings corresponding to the same year, are expected to be spatially correlated because a continuous sheath of wood is annually deposited along the tree stem. Similarly, the tree data (diameter at breast height, height to live crown and total tree height) used in the study were obtained from repeated measurements on trees cut for stem analysis in thinned plots and similar trees in adjacent stands for the control plots.

Since correct inference may be as important as the research itself, the application of an appropriate technique to obtain unbiased and efficient parameter estimates by accounting for correlation in the error structure is an important component of this research. Accordingly, the mixed-effects analysis technique is extensively used in this study to model both the mean response as well as in accounting for correlation.

The organization of the dissertation follows chapters in which issues common to the various topics are treated and self contained chapters for the major areas investigated. Whereas the use of OLS technique for research data analysis is common place, the method used in this thesis is relatively new to the forestry field. Accordingly, Chapter 2 is devoted to a detailed review of the analysis of longitudinal data, mixed-effects modeling in particular. Materials and methods are presented in Chapter 3. Chapter 4 presents works on thinning effects on specific gravity. Thinning effects on ring width distribution is a topic of Chapter 5, and stem profile modeling is covered in Chapter 6. Finally, Chapter 7 summarizes the findings of the study and outlines brief recommendations for further research.

1.2 Objectives

The specific objectives of the study include:

- i)* Study thinning effects on ring specific gravity variation along the stem over time (vertical and radial) and develop ring specific gravity prediction model based on tree, stand and site characteristics.
 - study effects of ring physiological age on specific gravity variation.
 - study the vertical variation in ring specific gravity.
 - investigate the effects of stand density and the rate of growth exemplified by both direct and indirect measures of growth rate on specific gravity.
 - evaluate the effects of the inherent productivity of site and environmental factors on variation in specific gravity.

- ii)* Study thinning effects on ring width distribution (vertical and radial) and develop ring width prediction model based on tree, stand and site factors.
 - investigate thinning effects on variation in the pattern of wood deposition at one time along the stem and at one point over time.
 - investigate the role of various tree, stand and site factors in determining ring width.
 - evaluate thinning effects on percent latewood.
 - develop percent latewood prediction model based on ring width measurements and available stand level information.

iii) Examine thinning effects on stem form and develop a *dynamic* stem profile model.

- investigate thinning effects on the form exponent of trees at one time along the stem and at one point over time.
- develop a stem profile model that accounts for changes in stand conditions and thinning treatment.
- evaluate the performance of the dynamic taper model developed in this study relative to selected static taper models in use.

iv) Employ statistical analysis tools that account for the correlation expected among observations in the data available for the study.

- employ analysis techniques that account for the expected correlation in the data by modeling the covariance structure or accounting for correlation indirectly.
- evaluate (empirically and qualitatively) the effects of accounting for correlation by comparing changes in hypothesis tests and qualities of fit criteria when the ordinary analysis techniques are employed.

1.3 Variable definition and notation

The following terminology and notations are used in the study:

<i>DBH</i>	Diameter at breast height (4.5 ft above ground) (in.).
<i>d</i>	Upper stem diameter at height <i>h</i> (in.)
<i>H</i>	Total tree height (ft).
<i>h</i>	Height above ground to diameter <i>d</i> (ft).
<i>RHT</i>	Relative height ($\frac{h}{H}$).
<i>BLC</i>	Height to base of live crown (ft).
<i>CR</i>	Crown ratio ($\frac{H-BLC}{H}$).
<i>BA</i>	Basal area (sq. ft).
<i>SI</i>	Site Index (ft).
<i>RLS</i>	Relative spacing.
<i>SPA</i>	Stems per acre.
<i>RD</i>	Relative density.
<i>QD</i>	Quadratic mean diameter (in).
<i>CI</i>	Competition index ($\frac{QD}{DBH}$).
<i>RS</i>	Ring specific gravity.
<i>ES</i>	Earlywood specific gravity.
<i>LS</i>	Latewood specific gravity.
R_p^2	Pseudo coefficient of determination.
<i>SEE</i>	Standard error of estimate.
<i>ML</i>	Maximum likelihood.
<i>MLE</i>	Maximum likelihood estimate.

<i>REML</i>	Restricted maximum likelihood.
<i>OLS</i>	Ordinary least squares.
<i>GLS</i>	Generalized least squares.
<i>AIC</i>	Akaike's Information Criterion.
<i>LRT</i>	Likelihood ratio test.
<i>F</i>	F -distribution.
<i>t</i>	Student's t-distribution.
χ^2	Chi-squared distribution.
<i>MB</i>	Mean bias.
<i>BLUP</i>	Best linear unbiased predictor.
<i>BLUE</i>	Best linear unbiased estimator.
<i>MSE</i>	Mean squared error.
<i>NDF</i>	Numerator degrees of freedom.
<i>DDF</i>	Denominator degrees of freedom.
<i>CV</i>	Coefficient of variation.
<i>FE</i>	Form exponent.
<i>GEE</i>	Generalized estimating equations.
<i>RW</i>	Ring width.
<i>EW</i>	Earlywood width.
<i>LW</i>	Latewood width.
<i>PA</i>	Population averaged.
<i>SS</i>	Subject specific.

CHAPTER TWO

2.0 The analysis of longitudinal data

2.1 Introduction

Much of the data used in this study consist of observations that are collected on individuals in repeated observations either in time and/or space. Since data collected from an individual tend to be more alike than different, in some ways because of the individual's deviation from the population average, they tend to be correlated.

The tree data that were obtained from repeated measures on permanent sample plots belong to the longitudinal data category. The bulk of the data, specific gravity and ring width data, obtained from stem analysis technically were not collected by repeated measurement on growth rings in the classical sense, but can also be regarded as longitudinal as well. Since the correlation structure in the data resembles those encountered in longitudinal studies, analyses techniques designed for longitudinal studies are appropriate.

In order to set the stage for subsequent works, it is appropriate to introduce longitudinal data analysis, and the chapter is devoted to issues related to longitudinal data analysis. Following a general introduction to the analysis of correlated observations in the context of longitudinal data analysis, alternative approaches to the analysis of such data are presented briefly. The major portion of the chapter is devoted to mixed-effects modeling.

2.1.1 Longitudinal vs cross-sectional studies

Longitudinal studies are studies in which individuals (here after referred to by the generic name *subjects*) are measured repeatedly or phenomena are observed through time. In contrast, studies where different subjects or phenomena are observed at a moment in time are *cross sectional* or *base line* studies. Longitudinal studies include repeated measure and growth curve studies. In designed studies, subjects on which repeated measurements are taken are assumed to remain constant over time and the primary object is to investigate treatment effects.

On the other hand, growth curve studies are concerned with the change which individuals undergo due to what is often called the *aging process* generic for change over time. In forestry, permanent sample plots are established in wide range of stand conditions and trees are monitored for long periods of time or information on tree history are retrospectively obtained through stem analysis as in growth curve studies. Repeated measures referred to here, unlike those in design studies, combine both treatment effects and change in subjects over time.

Cross-sectional studies involve observing several individuals at one point in time. That is, several individuals from a cross section of the population are observed at one time to draw inference about average population effect. In cross-sectional studies, deliberate attempts are made to obtain samples representative of the range of characteristics of interest to capture average effects due to differences among individuals in the population under study. For instance, if age is one of the covariates, subjects of different age groups are included, in essence, to capture age effects.

Implicitly then, it is assumed that subjects of different ages follow the same trajectory. That often this is not the case has been demonstrated in forestry for instance,

in tree height development in developing site-index curves. Sometimes, repeated cross-sectional studies are used to model changes over time (age effects), but the estimates obtained can be biased if the population is changing over time because of migration or attrition (Ware 1985).

Longitudinal studies enjoy several advantages over cross-sectional studies. Primarily, longitudinal studies offer an opportunity for controlled measurement hence a more reliable quantification of the history of subjects included in the study is possible than in cross-sectional studies. Secondly, longitudinal studies provide information about individual patterns of change. Estimates on age-related changes obtained from cross-sectional studies are based on differences between groups, rather than individual patterns, which may confound age and *cohort* effects (Ware 1985; Diggle *et al.* 1994). Finally, longitudinal studies can provide more efficient estimators of some parameters than cross-sectional studies with the same number and patterns of measurements due to their ability to distinguish between within-subject and between-subject effects.

If data collected from longitudinal studies are properly analyzed, it is possible to answer both cross-sectional and longitudinal questions. Cross-sectional questions are those that pertain to population characteristics such as the population mean whereas longitudinal ones are those that relate to individual change such as development in growth and aging. In the absence of selection or dropout bias, any parameter determining the cross-sectional mean can be estimated by an appropriate cross-sectional study, but, for instance, covariance parameters can only be estimated longitudinally (Louis 1988).

If the researcher is interested in changes in the subjects over time, the data analysis method must account for the change in the population and the change within subjects. Statistical analysis of longitudinal data is necessarily different from cross-sectional data analysis because within subject observations in the former are likely to be correlated.

Longitudinal studies lead to a data structure which is hierarchical in nature, imposing correlations among sub-units within units. The observations on subjects are nested within subjects resulting in variance components. A defining character of longitudinal data is that the observations within subjects are ordered either by time or position in space hence observations are not randomly assigned to “treatment” (Lindstrom and Bates 1990).

An illustration of the issue of cross-sectional versus longitudinal studies can be seen in this study using the basic measurements collected over twelve years. The measurements are DBH, height to live crown (BLC) and total tree height (H). Since the measurements were taken on several subjects during five time periods, the study can be considered repeated cross-sectional study. An analysis of the data within cross-sectional data analysis framework enables one to estimate changes in the population average over time (see Figure 2.1). Since the analysis technique does not preserve the relationship between observations over the time periods, nothing can be said about the rate of changes in individual trees over time. Consequently, the regression coefficients only have population averaged (PA) interpretation. From the scatter plots in Figure 2.1 it can be seen that these measurements, on average, increase over time.

Alternatively, the study can be considered a longitudinal study, which it is since individuals were visited over several time periods (see Figure 2.2). Under this setting we observe two levels of changes in the variables measured. One level enables evaluating average change in the population; whereas the second level can be used to evaluate changes in individuals over time *i.e.* subject specific (SS) interpretation is also possible. The concepts of PA and SS interpretations are much more technical than loosely used here hence they are treated more formally in § 2.2.4.1.3.

When longitudinal data analysis techniques are used, the relationship among observations from the same subjects or individuals are preserved to enable not only the

individualization of the regression coefficients, but also accounting for possible correlations among observations from the same subjects. As seen in the parallel profile plots in Figure 2.2, while on the average the population changes over time, the rate at which the changes occur vary from individual to individual. For instance, focusing on the DBH measurements, we see three distinct groups. One group tends to have values above the bulk of the trees, whereas one group shows a tendency to have values lower than the majority of the trees in the plots. The majority of the trees have their measurements bunched around the mean.

Thus, by analyzing the data using longitudinal data analysis technique we can make inferences on issues that we would not be able if cross-sectional analysis were entertained. In subsequent sections, the consequences of ignoring correlation among within subject observations and alternative ways of accounting for correlation are addressed.

2.1.2 Consequences of ignoring correlations

In forestry, a number of researchers attempted to account for correlation among observations in a variety of ways (see for instance Sullivan and Clutter 1972; Ferguson and Leech 1978 see also Davis and West 1981; West *et al.* 1984; Lappi 1986, Monserud 1986; Lappi and Bailey 1988 and others) the vast majority of growth and yield models relying on permanent plot and stem analysis data, however, fail to account for within plot or tree correlation. This sub-section is devoted to a discussion of the consequences of using ordinary analysis techniques which assume independence among observations when in fact the observations used in analysis are correlated.

Data from repeated measures on a subject (sampling unit) have a tendency to be correlated. Similarly, observations taken from sampling units close to each other, such as

clusters of trees, sample plots and points along a stem are usually spatially correlated (West et al. 1984). Stem analysis data are often used in forestry to reconstruct the past life history of individual trees and forest stands.

Because successive measurements or observations along a tree bole tend to be more alike than observations made from different trees, the observations are likely to be correlated. One can consider correlation as resulting among repeated responses because the regression coefficients vary across subjects-where here trees are the subjects. Alternatively, correlation arise among observations within subjects because of the individual's some what deviation from the average (Rutter and Elashoff 1994).

Many statistical data analysis are based on the assumption of independence among observations. For instance, when the ordinary least squares (OLS) technique is used to estimate parameters in model building, valid statistical inference depends, in part, on the assumption of independence of observations. If the OLS techniques are employed to analyze data which are temporally and/or spatially correlated, theoretical problems arise because the basic assumption of independence of observations is violated (Sullivan and Reynolds 1976; West *et al.* 1984).

The effect of ignoring the correlated nature of observations in using OLS has been widely investigated. Swindel (1968) presented bounds on the bias of the least-squares estimator of the variance when the covariance matrix is allowed to arbitrarily depart from the usual assumptions. These bounds are, however, too wide to be of practical use and are uninformative of the direction of bias since they include zero Gregoire (1992). Sullivan and Reynolds (1976) examined the case where two repeated measurements are conducted on a sampling unit. They presented results for situations of varying degree of correlations and changes in the magnitude of variance between measurements.

When ordinary least squares analysis is conducted on data obtained through multiple measurements on permanent sample plots or equivalently from stem analysis, the covariance matrix of the parameter estimates and the residual variance of the regression are biased (West *et al.* 1984). As a consequence, calculated confidence intervals are biased and tests of hypothesis operate at unknown levels of significance rather than the stipulated nominal level. Also due to the dependence of the bias on the covariance structure, it is impossible to tell whether the constructed intervals are uniformly narrower or wider than when the covariance structure is appropriately modeled (Gregoire 1992).

2.2 Alternative approaches

2.2.1 Maximum likelihood procedure

Alternative solutions have been suggested for overcoming problems posed by correlated observations generally in the form of using alternative estimation techniques. Concerned with the bias of variance estimator when ordinary analyses techniques (for instance, OLS) are employed when observations are correlated, researchers have sometimes used the maximum likelihood technique to obtain parameter estimates. Sullivan and Clutter (1972) employed this technique in developing simultaneous growth and yield models for loblolly pine.

Arner and Seegrift (1979, 1980) extended the works of Sullivan and Clutter (1972) so that a varying number of observations for each sampling unit is possible. They also developed computer programs for the maximum likelihood estimates of parameters, one of the bottlenecks in using the system at the time.

Maximum likelihood estimators of variance are asymptotically unbiased and efficient but are biased downward for small samples. Alternatively, restricted maximum likelihood which is unbiased for balanced designs and less biased than full maximum likelihood for unbalanced designs is advocated. Consistency and efficiency of maximum likelihood estimators also depend on correct specification of the marginal distribution of interest (Rutter and Elashoff 1994). Alternatives to the full likelihood approach via the use of quasi-likelihood are sometimes used to avoid strict distributional assumptions. Maximum likelihood procedure as an estimation technique is also used in mixed-effects modeling addressed in §2.2.4.

2.2.2 Multi-stage analysis

The problem of correlation in a data set in forestry setting has also been handled using multistage analysis technique or elementwise regression. West *et al.* (1984) discuss the merits of a two-stage analyses technique applied to a forestry problem. Biging (1985) used a two stage technique in developing site-index curves. Newberry and Burkhart (1986) used two-stage technique in developing taper equations.

In this procedure the analysis is broken into two stages to account for variations within and between sampling units. In the first-stage an appropriate model is fit to the data of each subject and parameters are estimated. The relation of parameter estimation from the first stage equations for each subject to the independent variables are used to account for variation between subjects in the second stage regression. Substitution of the second stage parameter estimates into the first-stage equations yields an equation which accounts for both within and between subject variations (West *et al.* 1984).

The drawback with this approach, especially when the number of repeated observations is small, has been that the first-stage coefficients are inefficient and unstable. In particular, fitting non-linear models may be difficult when the number of observations is small (Biging 1985). Moreover, the analysis techniques commonly used in the first-stage usually do not account for the serial correlations within subjects.

Davidian and Giltinan (1993, 1995) proposed methods of estimating intraindividual variation in non-linear mixed effects modeling (see §2.2.4.1.2) within multistage analysis framework. Assuming that a common intraindividual variance structure is present and sufficient observations per subject are available, individual regression parameters are first estimated from each individual's data. Then in the second stage, the individual parameter estimates are pooled and used in an iteratively reweighted least square to obtain final population parameter estimates.

2.2.3 Generalized least squares

An exact method for overcoming the problem of errors departing from the ideal case is the use of Generalized Least Squares (GLS) technique instead of OLS. Within a growth and yield context, Ferguson and Leech (1978; see also Davis and West 1981) are probably among the first to employ this method when they developed a two stage GLS procedure for estimating yield functions . For the generalized least squares model :

$$\mathbf{Y} = \mathbf{X}'\boldsymbol{\beta} + \boldsymbol{\epsilon} \quad [2.1]$$

Where

Y is an $N \times 1$ vector of observations on the dependent variable.

β is a $p \times 1$ vector of unknown regression coefficients.

X is an $N \times p$ non-stochastic matrix of rank k of observations on the explanatory variables;

ϵ is an $N \times 1$ vector of random unobservable errors with:

$E(\epsilon) = 0$, $E(\epsilon\epsilon') = \sigma^2 \Omega$, where Ω is a known symmetric, positive definite matrix and can be of different forms, and is used to account for correlation among observations, heteroscedasticity or a combination of both.

By Aitken's theorem (Fomby *et al.* 1984), the GLS estimator of β :

$$\hat{\beta} = (X' \Omega^{-1} X)^{-1} X' \Omega^{-1} Y \quad [2.2]$$

is most efficient (in the sense of having minimum variance) among the class of linear unbiased estimators of β .

Unfortunately, the method requires an *a priori* knowledge of the variance-covariance matrix of the residuals (Ω) which would be used for weighting in GLS regression. A prior knowledge of the variance-covariance matrix does not in general exist; and it is not estimable because $\frac{N(N+1)}{2}$ possibly distinct elements need to be estimated from N observations. As a result, auxiliary information is incorporated to limit the number of distinct elements in Ω that need to be estimated (Gregoire 1987).

In practice, iterative procedures in the form of estimated or feasible generalized least squares (FGLS) procedure, is used to overcome the problem and an appropriate estimator of Ω modifies to:

$$\tilde{\beta} = (X' \hat{\Omega}^{-1} X)^{-1} X' \hat{\Omega}^{-1} Y \quad [2.3]$$

where $\hat{\Omega}$ is consistently estimated by $\hat{\Omega}$.

However, the FGLS estimator does not possess the optimal efficiency of the GLS (Gregoire 1987). Fuller and Battese (1974) present sufficient conditions under which the FGLS is unbiased and possesses some of the desirable properties of the GLS. Under large sample situation the use of FGLS, depending on the true structure of Ω , yields most of the properties of GLS (Fomby *et al.* 1984). Extensive discussions of ways in which to obtain consistent estimates of Ω are presented in many econometric text books such as Fomby *et al.* (1984), Kmenta (1986), Judge *et al.* (1988), and in Searle *et al.* (1992).

However, missing data, unbalancedness, too few number of observations for some sampling units, and other characteristics of data often pose practical difficulties in application (Laird and Ware 1982). In particular the usual method of moments technique in estimating the variance parameter may be unreliable (Davis and West 1981; Wolfinger 1992).

2.2.4 Mixed effects modeling

An alternative technique used in longitudinal data analysis notably in the fields of medicine to account for correlation among repeated measures is the use of mixed-effects models. Mixed effects models are sometimes called random coefficient regression models (Rutter and Elashoff 1994), at times random-effects models (Laird and Ware 1982; Hirst *et al.* 1991) and mixed models (Wolfinger 1992). They all refer to the same modeling approach the details of which are outlined subsequently.

Longitudinal data analysis, received special attention particularly in the area of biomedical research where subjects are repeatedly observed. Such data besides being often correlated, also tend to be unbalanced and irregularly spaced requiring data analysis techniques that recognize and efficiently utilize their peculiar properties (Laird and Ware

1982). The technique is largely developed for studies in epidemiology and other health studies where subjects observed over a period of time have a tendency to drop out before studies are completed or for subjects to show up at time other than they are supposed to.

In forest growth and yield studies, where observations are obtained from permanent sample plots or are collected from stem analysis, observations are temporally or spatially correlated requiring the use of data analysis techniques that recognize and account for correlation. The structure of the data obtained from these studies also tend to be unbalanced and irregularly spaced. While variants of mixed-effects modeling have been attempted by some investigators within forestry research, Gregoire *et al.* (1995) were the first to extensively describe and effectively demonstrate the use of linear mixed-effects model analysis technique as applied to forestry problem using permanent plot data.

The technique accounts for correlation of the within subject errors through the use of various covariance structures, such as the continuous-time autocorrelation error structure (Diggle 1988) which, unlike its counterpart AR(1) in the discrete case, enables the use of irregularly spaced unbalanced data. The mixed effects model extends the GLM by allowing a more general specification of the covariance matrix of ϵ .

Assuming that the errors are normally distributed, correlation and heterogeneity of the σ_i^2 's is accommodated within the mixed model framework. In many longitudinal studies each subject has few observations making individual parameter estimation inefficient or impossible. Through the assumption that the random effect coefficients have a particular distribution, usually Gaussian, mixed effects modeling enables the borrowing of strength across subjects to estimate the fixed effects coefficients (Zeger *et al.* 1988).

2.2.4.1 Alternative models

2.2.4.1.1 Linear mixed-effects models

In the sequel, the notations of Laird and Ware (1982) is used to present linear mixed-effects modeling. We assume that there are m subjects each with possibly unequal number of observations n_i with a total of N observations ($N = \sum_{i=1}^m n_i$). Let β denote a $p \times 1$ vector of unknown population fixed-effect parameters, X_i be a known $n_i \times p$ matrix of fixed effect covariates; α_i be a $q \times 1$ vector of unknown subject specific random effects and Z_i a known $n_i \times q$ matrix of random effect covariates. Laird and Ware (1982) proposed the model:

$$Y_i = X_i' \beta + Z_i' \alpha_i + \epsilon_i \quad [2.4]$$

With the following assumed properties: $E(\epsilon_i) = 0$, $E(\alpha_i) = 0$, $Var(\epsilon_i) = R_i$, $Var(\alpha_i) = D$; $Cov(\epsilon_i, \alpha_i) = 0$; thus:

$$\epsilon_i \sim N(0, R_i)$$

$$\alpha_i \sim N(0, D)$$

where R_i and D are $n_i \times n_i$ and $q \times q$ positive-definite covariance matrices, respectively. Consequently;

$$E(Y_i) = X_i' \beta; \quad Var(Y_i) = V_i = Z_i D Z_i' + R_i$$

Thus the marginal distribution of Y_i , observations from subject i , is:

$$Y_i \sim N(X_i' \beta, Z_i D Z_i' + R_i) \quad [2.5]$$

With the above properties, given the subject's random effect coefficient (α_i), we can also deduce the moments of the conditional distribution of Y_i :

$$E(Y_i|\alpha_i) = X_i'\beta + Z_i'\alpha_i \quad [2.6]$$

and

$$Var(Y_i|\alpha_i) = R_i \quad [2.7]$$

which is an individualization of the regression specified in [2.4].

Model [2.4] for longitudinal data allows for serial correlation in two ways: The random effects variance matrix, D , models variability across subjects through the design matrix Z_i . The conditional covariance of $(Y_i|\alpha_i)$, R_i , models variability within individuals by explicitly modeling the within-subject error matrix R_i as a function of variance covariance parameters. Because any data set has finite variability to be divided between D and R_i , inclusion of random effects and parametrization of R_i must be considered together (Rutter and Elashoff 1994) as it may be impossible to model both D and R_i within the same model.

A point to consider is the selection of variables constituting Z_i among the set of predictors available. In practice, as pointed out by Louis (1988), the choice of covariance structure is dictated by data structures, subject area theories, available computer packages and personal judgment.

In many instances one analyst's covariate is another's covariance (cf. Gregoire *et al.* 1995). The analyst must often take a trade-off between including additional covariate (*i.e.* complicating the mean vector model) and increasing the complexity of the covariance

structure (*i.e.* increasing the dimension of Z_i and specifying D); in essence, covariance structures may be thought of as surrogates for unmeasured covariates.

Given the model as in [2.4] and stipulations thereof, parameters for the fixed effects (β) are obtained by generalized least squares technique using weights $W_i = V_i^{-1}$. The subject specific random effect parameters (α_i) are empirical Bayes predictors and are related to Stein-type shrinkage estimates (Laird and Ware 1982). Thus if V_i is known, using $W_i = V_i^{-1}$, we obtain:

$$\hat{\beta} = \left(\sum_{i=1}^m X_i' W_i X_i \right)^{-1} \sum_{i=1}^m X_i' W_i Y_i \quad [2.8]$$

and

$$\hat{\alpha}_i = D Z_i' W_i (Y_i - X_i' \hat{\beta}) \quad [2.9]$$

with variances

$$Var(\hat{\beta}) = \left(\sum_{i=1}^m X_i' W_i X_i \right)^{-1} \quad [2.10]$$

$$Var(\hat{\alpha}_i) = D Z_i' \{ W_i - W_i X_i \left(\sum_{i=1}^m X_i' W_i X_i \right)^{-1} X_i' W_i \} Z_i D \quad [2.11]$$

However, in assessing the error of estimation, to account for variation in α_i , Laird and Ware (1982) suggest using:

$$Var(\hat{\alpha}_i - \alpha_i) = D - D Z_i' W_i Z_i D + D Z_i W_i X_i \left(\sum_{i=1}^m X_i' W_i X_i \right)^{-1} X_i' W_i Z_i D \quad [2.12]$$

to account for the variation in α_i .

$\hat{\beta}$ maximizes the likelihood and is the minimum variance unbiased estimate. The expression for $\hat{\alpha}_i$ is derived by an extension of the Gauss-Markov theorem to cover random effects (Harville 1976). When V_i is known, the estimates of β , $\hat{\beta}$, are BLUE and $\hat{\alpha}_i$ is best (minimum mean squared error) linear unbiased predictor (BLUP) of α_i (Harville 1990; Robinson 1991).

Since V_i is generally unknown, its consistent estimator, $\hat{V}_i = Z' \hat{D} Z_i + \hat{R}_i$, is used instead with $Var(\hat{\beta})$ estimated by, $V\hat{a}r(\hat{\beta}) = (\sum_{i=1}^m X_i' \hat{W}_i X_i)^{-1} \cdot V\hat{a}r(\hat{\beta})$ underestimates $Var(\hat{\beta})$ because of the uncertainty in \hat{W}_i . An alternative estimator suggested by Liang and Zeger (1986) is the robust or sandwich estimator given by :

$$V\tilde{a}r(\hat{\beta}) = (\sum_{i=1}^m X_i' \hat{W}_i X_i)^{-1} S (\sum_{i=1}^m X_i' \hat{W}_i X_i)^{-1} \quad [2.13]$$

Where $S = (X_i' \hat{W}_i e_i e_i' \hat{W}_i X_i)$ and $e_i = y_i - X_i' \hat{\beta}$. If $e_i e_i' = \hat{V}_i$, [2.13] reduces to $V\hat{a}r(\hat{\beta})$.

Similarly, the variance of the random effects, $Var(\hat{\alpha}_i - \alpha_i)$ is estimated by $V\hat{a}r(\hat{\alpha}_i - \alpha_i)$ with W_i in [2.12] replaced by \hat{W}_i .

The problem is how to obtain consistent estimate of \hat{V}_i . Due to the unreliability of method of moment estimators (because they can give negative estimates for some variance components) the common choice is ML or REML; where, by appealing to the normality assumption on the errors and random effects parameters, the parameters in V_i , D and R_i , as well as $\hat{\beta}$ and $\hat{\alpha}_i$ are jointly estimated. The estimates are those values that maximize the likelihood function. Alternatively, quasi likelihood approaches have been used to relax distributional assumptions.

Assuming the ε_i and α_i are normally distributed, for a particular subject i its contribution to the data likelihood may be written as:

$$l_i = (2\pi^{n_i} |\sigma^2 V_i|)^{-\frac{1}{2}} \exp\left(-\frac{1}{2\sigma^2} \varepsilon_i' V_i^{-1} \varepsilon_i\right) \quad [2.14]$$

where the ε_i are the residuals $\varepsilon_i = y_i - X_i' \beta$. Now letting $L_i = -2\ln(l_i)$, twice the negative log-likelihood :

$$\begin{aligned} L &= \sum_{i=1}^m L_i \\ &= \sum_{i=1}^m \left\{ n_i \ln(2\pi) + n_i \ln(\sigma^2) + \ln|V_i| + \frac{\varepsilon_i' V_i^{-1} \varepsilon_i}{\sigma^2} \right\} \\ &= N \ln(2\pi) + N \ln(\sigma^2) + \sum_{i=1}^m \left\{ \ln|V_i| + \frac{\varepsilon_i' V_i^{-1} \varepsilon_i}{\sigma^2} \right\} \end{aligned} \quad [2.15]$$

Suppose $\varepsilon_i \sim N(0, \sigma_i^2)$ where $\sigma_i^2 = \sigma^2 X_i'$; i.e. $V_i = X_i'$, the errors follow a heteroscedastic structure where the variance is a function of an explanatory variable. For this special case, the derivatives of [2.15] with respect to the unknown parameters evaluated at zero, give the maximum likelihood estimating equations (Gregoire and Dyer 1989) :

$$\frac{\partial L}{\partial \beta} = 0 = \sum_{i=1}^m \frac{-2X_i' Y_i - 2 X_i' X_i \beta}{\sigma^2 X_i'} \quad [2.16]$$

$$\frac{\partial L}{\partial \sigma^2} = 0 = - \sum_{i=1}^m \left\{ \frac{N_i}{\sigma^2} - \frac{(Y_i - X_i' \beta)' (Y_i - X_i' \beta)}{\sigma^2 X_i'} \right\} \quad [2.17]$$

$$\frac{\partial L}{\partial \alpha} = 0 = \sum_{i=1}^m \left\{ \ln(X_i) - \frac{(Y_i - X_i' \beta)' (Y_i - X_i' \beta) \ln(X_i)}{\sigma^2 X_i'} \right\} \quad [2.18]$$

the solution of which yield estimates $\hat{\beta}$, $\hat{\sigma}^2$ and $\hat{\gamma}$.

However, since V_i 's are unknown in general, their elements are estimated, for instance, by using an OLS estimate of β as an initial estimate and concentrating out β . To further reduce computational burden of the procedure, σ^2 is often concentrated out of [2.15] such that L is expressed in a form which involves only elements of V_i , and a constant such that :

$$\hat{L} = N \ln(2\pi) + N \ln(\hat{\sigma}^2) + \sum_{i=1}^m \ln|V_i| + N \quad [2.19]$$

Where $\hat{\sigma}^2 = \frac{\sum_{i=1}^m e_i' V_i^{-1} e_i}{N}$; and $e_i = Y_i - X_i' \hat{\beta}$. For estimating variance (σ^2), equation [2.19] is biased downward especially if the sample size is small. Consequently, it is customary to use the restricted maximum likelihood given by:

$$\hat{L}_R = N + N \ln(2\pi) + (N - p) \ln(\hat{\sigma}^2) + \sum_{i=1}^m \ln|V_i| + \ln \left| \sum_{i=1}^m X_i' V_i^{-1} X_i \right| \quad [2.20]$$

Where $\hat{\sigma}^2 = \frac{\sum_{i=1}^m e_i' V_i^{-1} e_i}{N-p}$ and p is the number of fixed effect parameters. With some balanced designs, the solution of [2.20] gives an unbiased estimate of σ^2 . Within the mixed-effects modeling framework, to obtain the required estimates, \hat{D} and \hat{R}_i , Laird and Ware (1982) first suggested the EM (Expectation-Maximization) algorithm; a general-purpose optimization routine for computing maximum likelihood estimates in an incomplete data setting. While the EM algorithm is monotonic hence guarantees eventual

convergence if the maximum is away from the boundary of the parameter space, it's slowness and convergence to local rather than the global maxima are considered drawbacks in its implementation.

Various alternatives for speeding up the algorithm have been proposed. Jennrich and Schluchter (1986) proposed scoring in the M-step; Lindstrom and Bates (1988) use the Aitken accelerator. The MIXED procedure in SAS uses a modified Newton-Raphson method to numerically obtain the optimum values of \hat{D} and \hat{R}_i from the mixed model equation [2.21] (Wolfinger 1992). These estimates are then used to obtain the estimates [2.22] and [2.23]; which are REML for β and empirical Bayes for α_i (Laird and Ware 1982).

$$\begin{bmatrix} X_i' \hat{R}_i X_i & X_i' \hat{R}_i Z_i \\ Z_i' \hat{R}_i X_i & X_i' \hat{R}_i X_i + \hat{D}^{-1} \end{bmatrix} \begin{bmatrix} \hat{\beta} \\ \hat{\alpha}_i \end{bmatrix} = \begin{bmatrix} X_i' \hat{R}_i Y_i \\ Z_i' \hat{R}_i Y_i \end{bmatrix} \quad [2.21]$$

leading to the solutions:

$$\hat{\beta} = \left(\sum_{i=1}^m X_i' \hat{W}_i X_i \right)^{-1} \sum_{i=1}^m X_i' \hat{W}_i Y_i \quad [2.22]$$

and

$$\hat{\alpha}_i = \hat{D} Z_i' \hat{W}_i (Y_i - X_i' \hat{\beta}) \quad [2.23]$$

Due to the uncertainty in the estimates \hat{D} and \bar{R}_i the variances of the estimated parameters are underestimated and for accurate inference variance inflation is sometimes suggested (Wolfinger 1992).

2.2.4.1.2 *Nonlinear mixed effects models*

Much of the work on mixed effects model focused on data that could be modeled by linear or intrinsically linear models. In many cases, such as in growth curve data, linear models are not efficient in describing the process being modeled. Mixed effects modeling thus has been extended to address modeling nonlinear processes. The nonlinear counterpart of model [2.1] may be written as :

$$Y_i = f(X_i\beta + Z_i\alpha_i) + \epsilon_i \quad [2.24]$$

Where $f(\cdot)$ is a nonlinear function depending on known covariates, and others are as defined in §2.2.4.1. Many of the works on nonlinear mixed effects modeling involve linearization of $f(\cdot)$ using Taylor series expansion around the expected value of the random effects coefficient, around $\hat{\alpha}_i$ or around initial values. Sheiner and Beal (1980) linearize [2.24] by expanding around β and the expected value of α_i . Lindstrom and Bates (1990) use linearization about $\hat{\alpha}_i$, the best linear unbiased predictor of α_i , and $\hat{\beta}$ and then using Gaussian posterior approximation. Hirst *et al.* (1991) expand around the initial values β_0 and α_{i0} . Others (Vonesh and Carter 1992; Davidian and Gallant 1993; Davidian and Giltinan 1993) proposed methods that do not involve linearization of [2.24].

A variety of alternative approaches have been proposed for fitting nonlinear mixed effects models. Lindstrom and Bates (1990) method incorporates the concepts of the linear mixed-effects model of Laird and Ware (1982) for the individual parameter vectors

and then a first-order Taylor series expansion about current estimates of the random effects to approximate the marginal distribution of Y_i .

Sheiner and Beal (1980) proposed an extended least squares (equivalently MLE under normality) to a model which used first-order approximation to the nonlinear mixed model. Vonesh and Carter (1992) proposed a multi-stage approach where the parameters of the covariance structure are estimated from the residuals of an ordinary nonlinear least squares fit. The residuals are used in an estimated generalized least squares procedure to obtain estimates of the parameters (α_i and β). Their approach also handles the case where the α_i and ϵ_i are not necessarily normal, but approximately so.

Wolfinger (1993), proposed Laplace's approximation method as an alternative derivation of algorithms for fitting nonlinear mixed effects models where both fixed and random effects enter nonlinearly. Racine-Poon (1985) advocated a Bayesian approach to nonlinear mixed effects modeling based on vague prior and an assumption of normality for the error. Davidian and Giltinan (1993, 1995) put forth multistage analysis combined with weighted least squares to model within subject variability for situation where sufficient observations are available to estimate within subject parameters.

Much of the preceding discussion is based on the assumption that the α_i and the ϵ_i are normally distributed. To account for cases where such claims can not reasonably be made, techniques that are only semi-parametric have been proposed. Davidian and Gallant (1993) proposed a semi-parametric approach with the assumption that the random effect density is smooth otherwise unrestricted. Gregoire and Schabenberger (1996) employed generalized estimating equations approach in modeling cumulative tree bole volume.

Using the Lindstrom and Bates (1990)¹ approach and expanding around current estimates $(\hat{\beta}, \hat{\alpha}_i)$ yields (cf. Gregoire and Schabenberger 1996) :

$$Y_i \doteq f(X_i' \hat{\beta} + Z_i' \hat{\alpha}_i) + G_i'(\beta - \hat{\beta}) + Q_i'(\alpha_i - \hat{\alpha}_i) + \epsilon_i$$

where

$$G_i' = \left. \frac{\partial f(X_i' \beta + Z_i' \alpha_i)}{\partial \beta'} \right|_{\hat{\beta}, \hat{\alpha}_i} = f'(X_i' \hat{\beta} + Z_i' \hat{\alpha}_i) X_i$$

$$Q_i' = \left. \frac{\partial f(X_i' \beta + Z_i' \alpha_i)}{\partial \alpha_i'} \right|_{\hat{\beta}, \hat{\alpha}_i} = f'(X_i' \hat{\beta} + Z_i' \hat{\alpha}_i) Z_i$$

By rearranging one obtains:

$$Y_i' = G_i' \beta + Q_i' \alpha_i + \epsilon_i \quad [2.25]$$

where

$$Y_i' = Y_i - f(X_i' \hat{\beta} + Z_i' \hat{\alpha}_i) + G_i' \hat{\beta} + Q_i' \hat{\alpha}_i$$

Now, [2.25] is a linear mixed model whose parameters can be estimated using procedures described for linear mixed models. Landstrom and Bates (1990) suggest a two-step procedure – the pseudo data step and linear mixed effects step where the fitting routine iterates between linearization and fitting of the linear mixed effects to the pseudo-data until convergence.

¹ Lindstrom and Bates (1990) first expand only around the random effects current estimate to obtain what they call Pseudo-data step. The resulting expression does not quite correspond with the linear mixed effects estimation problem because it still is nonlinear in β . Consequently, another Taylor series expansion around the current estimates $\hat{\beta}$ is taken to obtain an expression corresponding to linear mixed effect model.

2.2.4.1.3 Generalized mixed effects models (GLIM)

Mixed effects modeling has been further extended to cover situations where data are not continuous and non-normal in the form of generalized linear models for longitudinal data. Stiratelli *et al.* (1984) studied the logistic Gaussian mixed model in which they assumed that $\text{logit}(\mu_i) = X_i'\beta + Z_i'\alpha_i$, with $\text{Var}(Y_i|\alpha_i) = \mu_i(1 - \mu_i)$ and α_i is distributed as independent random vector with mean $\mathbf{0}$ and covariance D .

In GLIM modeling interpretation of fixed effects coefficients is not as straight forward as in linear mixed effects modeling. One has to make distinction between whether the coefficients apply to the population or to individual subjects hence the concept of population-averaged (PA) and subject-specific (SS). SS effects model the expected within subject effect taking into account heterogeneity among subjects. Population averaged (PA) effects, on the other hand, model expected average effects across subjects based on the marginal expectation of Y_i without explicitly modeling variation among subjects.

The distinction between PA and SS modeling is a problem that sometimes can be confusing. Schabenberger and Gregoire (1996) provide an insightful discussion that dispels much of the confusion in the area. Models without random effects ($Z_i = 0$) are population-averaged since the model coefficients describe a change in response of the average population with a change in the covariates. On the contrary, models with random effects describe changes in the response of an individual with the change in the covariates hence are subject-specific. Moreover, PA models only describe the covariance among repeated observations for a subject whereas SS models explain the source of the covariance (Zeger *et al.* 1988)

Due to the asymptotic correlation between the SS parameters and of the random effects distribution, when SS parameters are of main interest, Zeger *et al.* (1988) suggest

care in their interpretation. PA effects estimate expected differences between subjects with different covariate values while SS effects estimate expected differences within individuals for different covariate values (Rutter and Elashoff 1994).

In the SS model, the focus is $E(Y_i|\alpha_i)$ and the correlation structure within subjects is modeled through parametrization of R_i . Let $\mu_i = E(Y_i|\alpha_i)$; following Zeger *et al.* (1988), the SS mixed generalized linear model is specified as:

$$h(\mu_i) = X_i'\beta + Z_i'\alpha_i \quad [2.26]$$

and

$$Var(Y_i|\alpha_i) = g(\mu_i)*\psi \quad [2.27]$$

Where α_i is an independent observation from a mixture distribution, F . The functions h and g are link (e.g. logit , probit) and variance, respectively. The objective of analysis is to estimate β , α_i and ψ . Here we note that β has SS interpretation and only under certain circumstances (such as when h is the identity link) does it also have the same interpretation as in PA.

The population-averaged approach deals with the marginal expectation, $u_i = E(Y_i)$. The PA response is modeled as a function of covariates much like parameter estimation in cross sectional studies. Distributional assumption about the heterogeneity across subjects is not required because no explicit accounting for subject to subject heterogeneity is needed. In PA models, the focus is the marginal expectation $E(Y_i)$ and the regression coefficients have interpretation for the population rather than for any particular individual.

$$h'(u_i) = X'_i \beta' \quad [2.28]$$

and

$$Var(Y_i) = g'(u_i) * \psi \quad [2.29]$$

for some link function h' and variance function g' . Here β' has population-averaged interpretation.

As elaborated in Schabenberger and Gregoire (1996), different authors provide different definition of when a particular model is PA and when SS. Since the link function in GLIM models is usually nonlinear, the marginal distribution of Y_i can not be evaluated in closed form. As a consequence, it is often approximated by linearizing it using Taylor series expansion around some value. A source of distinction between PA and SS model here is where the expansion is made. For models with random effects, if expansion is done around $E(\alpha_i) = 0$, the coefficients can have both PA and SS interpretation depending on whether or not $\hat{\alpha}_i$ is used in prediction. If the expansion is around current estimates of the random effects ($\hat{\alpha}_i$), the coefficients have SS interpretation. For models without random effects, as noted earlier, the coefficients have only PA interpretation.

Estimation in generalized linear model setting is difficult because, unlike in the linear mixed effects case, closed form expression for the fixed effect estimate cannot be obtained since the likelihood function is intractable. Liang and Zeger (1986) introduced estimating equations approach to longitudinal non-Gaussian discrete and continuous data analysis within the frame work of generalized linear models for members of the exponential family. Their approach avoids having to specify the joint distribution of a subject's observations while accounting for correlation that arise among those observations

using an assumed working correlation whose pattern could be estimated from the data during estimation.

Zeger *et al.* (1988) further explore generalized estimating equations (GEE) approach for SS and PA model fitting. Under GEE, the population averaged effects, β' , are estimated from :

$$\sum_{i=1}^m \left(\frac{\partial E(Y_i)}{\partial \beta'} \right)' V_i^{-1} (Y_i - E(Y_i)) = 0 \quad [2.30]$$

As shown by Liang and Zeger (1986), the solution of [2.30], $\hat{\beta}'$, is consistent and given the correct specification of the mean and certain regularity conditions, it is asymptotically Gaussian. The variance of $\hat{\beta}'$ is given by:

$$V(\hat{\beta}') = \left(\sum_{i=1}^m \left(\frac{\partial \mu_i}{\partial \beta'} \right)' V_i^{-1} \frac{\partial \mu_i}{\partial \beta'} \right)^{-1} \quad [2.31]$$

and is estimated by $\hat{V}(\hat{\beta}')$ where β' is replaced with $\hat{\beta}'$. $\hat{V}(\hat{\beta}')$ is a model based variance estimate of $\hat{\beta}'$. A robust (or sandwich) variance estimator of $\hat{\beta}'$ is given by:

$$V'(\hat{\beta}') = G_b^{-1} G_h G_b^{-1} \quad [2.32]$$

where

$$G_b = \sum_{i=1}^m \left(\frac{\partial \hat{\mu}_i}{\partial \beta'} \right)' V_i \frac{\partial \hat{\mu}_i}{\partial \beta'}$$

$$G_h = \sum_{i=1}^m \left(\frac{\partial \hat{\mu}_i}{\partial \beta'} \right)' \hat{V}_i^{-1} \text{Var}(Y_i) \hat{V}_i^{-1} \frac{\partial \hat{\mu}_i}{\partial \beta'}$$

and

$$\hat{\mu}_i = E(\hat{Y}_i)$$

If $\widehat{Var}(Y_i) = \hat{V}_i$ then $V(\hat{\beta}')$ and $V'(\hat{\beta}')$ are identical.

$V'(\hat{\beta}')$ is a consistent estimate regardless whether the specification of $Var(Y_i)$ is correct.

In the GEE setting, only the link function needs to be correctly specified to make consistent inferences about PA coefficients. For SS mixed models however, both the link function and the distribution of random effects must be correctly specified for consistent inferences.

2.2.4.2 Modeling correlations

Within the mixed effects modeling framework correlations among observations can be modeled in two ways. First, if random effects are present correlation can be modeled either using the random effects Z_i , R_i or both. For models with no random effects, correlations can only be modeled in R_i . We discuss the case with models where random effects are present.

Two approaches are often taken in modeling correlation among observations. Correlation within subjects can be modeled through direct parametrization of R_i or indirectly by using random effects. Given model such as the one in [2.4], the variance of $Y_i = V_i = Z_i D Z_i' + R_i$. Since correlation among observations is partly explained by the deviation from the overall trend (Rutter and Elashoff 1994), it can be accounted for by specifying D and the matrix of random effects, Z in which case correlations are accounted for indirectly. After accounting for part of the correlation in the data due to variation from

subject to subject through the random effects (α_i), we can assume conditional independence model; *i.e.* given α_i , $Var(\epsilon) = \sigma^2 I = R_i$.

Alternatively, the within subject covariance structure R_i can be of more interest. In that case, an assumed covariance structure is specified and its parameters are estimated from the data. A common assumption is that observations from different subjects are uncorrelated. The typical assumption made is that correlation among observations within a subject decrease with distance (temporal or spatial) between observations. A covariance structure that has been found to give good results under very general condition is the continuous time auto correlation structure. This covariance structure enables modeling correlation in unbalanced and irregularly spaced data structure which poses problems when the contemporary analysis techniques are employed.

The choice between the two approaches depends on the objectives of the study. If the main interest of the study is variation between subjects, then assuming local independence is reasonable. If, however, the correlation within subjects is the primary interest, then direct specification and modeling of R_i should be given consideration. Since any data set has finite variability to be divided between the two components of variance, D and R_i , it is often impossible to model correlation using the random effects as well as R_i simultaneously.

In choosing a covariance structure in direct correlation modeling a question as to whether the correct form is specified may arise. As Rutter and Elashoff (1994) pointed out, correct specification of the covariance matrix is not crucial in linear mixed-effects modeling since a sufficient condition for consistent estimation of the fixed effect parameters is the correct specification of the mean *i.e.* the fixed effects component. Table 2.1 presents a sample of covariance structures for within subject correlation.

Table 2.1 Examples of covariance structures²available for modeling within subject correlation

Structure	Variance	Form
Simple	SIM	$\sigma^2 \begin{pmatrix} 1 & 0 & 0 & 0 \\ 0 & 1 & 0 & 0 \\ 0 & 0 & 1 & 0 \\ 0 & 0 & 0 & 1 \end{pmatrix}$
Unstructured	UN	$\begin{pmatrix} \sigma_{11}^2 & \sigma_{12}^2 & \sigma_{13}^2 & \sigma_{14}^2 \\ \sigma_{21}^2 & \sigma_{22}^2 & \sigma_{23}^2 & \sigma_{24}^2 \\ \sigma_{31}^2 & \sigma_{32}^2 & \sigma_{33}^2 & \sigma_{34}^2 \\ \sigma_{41}^2 & \sigma_{42}^2 & \sigma_{43}^2 & \sigma_{44}^2 \end{pmatrix}$
First-order autoregressive	AR(1)	$\sigma^2 \begin{pmatrix} 1 & \rho & \rho^2 & \rho^3 \\ \rho & 1 & \rho & \rho^2 \\ \rho^2 & \rho & 1 & \rho \\ \rho^3 & \rho^2 & \rho & 1 \end{pmatrix}$
Spatial	SP(POW)(c)	$\sigma^2 \begin{pmatrix} 1 & \rho^{d_{12}} & \rho^{d_{13}} & \rho^{d_{14}} \\ \rho^{d_{21}} & 1 & \rho^{d_{23}} & \rho^{d_{24}} \\ \rho^{d_{31}} & \rho^{d_{32}} & 1 & \rho^{d_{33}} \\ \rho^{d_{41}} & \rho^{d_{42}} & \rho^{d_{43}} & 1 \end{pmatrix}$

Where d_{ij} is some measure of spatial distance.

²SAS Technical Manual, Version 6.07.

2.2.4.3 Inference

Inferences about the estimated parameters depend on the model and estimation method used. In the linear mixed effects modeling framework, the properties of $\hat{\beta}$ and $\hat{\alpha}_i$ depend on whether D_i and R_i are known. If D_i and R_i are known, $\hat{\beta}$ is the best linear unbiased estimator (BLUE) of β and $\hat{\alpha}_i$ is the best linear unbiased predictor (BLUP) of α_i in terms of having the minimum mean squared error (Harville 1990). However, since D_i and R_i are generally unknown, but are respectively estimated by \hat{D}_i and \hat{R}_i instead, the properties of estimated coefficients are asymptotic. Further, the t - and F -tests no longer have the corresponding t - and F -distribution though the approximations are good (Wolfinger 1992).

With respect to nonlinear mixed-effect model [2.24], $E(Y_i) = \eta$ is nonlinear function in β and α_i , no closed form solution exist for both $\hat{\beta}$ and $\hat{\alpha}_i$. Consequently, as observed in § 2.2.4.1.2 they are usually approximated by first-order Taylor approximation around some value. The estimation technique often involve a nonlinear least-square stage (Lindstrom and Bates 1990; Vonesh and Carter 1992). Inferences, thus in general rely on asymptotic properties of the parameters and tests only hold approximately.

Under generalized mixed effects modeling framework [2.28] - [2.30], the link function in general is nonlinear and iterative methods are used to obtain parameter estimates. Whether or not invoking the normality assumption is appropriate to use ML or GEE is employed in parameter estimation, again inference is based on asymptotic properties and tests are approximate.

2.2.4.4 Model fitting criteria

Model fitting and evaluation criteria in common use in the mixed effect modeling framework are the Akaike's Information Criterion (AIC) and the Likelihood Ratio Test (LRT). Both the AIC and LRT make use of the likelihood values obtained in model fitting.

2.2.4.4.1 The AIC

The AIC is a measure of information which seeks to incorporate accuracy with parsimony (Judge *et al.* 1988) as it takes into account the number of parameters estimated in much the same spirit as the adjusted- R^2 and the C_p statistic. The AIC is calculated as:

$$\text{AIC} = -2\hat{l} + 2q \quad [2.33]$$

where \hat{l} is the log likelihood evaluated at the MLE's and q is the number of parameters estimated in the model. So, in essence AIC is a penalized likelihood; penalized by the number of estimated parameters. In the mixed effects modeling considered here, q is the number of covariance parameters estimated and the AIC is used to compare models with the same fixed effects but different covariance structures. The goal is to minimize AIC.

2.2.4.4.2 The LRT

The LRT procedure compares the maximum value of the likelihood function under the assumption that the null hypothesis (restricted) is true to the maximum value under the alternative hypothesis (unrestricted). If the restricted likelihood value is close to the unrestricted in comparison with the distribution under the null hypothesis, then the hypothesis is accepted, otherwise it is rejected.

The LRT defined as:

$$\lambda(\theta) = -2\ln\left(\frac{l(\omega)}{l(\Omega)}\right) \quad [2.33]$$

Where

$l(\omega)$ = likelihood under H_0 , and

$l(\Omega)$ = likelihood under H_1 .

$\lambda(\theta)$ is asymptotically distributed χ_r^2 where r is the number of extra parameters in the unrestricted model. The value obtained in [2.33] is compared with $\chi_{r, \alpha}^2$ where large values lead to rejection of the null hypothesis. The LRT is useful in two instances:

i) To test whether significant gain is achieved over $\sigma^2 I$, as for instance when GLM is used, by modeling covariance the hypothesis:

$$H_0: V = \sigma^2 I$$

$$H_1: V \neq \sigma^2 I$$

is tested. Rejection at the specified α -level favors modeling covariance.

ii) To compare the reduction in sum of squares in nested models :

$$H_0: \beta_2 = 0$$

$$H_1: \beta_2 \neq 0$$

Where $\beta' = [\beta'_1, \beta'_2]$

The hypothesis is rejected if $\lambda(\beta_2|\beta_1)$ exceeds $\chi^2_{r, \alpha}$ quantile where r is the number of additional parameters due to including β_2 in the model.

The behavior of the LRT test has recently been studied when non-standard conditions are encountered in hypothesis testing (Morgan *et al.* 1995; Stram and Lee 1994). When the null value of the parameter is on the boundary of the parameter space, such as when we test whether or not a variable is random, the asymptotic distribution of [2.33] can no more be considered χ^2_r (Stram and Lee 1994) but a mixture of χ^2_r and χ^2_{r-1} (Morgan *et al.* 1995). The upshot of the result is that hypothesis tests operate at a level different from the nominal level. In these situations, using approximations or semi-parametric approaches have been suggested (Stram and Lee 1994; Morgan *et al.* 1995).

2.2.4.5 Model diagnostics

Once a model is selected and fitted, it is necessary to evaluate the appropriateness of the model using diagnostic tools. In the standard regression analysis diagnostic tools are available and readily accessible (for instance Belsley *et al.* 1980). While various diagnostic tools in the same general line as the case for standard regression have also been suggested for mixed effects modeling, they are not readily accessible particularly to the novice user of available statistical software. Gregoire *et al.* (1995) extensively discuss alternative approaches and provide examples in their work. Rutter and Elashoff (1994)

also address diagnostic techniques used to detect departure from assumptions and validity of fitted models.

Parallel profile plots and residual analysis are the primary tools in determining the appropriateness of a fitted model. Analysis of residuals, studentized residuals in particular, may be used to identify outliers, influential data points and model misspecification. For models containing random effects, one has to distinguish between the fixed effect residuals $e_{ij} = Y_{ij} - X'_{ij}\hat{\beta}$ and random effects residuals $r_i = Y_i - X'_i\hat{\beta} - Z'_i\hat{\alpha}_i$. The fixed effects residuals can be used to detect departure from the assumed structure of V_{ij} ; whereas the random effects residuals are useful in detecting misspecification of the random effects (Wolfinger 1992).

In addition, while alternative approaches are available in the case where the assumption on normality does not necessarily hold via GEE and other techniques, the normality assumption is fundamental to mixed effects modeling. It is, therefore, appropriate to check if the normality assumption holds using normal probability plots of the random effects residuals as suggested in Gregoire *et al.* (1995) and others.

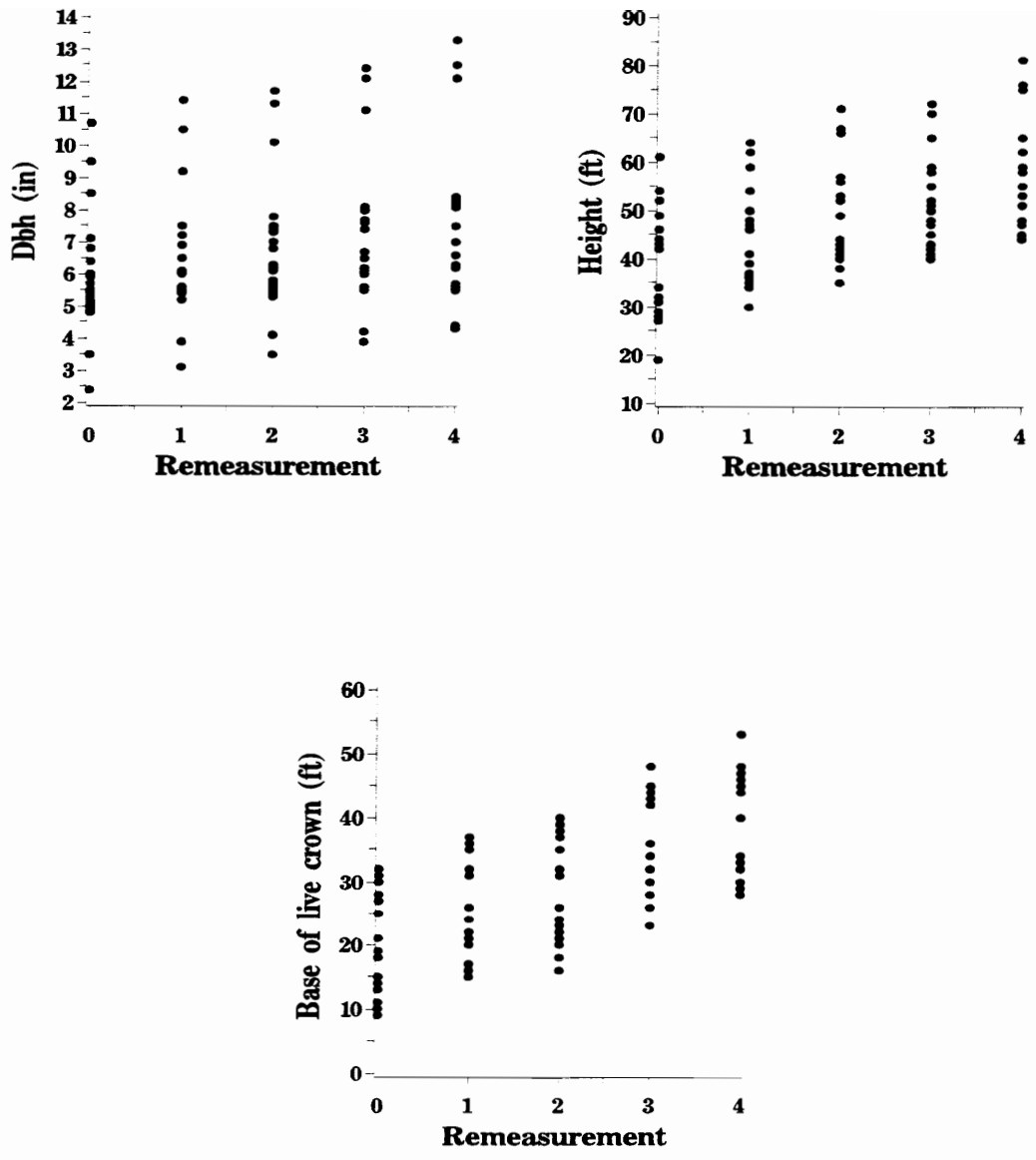


Figure 2.1: Scatter plots of DBH, total tree height and height to the base of live crown over remeasurement periods.

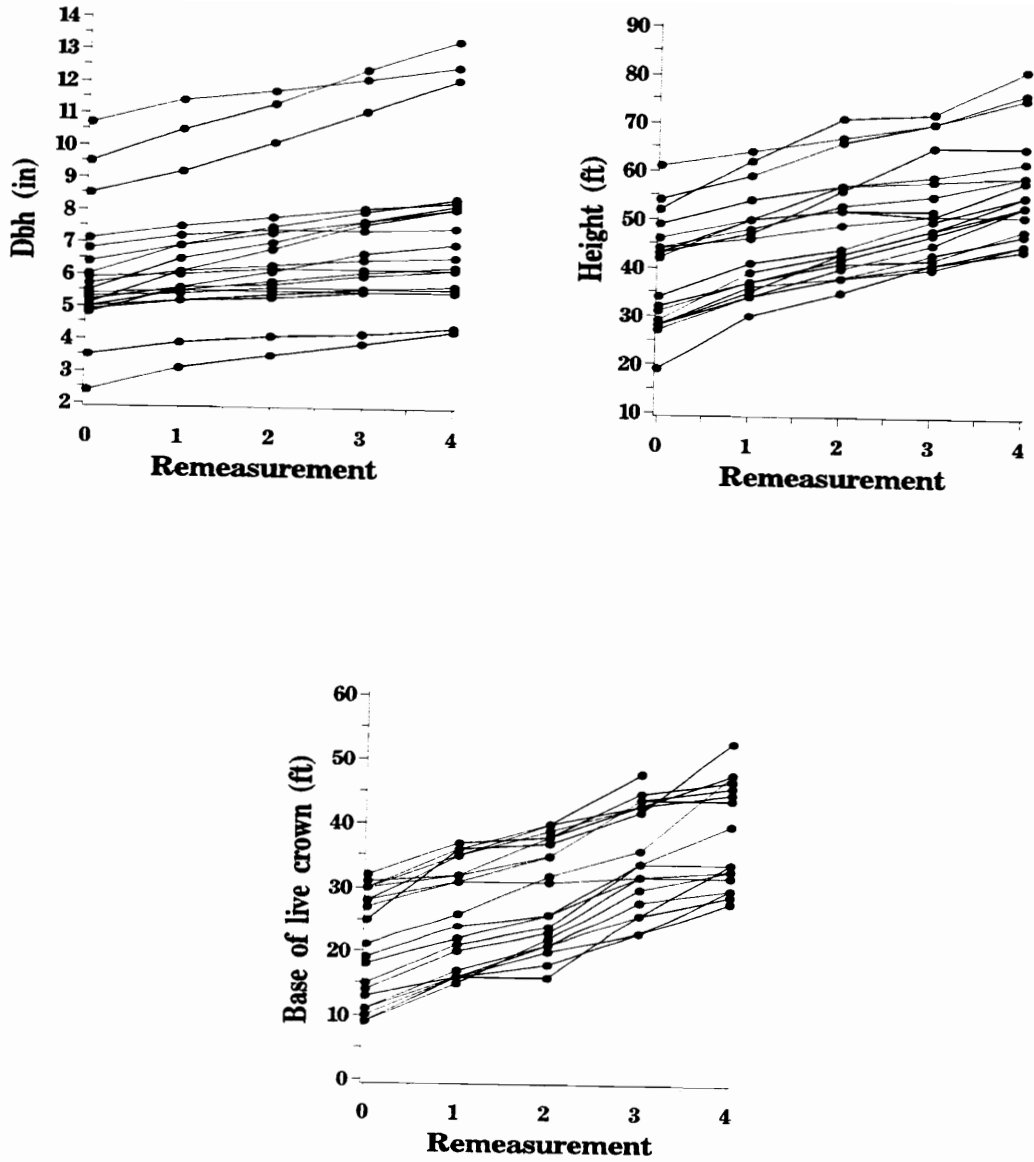


Figure 2.2: Parallel profile plots of DBH, total tree height and height to the base of live crown.

CHAPTER THREE

3.0 Materials and Methods

3.1 Data description

The data used in this study were obtained from stem analysis conducted on trees removed in a second thinning from a thinning study in loblolly pine plantations that was established on cutover site-prepared lands (Burkhart *et al.* 1985). The thinning study established in 1981-82 consisted of two thinning treatments and a control. At the time of plot establishment two levels of thinning treatment were applied. In the heavily thinned plots, approximately 50 % of the total basal area was removed, whereas in the lightly thinned plots approximately 30% of the total basal area was removed. A second thinning was applied in roughly half of the thinned plots 12 years after plot establishment.

During the second thinning, two trees were randomly selected from each plot (control, light thin and heavy thin) for stem analysis; and then the balance of the number of trees prescribed for removal were marked using regular operational procedure. In light thinned and heavy thinned plots, the actual trees randomly selected for removal were felled. In the control plots, however, trees characteristically (in DBH, total height, stem form, etc.) similar to those randomly selected were felled from trees in the buffer zone bordering the plots.

The selected trees were sectioned at 4-foot intervals from stump to a top diameter of approximately two inches. A disk approximately 1-inch in thickness was cut from the top of each section and sent to the laboratory. At the laboratory, 5 mm square radial cores for the stump, DBH, and every 4 feet thereafter to a 2-inch top were removed from each disk. Cores for the following heights: stump, DBH, 8-foot, 16-foot and every 16 feet thereafter were sent to the Weyerhaeuser Technology Center in Tacoma, Washington for x-ray scanning to obtain ring-by-ring specific gravity. In addition, all cores removed at 4 feet intervals from stump to 2 inch top diameter were image analyzed at the USDA Forest Service laboratory in Athens, Georgia to obtain ring width measurements.

A number of steps were required for the x-ray densitometry technique used to determine ring by ring specific gravity. In order to prepare each core for x-ray scanning, the sample was sawn in the grain direction to about 2 mm (plus or minus 0.025 mm) thickness throughout its length. The sample was then treated with alcohol/benzene solution to extract the pitch and phenolic colorings and then conditioned to uniform moisture content (75 degrees, 50 % relative humidity) coming from the lower moisture content direction.

The scanning was conducted with a system using customized scanning stage with a standard commercial x-ray diffractometer. The sample was scanned past a 50μ by 400μ collimated x-ray beam where the x-ray conditions are chosen to achieve maximum discrimination between the highest and lowest density to be encountered. A reference standard (calibrated step wedge) was x-rayed along with every sample. Each transmitted x-ray intensity value from the sample was converted to a specific gravity value by relating it to a sixth-order regression fit between the step wedge intensity values and the calibrated wood specific gravity values assigned to the steps. The samples were continuously measured — typically about 2.5 sample points per 0.25 mm.

The x-ray densitometry technique used a 0.500 specific gravity value to signal the end of one ring and the beginning of another. For example, scanning a core begins at the outer edge and proceeds toward the pith. The first ring measured is the latewood ring laid down by the tree the summer prior to harvest. It should have a specific gravity value above 0.500. As scanning proceeds, the specific gravity drops below 0.500 signaling the end of the latewood ring component and beginning of the earlywood ring component. A rise in specific gravity above 0.500 signals the end of the complete annual ring and the beginning of another. The actual width of latewood is obtained by multiplying the volume proportion of latewood by the total ring width. Thus, ring widths are obtained indirectly from the frequency of specific gravity measurements as the sample core is passed beneath the scanner.

The specific gravity data from each sample core were tabulated on a ring-by-ring and within-ring basis so that for each ring the following data were collected: ring width, ring average specific gravity, average earlywood specific gravity, average latewood specific gravity, weight percentage of latewood fiber and volume percentage of latewood fiber. All of the specific gravity values are expressed on an oven-dry weight, green volume basis. A total of 256 trees were sampled giving 27,571 specific gravity observations. Approximately half of the data were used in fitting models and the rest were used for model validation.

The image analysis technique is a computer controlled visual system that enables a direct measurement of growth rings as the core is passed beneath an optical scanner. The operator has visual resolution of the core and the obvious visual contrast between the dark latewood and the light earlywood signals the boundary between rings. As in the case of specific gravity, data from each sample core were tabulated on a ring-by-ring and within-ring basis so that for each ring earlywood width, latewood width and total ring width

values were available. A total of 185 trees from which 42,963 observations were obtained were used in this study. Approximately half of the observations were used for model fitting and half were used for model validation.

One of the objectives of this study was to develop a dynamic stem profile model. This requires upper stem diameter measurements along the stem as well as DBH and total tree height measurements over time. Since upper stem diameters were not measured directly during the remeasurement periods, they were generated from ring width data by cumulating ring width at each 4-foot interval. A total of 158 trees from which 25,332 measurements were used in analysis. Approximately half of the observations were used for model fitting and half used for model validation.

Besides the ring by ring data, data were available from measurements collected since plot establishment for the thinning study. These data pertain to tree conditions from which stand attributes were also generated. The measurements were conducted every three years during the dormant season. Among measurements taken were: DBH, total tree height, height to base of live crown, crown width, and other subjective measures on tree vigor and stem quality. For this study, measurements on DBH, total tree height, height to base of live crown were utilized. Crown ratio, was derived from measurements on the base of live crown height and total tree height. The stand density measures derived include: quadratic mean diameter at breast height, basal area per acre, stems per acre, relative spacing, and relative density.

Site index (for base age 25) was calculated using the Burkhardt *et al.* (1987) equation. During the development of the site index model, trees which were very young were included. To counter this and to make site index prediction more reliable, the measurement age closest to age 25 among remeasurement ages were used in the site index prediction equation. It is common to assume that site index remains constant irrespective

of silvicultural treatment (with the exception of major draining and fertilization treatments which are known to increase site quality). This basic principle was assumed to hold in this study.

The sample plots used in the analysis are spread throughout the range of loblolly pine. Due to regional variation in climate, variation in response to thinning treatment is to be expected. While no climatic data were available for the sample plot locations *per se*, rainfall and temperature data available for nearby weather stations were interpolated (Doruska 1995)³ and monthly precipitation, mean minimum temperature and mean maximum temperature for the period 1980 to 1990 were generated.

The weather data did not have measurements such as humidity and evapotranspiration to enable the use of existing climatic indices such as the Palmer draught index. Consequently, variables combining precipitation and temperature figures were generated for the growing season as follows. The March and April precipitation figures were combined to form spring precipitation; and precipitation for the months of June, July and August were combined to form summer precipitation figures. The mean maximum temperatures for the months of July and August were combined to form mean maximum summer temperature. A variable where the precipitation figures were standardized by the summer temperature were used to obtain approximate effects of climatic variables.

In order to determine thinning effects on stem form variation, one needs a measure directly associated with stem form. In this study the form exponent was used as a measure of stem form and variation in the form exponent along the stem over time was used to approximate thinning effects on stem form variation over time. A description of the method used to calculate the form exponent is presented in Appendix A3.1.

³Personal communications with Mr. P.F. Doruska, a former graduate student at VPI & SU.

Typical characteristics of the ring specific gravity and ring width data, is unbalancedness since both the number of disks vary from tree to tree and number of rings vary from disk to disk. Moreover, while measurements were planned to be taken at pre-specified fixed heights (h), difficulties in practice frequently dictated that heights from which disks are extracted to be shifted – making the data irregularly spaced. Descriptive summary statistics for the various data sets are given in the respective chapters in which they are investigated.

3.2 Methodology

As most observations used in this study are repeated measures on individuals in which measurements were taken over a period of time (the tree data) or over short distances apart (the disk data) these observations are likely to be temporally or spatially correlated. Moreover, because of the nature in which the measurements were taken (*i.e.* ordered by time or position), these data fall within the realm of longitudinal data category. Accordingly the principles of mixed-effects⁴ analysis technique, which is suitable for analyzing longitudinal data, were used in hypothesis testing and model development in the various problems investigated in the subsequent chapters .

Many of the optimality properties of mixed-effects modeling assume that the errors and the random effects parameters are normally distributed. Normal probability plots were used to ascertain whether such claim can be made for the various data sets used in this thesis. The specific gravity data showed a pattern close to normality⁵ (Figure 4.11), whereas the ring width data showed some departure, but can also be considered approximately normal (Figure 5.13). Also, given the size of data available, appeal was made to the large sample asymptotic properties. Model fitting was undertaken using the REML method in procedure MIXED (SAS 1992) for the linear models, and the NLINMIX⁶ SAS macro for the nonlinear models.

⁴ While the use of the term "mixed-effects" implies the presence of fixed effects and random effects in a model, the term is often freely used to refer to the analysis technique even if random effects are not included in the model, but correlation is directly modeled *i.e.* $Z_i = 0$. In many cases distinctions are made between the two.

⁵ Based on residuals from prediction models developed in the study.

⁶NLINMIX macro was developed by Russ Wolfinger at SAS Institute, Cary, North Carolina and is available to the public through anonymous ftp.

To provide the basis for the subsequent analysis, the data should be represented in a mathematically compact form. Accordingly,

Let:

t = tree sampled; $t= 1,2, \dots T$

h_t = number of discs on the t^{th} tree.

n_{th} = the number of rings on the h^{th} disk of the t^{th} tree.

N_t = total number of rings in the t^{th} tree; $N_t = \sum_{h=1}^{h_t} n_{th}$

N = total number of rings in the sample; $N = \sum_{t=1}^T N_t$.

Pursuant to the data analysis technique adopted in this study, a general model for expressing measurement on a particular ring is:

$$Y_{thi} = \sum_{k=1}^p \beta_{thik} X_{thik} + \sum_{m=1}^q \alpha_{thim} Z_{thim} + \epsilon_{thi} \quad [3.1]$$

where

Y_{thi} is measurement on the i^{th} ring of the h^{th} disk of the t^{th} tree.

X_{thik} is the value of k^{th} fixed effect covariate of the i^{th} ring at the h^{th} height of the t^{th} tree.

Z_{thim} is the value of k^{th} random effect covariate of the i^{th} ring at the h^{th} height of the t^{th} tree.

β_k is the fixed effects parameter; $k = 1, 2, \dots, p$.

α_m is the random effect parameter, $m = 1, 2, \dots, q$; $q \leq p$

ϵ_{thi} is the error.

In the sequel we will suppress the use of Y_{thi} , but instead use Y_t to refer to data coming from a specific tree. As usual [3.1] can be compactly and efficiently presented in a matrix form as:

$$Y_t = X_t' \beta + Z_t' \alpha_t + \epsilon_t \quad [3.2]$$

where

- Y_t is an $N_t \times 1$ vector of observations for the t^{th} tree,
- β is a $p \times 1$ vector of unknown population fixed-effect parameters,
- X_t is a known $N_t \times p$ matrix of fixed effect covariates,
- α_t is a $q \times 1$ vector of unknown and unobservable random-effect parameters,
- Z_t a known $N_t \times q$ matrix of random effect covariates.
- ϵ_t is an $N_t \times 1$ vector of random unobservable errors.

It is assumed that the α_t and ϵ_t are normally distributed, and thus :

$$\begin{aligned} \alpha_t &\sim N(0_q, D) & \text{and} & \quad \text{Cov}(\alpha_t, \epsilon_t) = \mathbf{0} \text{ (a } q \times N_t \text{ null matrix).} \\ \epsilon_t &\sim N(0_{N_t}, R_t) \end{aligned}$$

Where 0_q and 0_{N_t} are the null vectors of orders q and N_t , respectively; and D is a $q \times q$ covariance matrix of the random effects, and R_t is an $N_t \times N_t$ covariance matrix of the errors. And consequently as observed in § 2.2.4.1.1,

$$E(Y_t) = X_t' \beta \quad [3.3]$$

$$Var(Y_t) = V_t \quad [3.4]$$

where $V_t = Z_t D Z_t' + R_t$

In the various modeling works undertaken, the objectives of this study was to estimate β , α_t and to make inferences about them. Since V_t is unknown, elements of its components were estimated using the Newton-Raphson algorithm in SAS, and \hat{V}_t was used. Consequently,

$$\hat{\beta} = \left(\sum_{i=1}^m X_i' \hat{W}_i X_i \right)^{-1} \sum_{i=1}^m X_i' \hat{W}_i Y_i \quad [3.5]$$

and

$$\hat{\alpha}_t = \hat{D} Z_t' \hat{W}_t (Y_t - X_t' \hat{\beta}) \quad [3.6]$$

Where $W = V_t^{-1}$.

The variances of $\hat{\beta}$ and $\hat{\alpha}_t$ are as discussed in §2.4.1.1.

In some cases, especially when correlation is directly modeled, an understanding of the structure of within tree covariance (R_t) is important. As the structure depends on the ϵ_{thi} , a full distribution of the errors is necessary. To do so, one has to examine the method in which the data were collected.

Since the nature of correlation (temporal) in the tree data (DBH, total height, etc.) is straightforward, here we focus on the disk data. The ring measurements are observations collected on an individual at several locations *within* a tree because several disks were removed from a tree and ring by ring observations were recorded.

Alternatively, one can consider the observations as if measurements were taken during several visits to the tree from the time it was a mere seedling to the time it was felled for the study. Consequently, it is reasonable to assume that the ring measurements are spatially and/ or temporally correlated.

It is further assumed that the correlation is patterned due to tree physiology and the sampling method. To accommodate this assumption, the following correlation structure is provisionally specified. We assume the errors (ϵ_{thi}) in [3.1] have the following properties:

$$E(\epsilon_{thi}) = 0. \quad [3.7]$$

$$Var(\epsilon_{thi}) = \sigma^2; \forall t, h, i. \quad [3.8]$$

$$Cov(\epsilon_{thi}, \epsilon_{t'h'i}) = 0 \text{ for } t \neq t'. \quad [3.9]$$

$$Cov(\epsilon_{thi}, \epsilon_{th'i}) = \sigma^2 \xi_{th}; \text{ for } h \neq h'. \quad [3.10]$$

$$Cov(\epsilon_{thi}, \epsilon_{th'i'}) = \sigma^2 \xi_{ti}; \text{ for } i \neq i'. \quad [3.11]$$

$$Cov(\epsilon_{thi}, \epsilon_{th'i'}) = 0 \text{ for } h \neq h', i \neq i'.^7 \quad [3.12]$$

Where the ξ_{th} , ξ_{ti} are correlation structures that will be specified subsequently to depict correlation among observations sharing common subjects. For instance, it is reasonable to posit the continuous time/space autoregressive structure for $\xi_{(.)}$ such that $\xi_{th} = \exp(-|\frac{\delta_{th}}{\alpha_{th}}|)$; and $\xi_{ti} = \exp(-|\frac{\delta_{ti}}{\alpha_{ti}}|)$; where $\delta_{(.)}$ is some measure of spatial or temporal distance. Specifically, $\delta_{th} = |h - h'|$ and $\delta_{ti} = |A_p - A'_p|$ where h is height above ground to the point of measurement and A_p is ring physiological age. Alternatively, to model correlation among growth rings at one point, one might posit a first order

⁷ Following Gregoire *et al.* (1995) for different rings at different height, one might conceivably posit $Cov(\epsilon_{thi}, \epsilon_{th'i'}) = \sigma^2 (\xi_{th})(\xi_{ti})$ for $h \neq h', i \neq i'$ which would obviously add complexity to the covariance structure, but may not be supported by the data.

autoregressive structure in which case for instance $\xi_{ti} = \rho^{|\delta_{ti}|}$; where $\rho = \exp(-\frac{1}{\alpha_{ti}})$, $\alpha_{ti} > 0$, is correlation between two measurements.

In the specification put forth in [3.8]-[3.12], ring measurements on different trees are uncorrelated; ring measurements on rings deposited in subsequent years at a specific height are correlated possibly with correlation diminishing as the age difference between rings increase; ring measurements on a particular ring taken at different heights are correlated with correlation also likely diminishing with distance between disk heights. Finally, ring measurements taken on rings of different years at different height are uncorrelated.

As a consequence of [3.8]- [3.12], the $(N_t \times N_t)$ matrix R_t of ϵ_t (assumed to be symmetric), for the t^{th} tree assuming data within a tree are first sorted by disk and then by ring, has the form:

$$R_t = \sigma^2 \begin{pmatrix} \begin{pmatrix} 1 & \xi_{t1} & \dots & \xi_{t1} \\ & 1 & \dots & \vdots \\ & & \ddots & \xi_{t1} \\ & & & 1 \end{pmatrix} & \begin{pmatrix} \xi_{t1} & 0 & \dots & 0 \\ & \xi_{t1} & \dots & \vdots \\ & & \ddots & 0 \\ & & & \xi_{t1} \end{pmatrix} & \dots & \begin{pmatrix} \xi_{t1} & 0 & \dots & 0 \\ & \xi_{t1} & \dots & \vdots \\ & & \ddots & 0 \\ & & & \xi_{t1} \end{pmatrix} \\ \begin{pmatrix} 1 & \xi_{t1} & \dots & \xi_{t1} \\ & 1 & \dots & \vdots \\ & & \ddots & \xi_{t1} \\ & & & 1 \end{pmatrix} & \begin{pmatrix} \xi_{t1} & 0 & \dots & 0 \\ & \xi_{t1} & \dots & \vdots \\ & & \ddots & 0 \\ & & & \xi_{t1} \end{pmatrix} & \dots & \begin{pmatrix} \xi_{t1} & 0 & \dots & 0 \\ & \xi_{t1} & \dots & \vdots \\ & & \ddots & 0 \\ & & & \xi_{t1} \end{pmatrix} \\ \dots & \dots & \dots & \dots \\ \begin{pmatrix} 1 & \xi_{t1} & \dots & \xi_{t1} \\ & 1 & \dots & \vdots \\ & & \ddots & \xi_{t1} \\ & & & 1 \end{pmatrix} & \dots & \dots & \begin{pmatrix} 1 & \xi_{t1} & \dots & \xi_{t1} \\ & 1 & \dots & \vdots \\ & & \ddots & \xi_{t1} \\ & & & 1 \end{pmatrix} \end{pmatrix} \quad [3.13]$$

$N_t \times N_t$

The diagonal matrices of R_t are $n_{th} \times n_{th}$, i.e. the number of rings per disk with up to h_t matrices. From the off-diagonal elements of the matrices on the diagonal of R_t

one obtains correlation between different rings at a common height (ξ_{ti}). The diagonal elements of the off-diagonal matrices of R_t provide correlation among measurements on one-year growth rings measured at different heights (*i.e.* the ξ_{th}). Because of the stipulation in [3.12], the off-diagonal elements of the matrices in the off-diagonal matrices of R_t are all zeros.

An alternative to [3.13] is to consider sorting⁸ observations first by ring then by height. In this setting, tree rings are considered the *primary* units on which several measurements were taken. Disk heights now assume secondary importance as fixed locations at which ring measurements were taken for practical convenience. Now R_t assumes the form:

$$R_t = \sigma^2 \begin{pmatrix} \begin{pmatrix} 1 & \xi_{th} & \dots & \xi_{th} \\ & 1 & \dots & \vdots \\ & & \ddots & \xi_{th} \\ & & & 1 \end{pmatrix} & \begin{pmatrix} \xi_{ti} & 0 & \dots & 0 \\ & \xi_{ti} & \dots & \vdots \\ & & \ddots & 0 \\ & & & \xi_{ti} \end{pmatrix} & \dots & \begin{pmatrix} \xi_{ti} & 0 & \dots & 0 \\ & \xi_{ti} & \dots & \vdots \\ & & \ddots & 0 \\ & & & \xi_{ti} \end{pmatrix} \\ \vdots & \begin{pmatrix} 1 & \xi_{th} & \dots & \xi_{th} \\ & 1 & \dots & \vdots \\ & & \ddots & \xi_{th} \\ & & & 1 \end{pmatrix} & \dots & \begin{pmatrix} \xi_{ti} & 0 & \dots & 0 \\ & \xi_{ti} & \dots & \vdots \\ & & \ddots & 0 \\ & & & \xi_{ti} \end{pmatrix} \\ \vdots & \vdots & \ddots & \vdots \\ \vdots & \vdots & \vdots & \begin{pmatrix} 1 & \xi_{th} & \dots & \xi_{th} \\ & 1 & \dots & \vdots \\ & & \ddots & \xi_{th} \\ & & & 1 \end{pmatrix} \end{pmatrix} \quad [3.14]$$

$N_t \times N_t$

Here the matrices on the diagonal of R_t have dimensions $h_{ti} \times h_{ti}$ (*i.e.* number disks spanned by successive growth rings) with a total of up to $max(n_{th})$ sub-matrices. In this setting, the off-diagonal elements of the diagonal matrices in R_t yield correlation

⁸ This is just for illustration. In practice sorting is not necessary to use the correlation structure described here because the location of a measurement is tied to the height and ring number. *i.e.* its (x, y) coordinate is known.

among measurements conducted at different height in one-year growth rings (ξ_{th}). The diagonal elements of the off-diagonal matrices give correlation among growth rings at common height (ξ_{ti}); again due to [3.12] the off-diagonal elements are zeroes. Thus, [3.14] essentially reverses the correlation pattern stipulated in [3.13]. Because the structure in [3.13] and [3.14] are mutually exclusive, the choice between them is based on some measure of fit.

3.2.1 Accounting for correlation

Accounting for correlations among observations was undertaken both by direct covariance modeling and including random effects, the AIC values dictating selection between the two approaches. Specifying both Z_t and R_t was not possible in almost all cases considered in this thesis because the various data sets did not support combination mixed models.

In many instances, it was found more appropriate to model the correlation directly in R_t rather than including random effect covariates. In these situations, covariance structures that depict patterns in which correlations decrease with distance (temporal or spatial) between observations were generally preferred. Particularly patterns which show the AR(1) covariance structure and the continuous time/space autoregressive structure were commonly employed.

The continuous time/space autoregressive structure is often preferred because it is less restrictive as to the number of measurements in different subjects (balance) and the timing and/or position of measurements (spacing) (Diggle 1988). Because of the nature of the data, whenever possible the continuous time autoregressive structure was selected. However, sometimes numerical difficulties caused problems in parameter estimation with

this structure. In such cases the AR(1), which yields similar results in general and practically identical results if observations are equally spaced, was used.

When the mixed model approach was used to account for correlations indirectly, an iterative procedure was employed first starting with all effects random and dropping variables one at a time as the fitting procedure tended to fail due to over parametrization. In some cases an effect (usually fixed) which was significant at one stage turned insignificant at a later stage; in such cases, the effect was dropped from the model and parameters were re-estimated.

3.2.2 Tests on thinning effects – design considerations

In testing thinning effects on the various attributes of the loblolly pine trees, it was necessary to appreciate the design in which the data were collected to make correct inferences. The thinning study plots are unequally distributed into three broad physiographic regions: Coastal Plain, Piedmont and “Others” also referred to as “Highlands”. Furthermore, since several measurements were taken per tree, the thinning study design can be considered a generalized randomized (incomplete) block design (GRIBD) with sub-sampling where the blocking factor is physiographic region. The sub-sampling part was important to note in order to avoid inflating the degrees of freedom in hypothesis testing as the sub-samples do not contribute to the error degree of freedom for testing thinning effects. Consequently, the degrees of freedom for error were adjusted accordingly in all hypothesis tests⁹.

⁹ As the data used in this study are large (at least 158 trees), the problem of inflating the degrees of freedom for error is not crucial in practice: it is important in theory nonetheless.

In their studies on yield level variation, Hasenauer *et al.* (1994) found variation in various tree and stand attributes between plantations in the Gulf Coastal Plain and the Atlantic Coastal Plain. To determine if such variation is also evident in the issues investigated in this study, the Coastal Plain was further subdivided into Atlantic Coastal Plain and Gulf Coastal Plain, and tests were conducted to determine if the Coastal Plain should be separated.

In the various test results presented p-values associated with region effects are not reported because physiographic region is considered a blocking factor. From the design point of view, blocking is conducted to reduce experimental error based on an *a priori* knowledge or belief that the experimental materials to which treatments are applied differ across the blocking factor. This indeed enables the researcher to make stronger statement about treatment effects than would be the case with a completely randomized design, say.

Unfortunately, fixed block effects are not testable. The reason is that since there is no randomization involved in assigning blocks to treatments, tests on block effects cannot be approximated by the usual F-test (Hinkelmann and Kempthorne 1994) hence it is not appropriate to attach significance to the p-values obtained in statistical analysis outputs.

An approach that is sometimes taken is, to think of physiographic regions as randomly selected among all possible physiographic regions and assigned the different thinning treatments. In this case, approximate Z-test (Wald test) is available to test block factor as a variance component within the mixed effects modeling framework. However, knowing that the thinning study covered the entire range of loblolly pine which has a limited number of physiographic regions, regarding the regions as having been randomly selected from a population of physiographic regions is inappropriate; consequently, blocks are considered fixed and p-values for block effects are not reported.

In some cases it was necessary to determine if the physiographic regions can all be considered separate or if some could be combined for the particular issue being addressed; for instance, to determine if separate prediction models are required in different regions. To address this point dummy variable regressions were undertaken. Dummy variable regression is equivalent to analysis of variance with an appropriate constraint (Myers 1990) and provides a useful tool especially if further analysis, such as model fitting, is to be conducted.

As the first thinning was applied in 1981-82 and the ring by ring data were collected during 1993-94, only the rings deposited since are affected by thinning treatment. All thinning effects were thus evaluated for measurements on the outer 12 growth rings.

3.2.3 Model selection and validation criteria

The AIC and the LRT results guided model selection. In this thesis, the AIC was calculated as:

$$AIC^{10} = L - q \quad [3.15]$$

where L is the log likelihood evaluated at the MLE's and q is the number of covariance parameters estimated in the model. The goal is to maximize AIC. The AIC was used to discriminate among models having the same fixed effects, but different covariance structures.

¹⁰ This is the definition used by SAS. Classical definition of AIC is $-2L + 2q$, where the goal is to minimize AIC rather than maximize it (See also § 2.2.4.4.1).

The LRT was used in the study to test whether significant gain is achieved by modeling covariance structure compared to using the default (*i.e.* $\sigma^2 \mathbf{I}$). The p-values from the LRT were used to get a general indication of the gain obtained over GLM as the test is generally considered too liberal.

It was also found useful to make comparison among models also on a more familiar scale by comparing values of statistics similar to those available in conventional analyses. One criterion that was used to evaluate models was an R^2 like statistic commonly used in model validation, R_p^2 (sometimes called the Fit Index), computed as :

$$R_p^2 = 1 - \frac{\sum_{t=1}^{T_V} \sum_{h=1}^{h_t} \sum_{i=1}^{r_{ht}} (Y_{thi} - \hat{Y}_{thi})^2}{\sum_{t=1}^{T_V} \sum_{h=1}^{h_t} \sum_{i=1}^{r_{ht}} (Y_{thi} - \bar{Y})^2} \quad [3.16]$$

where

R_p^2 proportion of variation predicted by the model.

\bar{Y} is overall mean.

\hat{Y}_{thi} is predicted value.

T_V is the number of trees in the validation data set.

Models with large R_p^2 values are preferred.

Other quantities considered were the estimated standard error (S E E), the mean

bias (MB) and mean squared error¹¹ (MSE). Where:

¹¹ This value is the mean of squared difference between the predicted and actual (bias), but technically it is Mean Squared Error (MSE) as it is the expected value of the squared difference of an estimate from its expected value: *i.e.* $E(\hat{\theta} - \theta)^2$, where $\hat{\theta}$ is an estimate of θ . The MSE referred to here should not be confused with the "MSE" from regression outputs because the former is based on validation data and the difference in the divisor *i.e.* N versus $N - p$.

$$SEE = \sqrt{\frac{\sum_{t=1}^{T_f} \sum_{h=1}^{h_t} \sum_{i=1}^{r_{th}} (Y_{thi} - \hat{Y}_{thi})^2}{N_f - p}} \quad [3.17]$$

$$MB = \frac{\sum_{t=1}^{T_v} \sum_{h=1}^{h_t} \sum_{i=1}^{r_{th}} (\hat{Y}_{thi} - Y_{thi})}{N_v} \quad [3.18]$$

$$MSE = \frac{\sum_{t=1}^{T_v} \sum_{h=1}^{h_t} \sum_{i=1}^{r_{th}} (\hat{Y}_{thi} - Y_{thi})^2}{N_v} \quad [3.19]$$

N_f and N_v are the numbers of observations in the fitting data set and validation data set, respectively; p is the number of fixed effects parameters in the model; T_f is the number of trees in the fitting data set. Models with small SEE , MB and MSE are preferred. Whenever appropriate, double cross validation was used by exchanging the roles of the fitting and validation data.

CHAPTER FOUR

4.0 Thinning effects on ring specific gravity and ring specific gravity prediction model

4.1 Introduction and literature review

4.1.1 Introduction

As forest management becomes more and more intensive, the demand for management information on the quality of wood expected to be produced given a set of silvicultural prescriptions is increasing. In particular, it is necessary to quantify effects of silvicultural treatments such as thinning so that they can be appropriately accounted for and incorporated into growth simulators. Since the value of a piece of wood depends on the end product for which it is used, a variety of attributes may be used to assess quality.

Many wood quality factors are directly related to specific gravity. The strength, stiffness and pulp yield per unit volume tend to increase with specific gravity. Thus, specific gravity of a wood is its single most important indicator of quality (Haygreen Bowyer 1996). Wood specific gravity is an extensively studied subject, but most studies tended to focus on a single aspect of the issues and seldom had the scope to

Chapter four: Thinning effects on ring specific gravity and ring specific gravity prediction model

simultaneously evaluate more than one of the many sources of variation. As a result, conclusions drawn from studies sometimes tend to be contradictory. This study aims at addressing thinning effects on wood quality by evaluating its effects on the specific gravity of loblolly pine trees along the stem over time by accounting for some of the sources of variation.

Also, a specific gravity prediction model which seeks to effectively predict tree ring specific gravity based on tree, stand and other factors was developed. The ring specific gravity prediction model developed in this study, with the ring width prediction model also developed, establishes the missing link in growth simulators to provide users with additional power to make informed management decisions.

4.1.2 Literature review

Wood specific gravity is the best single wood quality indicator without considering specific end uses (Olson and Arganbright 1977). Specific gravity shows considerable variation within a single tree and among trees within a species (Choong *et al.* 1989), and consequently has been the topic of numerous research studies.

Studies on ring specific gravity may be divided into those concerned with assessing treatment effects and those concerned with predicting average tree specific gravity. Some investigators (Heger 1974; Lenhart *et al.* 1977; Talbert and Jett 1981) attempted to model specific gravity using a set of predictor variables mostly functions of relative height and age. Walker (1981) used a specific gravity prediction model developed by Bethel in 1940 in his studies on effects of management on dry weight production in loblolly pine plantations. Burkhart and Beckwith (1970) used a combination of age and diameter at breast height to predict average specific gravity of a tree. Larocque and Marshall (1995)

Chapter four: Thinning effects on ring specific gravity and ring specific gravity prediction model

developed a ring specific gravity model for red pine (*Pinus resinosa* Ait.) using ring physiological age and proportion of latewood. Most studies on specific gravity are descriptive, however, generally aimed at either describing vertical and radial variation of specific gravity or specific gravity variations due to cultural treatments.

Effects of silvicultural treatments, particularly thinning, on wood specific gravity generated much interest in the field. A crucial issue is the effect of the rate of growth on specific gravity. It is common knowledge that certain cultural practices, notably thinning and fertilization, increase the rate of diameter growth so that more useful products are obtained within relatively short period of time. It has been a concern to the scientist whether the gain in shortened rotation comes at the expense of wood quality or its best indicator specific gravity (Bendtsen 1978; Szymanski and Tauer 1991 and others). The concern mostly emanated from the similarity between the growth rate of juvenile wood, which inherently has low specific gravity and the rapid rate of growth following fertilization or thinning.

While investigators seem in general agreement that juvenile wood has a tendency to have a lower specific gravity than mature wood (Paul 1957; Bendtsen 1978 ; Talbert and Jett 1981), many researchers failed to see similar correlation between fast growth and low specific gravity (Burton and Shoulders 1974; Cregg *et al.* 1988; Bendtsen 1978; Taylor and Burton 1982; Larocque and Marshall 1995) in the loblolly pine and red pine trees they studied.

For instance, results of investigations conducted to determine thinning effects on specific gravity are not consistent. Some researchers (Erickson and Lambert 1958; Shepard and Shottafer 1990) reported that specific gravity decreased following thinning, for Douglas-fir and black spruce (*Picea mariana* (Mill.) B.S.P.), respectively; whereas others (Burton and Shoulders 1974; Taylor and Burton 1982; Barbour *et al.* 1992) found

Chapter four: Thinning effects on ring specific gravity and ring specific gravity prediction model

that specific gravity is unaffected by thinning for loblolly pine and red spruce trees. Yet others (Paul 1957; Jackson 1968; Choong *et al.* 1989), reported that thinning increased specific gravity in red pine, loblolly pine and slash pine (*Pinus elliotii* Engelm.) trees.

According to Megraw (1985) cultural treatments can have an impact on resulting wood properties because of the induced changes to the vigor and size of crown. In particular, he suggested that by slowing down crown recession and prolonging formation of lower density juvenile wood in the lower bole, thinning under normal circumstances has a tendency to reduce wood specific gravity. On the other hand if moisture is a limiting factor towards the end of the growing season, thinning may tend to increase in specific gravity by extending latewood growth.

Species variation, genetic variation, climatic factors, measurement techniques, and sampling techniques all appear to contribute to the seemingly contradictory results. Wiemann and Williamson (1989) studied radial gradients in the specific gravity of various tropical and temperate species. They found considerable variation particularly between tropical and temperate species. Barbour *et al.* (1992), for instance, report that in red spruce (*Picea rubens*) specific gravity decreases with distance from the pith, whereas for many pine species, notably loblolly pine, specific gravity increases with distance from the pith (Haygreen and Bowyer 1996); which indicates that some patterns are not universal. In a review of the literature on wood in intensively managed trees, Bendtsen (1978) also indicates findings on cultural effects reported by researchers tended to vary from species to species.

Some of the inconsistencies among different research reports probably are attributable to measurement techniques employed. The degree of precision of actual measurements can differ among research studies depending on the precision of equipment used. More importantly, however, some investigators used specific gravity of relatively

Chapter four: Thinning effects on ring specific gravity and ring specific gravity prediction model

large portions of tree stems, usually disks (Erickson and Lambert 1958; Lenhart *et al.* 1977; Shepard and Shottafer 1990) whereas others (Shepard and Shottafer 1992; Wiemann and Williamson 1989; Ezell and Schilling 1980; Petty *et al.* 1990; Larocque and Marshall 1995) either determined ring by ring specific gravity or specific gravity of groups of rings in a disk.

Variation in the sampling design of rings and disks is also evident. Many researchers that set out to determine the effects of cultural treatments on specific gravity often examined single samples taken at or in the general vicinity of breast height (Smith 1980; Cregg *et al.* 1988; Wiemann and Williamson 1989; Szymanski and Tauer 1991; Larocque and Marshall 1995) others (Jackson 1968; Lenhart *et al.* 1977; Ezell and Schilling 1980; Petty *et al.* 1990; Shepard and Shottafer 1992) used samples taken from several locations along the stem. The latter being generally those interested in the vertical variation of specific gravity. Since specific gravity varies by height and physiological age in some species, notably loblolly pine, one needs care in interpreting results from single point samples.

Many investigations have shown that wood specific gravity is not uniform, but shows both longitudinal and radial variation. Specific gravity decreases with increasing height (Lenhart *et al.* 1977; Bendtsen 1978) and increases with distance from the pith (Paul 1957; Clark and Saucier 1989). Ezell and Schilling (1980) reported inconsistencies in both longitudinal and radial variation among sweetgum (*Liquidambar styraciflua* L.) trees they studied perhaps due to species variation.

Because age also is known to be positively correlated with specific gravity, it seems that part of the inconsistencies reported on the effects of cultural treatments on wood specific gravity is a result of confounding between age and cultural treatments.

Larocque and Marshall (1995) presented results on specific gravity development of red

Chapter four: Thinning effects on ring specific gravity and ring specific gravity prediction model

pine stands as affected by different initial spacings based on ring specific gravity samples taken at breast height. They concluded that relative density of whole rings and proportion of early or latewood did not differ with spacing in young stands, but did so as stands grew older and competition increased, apparently confirming the age-treatment confounding that often make conclusions drawn from specific gravity studies sometimes contradictory.

Studies also confirm that trees show variations in specific gravity due to climatic and regional variations (Cregg *et al.* 1988; Clark and Saucier 1989; Wiemann and Williamson 1989). Loblolly pine, for instance reportedly shows regional variation in specific gravity. Talbert and Jett (1981) reported a general northward decrease in specific gravity; similarly, Szymanski and Tauer (1991), in a provenance trial conducted in Arkansas, found the highest specific gravity reading at breast height in trees from a seed source from the northwestern part of loblolly pine's range. These regional variations may largely be due to different climatic conditions prevailing in these regions.

4.2 Data and methods

4.2.1 Data

The specific gravity data used in this study was fully described in Chapter 3. Tables 4.1 and 4.2 present a summary of the tree and disk data utilized for model fitting and validation. Patterns in average specific gravity for selected trees are presented graphically. Figure 4.1 shows parallel profile plots of ring specific gravity by height and by physiological age for a particular tree. Figures 4.2 - 4.4 depict three-dimensional views of ring specific gravity, earlywood specific gravity and latewood specific gravity, respectively, for the same tree. Average ring specific gravity by height and physiological age is shown in Figure 4.5a , 4.5b, respectively.

Table 4.1 : Tree summary statistics for ring specific gravity prediction model fitting and validation data.¹²

Variable	n	mean	CV	Minimum	Maximum
<u>Fitting</u>					
DBH (in)	128	8.5	23.1	4.3	14.0
BLC (ft)	128	36.7	21.0	17.7	55.8
H (ft)	128	59.4	14.4	38.6	85.0
<u>Validation</u>					
DBH (in)	128	8.6	23.1	4.5	14.0
BLC (ft)	128	36.3	21.1	19.0	61.3
H (ft)	128	59.6	14.5	33.8	87.9

¹² See § 1.3 “variable definition and notation” for definition of symbols in Tables.

Table 4.2 : Ring summary statistics for specific gravity prediction model fitting and validation data.

Variable	n	Mean	CV	Minimum	Maximum
<u>Fitting</u>					
RS	13958	0.455	17.2	0.252	0.760
ES	13958	0.339	12.2	0.000	0.642
LS	13958	0.637	22.3	0.000	0.861
<u>Validation</u>					
RS	13613	0.451	17.0	0.252	0.763
ES	13613	0.339	11.9	0.000	0.600
LS	13613	0.636	22.2	0.000	0.842

4. 2.2 Methods

To describe the specific gravity of a particular tree, a model of the form described in [3.2] was used. Thus the the specific gravity data may be represented by:

$$Y_t = X'_t\beta + Z'_t\alpha_t + \epsilon_t \quad [4.1]$$

where

Y_t is a vectors of specific gravity observations for the t^{th} tree, and other variables are as defined in § 3.2.

The distributional properties of the random variables in [4.1] are as described in §3.2. The error terms are assumed to be normally distributed with the covariance matrix stipulated in [3.8]-[3.12].

To investigate thinning effects on specific gravity and for specific gravity prediction models, various linear and nonlinear models were considered (see Appendix

A4.1). Correlation among observations were accounted for by either specifying random effects covariates, but mostly through direct covariance modeling. Modeling both D and R simultaneously was also considered though generally unsuccessful.

4.3 Results and analyses

4.3.1 Covariance structure

Modeling both D and R was not supported by the available data. Thus, a choice had to be made between specifying random effect covariates and direct covariance modeling. Comparing the performance of models in which random effects were specified with the ones in which correlation was directly modeled, the latter consistently exhibited superior performance when compared using AIC.

For the specific gravity data, the continuous time autoregressive structure specified in [3.8] - [3.12] as detailed in [3.13] and [3.14], implies the use of a structure with spatial pattern. While the continuous time autoregressive structure is ideal for the data at hand, alternative specifications were also considered. Based on the AIC, many of the alternative covariance structures specified showed poorer but comparable performance.

As observed earlier, because the specifications in [3.13] and [3.14] weigh correlation among observations in a tree (the ξ_{ti} and ξ_{th}) differently, choosing between them was necessary. Moreover, due to numerical constraints, the parameters in the diagonals of the off-diagonal matrices of R_t in both [3.13] and [3.14] could not be estimated. Consequently, the structure of R_t had to be modified to make it block diagonal *i.e.* the covariance specifications in § 3.2 had to be modified either to $Cov(\epsilon_{thi}, \epsilon_{th'i}) = 0$ or $Cov(\epsilon_{thi}, \epsilon_{th'i'}) = 0$; because correlation between observations on successive rings and observations within a one year ring could not be modeled simultaneously¹³.

¹³ This has to do with how the repeated option in the MIXED SAS procedure works.

The choice was whether the correlation between observations on rings in a disk (ξ_{ti}) or that between observations on rings of the same year (ξ_{th}) is more important. Based on AIC, it was consistently observed that models in which [3.13] was stipulated performed better than those in which [3.14] was used. That is correlation among observations in a disk tended to be higher than those between observations on rings of the same year. Considering that disks are spaced farther apart along the stem than annual rings are within a disk, this is not unreasonable outcome.

Thus, model [4.1] was modified to:

$$Y_t = X_t' \beta + \epsilon_t \quad [4.2]$$

Where,

$$\epsilon_t \sim N(0, R_t)$$

$$Y_t \sim N(X_t' \beta, R_t)$$

$$R_t = BD \left(\sigma^2 \exp\left(-\left|\frac{\delta_{ti}}{\alpha_{ti}}\right|\right) \right)$$

BD = block diagonal matrix and other symbols are as defined in § 4.2.2.

The specification [4.2] is a special case of [4.1] where $Z_t = 0$. The structure is simpler than that originally specified in [3.8]-[3.12], but it is different from the usual general linear model as it does take correlation among observations into account; hence it meets one of the objectives of the study. Empirical evaluation using covariance structure where all parameters are estimated, though unreasonable, showed that this form is quite adequate.

The LRT test comparing this structure with the default ($V = \sigma^2 I$) also showed substantial improvement ($p < 0.0001$) in maximizing the likelihood function. Accordingly, all subsequent works in this study follow models fitted and tests conducted under the error structure stipulated in [4.2].

4.3.2 Thinning effects on ring specific gravity

The results of thinning effects on ring specific gravity under the model specified in [4.2] are presented for the entire specific gravity data (12 outer rings) adjusted for the degrees of freedom as outlined in §3.2.2 (Table 4.3).

Table 4.3: A test of thinning effects on ring specific gravity for all data combined

Source	NDF	DDF	Typ III F	Pr > F
Region	2	247	68.49	*** ¹⁾
Thinning	2	247	1.47	0.2464
Region* Thinning	4	247	2.84	0.0250

¹⁾ p – values for region are not reported (see § 3.2.2).

The test results indicate that thinning does not affect specific gravity of loblolly pine trees significantly ($\alpha = 0.05$)¹⁴. The thinning by region interaction result, however, shows that thinning effects vary by physiographic region. Because thinning effect on ring

¹⁴ In this study all tests with $p < 0.05$ are considered significant.

width varies by height (Larson 1963; Myers 1963 and others), it was conjectured that thinning effects on specific gravity may have a similar trend and the hypothesis of no thinning treatment effect was tested at the various heights from which samples were taken. The results are displayed in Table 4.4.

Table 4.4: Tests of thinning effects on specific gravity by selected heights.

Height (ft)	Region	Thinning	Thinning*Region
0.5	***	0.5793 ¹⁾	0.0718
4.5		0.1819	0.3145
8.5		0.4442	0.0798
16.5		0.6413	0.3492
32.5		0.7458	0.1803
48.5		0.3541	0.2396

¹⁾ The numbers in the table are *p*-values

The results show that thinning effects are still not significant when different heights are considered. Moreover, there is no significant thinning by region interaction indicating that thinning treatments perform similarly at the various heights in the different physiographic regions.

In each of the above cases, the data for the 12 years were pooled either entirely or at the height level. It has been suggested (see for instance Liu *et al.* 1995) that thinning responses are not immediate, but that a period of time elapses before thinning response is evident and a maximum is achieved from where on response diminishes until eventually the pre-treatment level is achieved.

If such pattern indeed holds for specific gravity response, it is possible to miss the thinning treatment response if data over a long period of time are pooled. To alleviate this problem it is necessary to analyze response data over relatively short periods of time. In

this study, there is a potential for testing thinning effects on an annual basis. In addition, the possibility of thinning effects variation by height within annual rings has to be entertained.

Even with the wealth of data enjoyed in the study, such fine analysis would stretch the data making some tests less reliable without necessarily providing more insight into the issue. Thus, assuming that thinning treatment effects last at least for up to three years, the data for each measurement period (every three years) were pooled by height to test thinning effect variation by time and height (Table 4.5).

The results in Table 4.5 confirm results obtained earlier (Table 4.3 and 4.4), that thinning effects over measurement periods by height are not significant. It thus seems reasonable to conclude that for the thinning treatment levels applied, ring specific gravity of the loblolly pine trees in cutover site-prepared lands is not significantly affected. Figure 4.9 shows average ring, earlywood and latewood specific gravity variation by height and physiological age as affected by thinning treatment.

Table 4.5 : Thinning effects on ring specific gravity over measurement periods by selected heights

Height (ft)	Years since thinning											
	0-3			4 - 6			7-9			10-12		
0.5	* ¹	0.9850 ²	0.5751 ³	*	0.2191	0.1123	*	0.3595	0.5708	*	0.6441	0.3323
4.5		0.7803	0.7418		0.3282	0.6295		0.0332	0.2832		0.3357	0.8724
8.5		0.3023	0.3713		0.7521	0.3048		0.6941	0.4615		0.2226	0.1891
16.5		0.5035	0.4436		0.7329	0.5161		0.2848	0.9618		0.3327	0.2572
32.5		0.9907	0.7732		0.6244	0.4424		0.8731	0.8006		0.8442	0.1163
48.5		0.6542	0.0199		0.5455	0.3204		0.4619	0.9676		0.3972	0.4470

The numbers in the table are p – values for: ¹ Region ² Thinning ³ Region *Thinning.

As a follow up to the results displayed in Tables 4.3-4.5 and to assist in the second objective of the specific gravity study, developing specific gravity prediction model, dummy variable regression was used to determine whether regions require separate regression lines or if the differences can be accounted for by just a location shift. This was accomplished by running simple linear regressions (within the context of [4.2]) with dummy variables using alternative explanatory variables such as percent latewood volume, relative height and physiological age.

Tests on the intercept parameter tended to vary with the specific gravity prediction variable used, but overall the tests seemed to indicate that data from the Piedmont and the others (the highlands) can be combined. With respect to the Coastal Plains, the results indicated that separate intercepts are required with plantations from the Gulf Coastal Plain having, on the average, higher ring specific gravity than the plantations from the Atlantic Coastal Plain. For the slope parameter, however, the difference between the two regions was not significant. Figure 4.10 shows ring, earlywood and latewood specific gravity variation by physiographic region.

Though the tests indicated only a shift in the intercept parameter, in reality the ring specific gravity model involves several variables making it difficult to visualize which parameters are indeed different. As large number of observations were available, it was decided to take a more general approach by fitting three separate regressions for the Gulf Coastal Plain, the Atlantic Coastal Plain, and the Piedmont.

4.3.3 Specific gravity prediction model

A major goal of this study was to develop a ring specific gravity prediction model based on site, stand, tree characteristics and ring position within a tree. The ability to

Chapter four: Thinning effects on ring specific gravity and ring specific gravity prediction model

predict ring specific gravity enables one to evaluate wood in the main stem of a tree for use in various products. Coupled with volume information, wood density information can assist management to make informed decisions on when and how much to cut to obtain optimum product mixes.

The general framework of the specific gravity prediction model considered was:

$$RS = f(\text{tree, stand, site, ring attributes}) + \text{error} \quad [4.3]$$

RS = Ring specific gravity.

tree attributes = DBH, total height, crown size, competition index.

stand attributes = basal area per acre, relative spacing, relative density, number of trees per acre, quadratic mean diameter, thinning treatment .

site attributes = site index, climate, physiography.

ring attributes = physiological age, relative vertical position within a tree.

Even from the incomplete list, it is clear that it is impossible to include every factor that potentially affects ring specific gravity in the prediction model. The goal of this study was to come up with a model that effectively, yet parsimoniously, predicts ring specific gravity. Figures 4.7 and 4.8 show relationships between average specific gravity and various tree and stand attributes.

Several models with alternative forms of expressing tree, stand and site attributes were considered. Many site and stand density attributes failed to enter the model significantly. Appendix A4.1 shows the various models considered and their fit and prediction performance. Of the models considered, the following model appeared to be the best and was selected for further evaluation.

Chapter four: Thinning effects on ring specific gravity and ring specific gravity prediction model

$$RS = \beta_0 + \beta_1 LA + \beta_2 RHT + \beta_3 PLV + \beta_4 RW + \beta_5 CI + \epsilon \quad [4.4]$$

where

RS is ring specific gravity.

LA is the natural logarithm of ring physiological age.

RHT is relative height.

PLV is percent late wood volume of a growth ring.

RW is ring width (inches).

CI is competition index; defined as quadratic mean diameter of the stand divided by tree DBH.

β_i ($i=1,2,\dots,5$) are regression coefficients,

ϵ_i 's are errors, as stipulated in [4.2].

As seen from the results (see Table A4.1.1 in Appendix A4.1) many of the models performed quite poorly failing to effectively predict ring specific gravity. Model [4.4] and a nonlinear variant model [4.4e], performed superior to the other models considered. Overall, however, model [4.4] was the best both in terms of quality of fit (AIC, estimated SEE) and prediction (MSE and R_p^2). This model was further evaluated through double cross validation by fitting it to the validation data and evaluating its performance on the fitting data (see Table 4.6). From the results, it can be concluded that model [4.4] performs well in predicting ring specific gravity. This model is proposed to be used for predicting the ring specific gravity of loblolly pine trees in thinned and unthinned stands on cutover site-prepared lands.

Chapter four: Thinning effects on ring specific gravity and ring specific gravity prediction model

The coefficient estimates, their asymptotic standard errors, covariance parameter estimates and various fit statistics for the combined data set and separately for the Atlantic Coastal Plain, the Gulf Coastal Plain and the Piedmont are presented in Table 4.7.

Table 4.6: Quality of fit and prediction statistics double cross-validated on the fitting and validation data.

Data	$\hat{S}\hat{E}\hat{E}$	MB	MSE	R_p^2
Fitting	0.0295	0.00281	0.00087	0.853
Validation	0.0292	-0.00151	0.00087	0.857

Table 4.7 : Coefficient estimates and their asymptotic standard errors (italicized) for the combined data and by physiographic region.

Regions	<i>Coefficient estimates</i>						AIC	$\hat{\sigma}^2$	$\hat{\alpha}$
	$\hat{\beta}_0$	$\hat{\beta}_1$	$\hat{\beta}_2$	$\hat{\beta}_3$	$\hat{\beta}_4$	$\hat{\beta}_5$			
Combined	0.357318 <i>0.002064</i>	-0.010267 <i>0.000380</i>	-0.041291 <i>0.002722</i>	0.003544 <i>0.000014</i>	-0.041054 <i>0.001247</i>	0.014923 <i>0.001420</i>	61345	0.00086	1.3637 <i>0.0227</i>
Atlantic coastal Plain	0.365798 <i>0.003590</i>	-0.008495 <i>0.000712</i>	-0.041527 <i>0.003691</i>	0.003467 <i>0.000025</i>	-0.057745 <i>0.004855</i>	0.008902 <i>0.002325</i>	18974	0.0009	1.4170 <i>0.0423</i>
Gulf coastal Plain	0.355176 <i>0.004024</i>	-0.006161 <i>0.000810</i>	-0.046069 <i>0.002593</i>	0.003492 <i>0.000028</i>	-0.037072 <i>0.005648</i>	0.016828 <i>0.002637</i>	13747	0.0009	1.8994 <i>0.0405</i>
Piedmont	0.353656 <i>0.003292</i>	-0.012369 <i>0.000533</i>	-0.032300 <i>0.004002</i>	0.003571 <i>0.000020</i>	-0.038113 <i>0.001751</i>	0.016953 <i>0.002432</i>	28736	0.00078	1.3668 <i>0.0331</i>

Partial F-tests show that percent latewood volume is the most important variable in predicting ring specific gravity. Also, the pattern of ring specific gravity follows close

relationship to the proportion of latewood. This is consistent with the strong linear trend observed in Figure 4.7d.

To obtain more insight into the pattern and property of ring specific gravity, graphical analyses were also undertaken. Low on the bole growth rings are dominated by latewood fibers. With increasing height, the proportion of latewood continuously decreases hence the specific gravity also decreases (Figures 4.5a, 4.5c). Regarding ring age, at young physiological age growth rings are dominated by earlywood; consequently rings tend to have low specific gravity. As age increases (from approximately age 10 onwards) the proportion of latewood increases substantially as does ring specific gravity (Figures 4.5b, 4.5d). The decrease in specific gravity past age 25 is probably due to too few observations at the data boundary. Relative position in height seems to have a stronger effect on ring specific gravity than relative position in physiological age.

In order to examine whether specific gravity pattern varies by ring position in terms of physiological age and vertical position, rings were grouped into 5-year age classes and selected sampling heights. Average ring, earlywood and latewood specific gravity values for the age and height classes were plotted by physiological age and height, respectively (Figure 4.6). While the general trend in specific gravity variation is maintained, it appears that ring position both in terms of distance from the pith (physiological age) and vertical distance have an effect on specific gravity profile.

Rings in the juvenile region (1-5 years) have a tendency to exhibit lower specific gravity profile along the stem. Similarly as one proceeds up the stem, specific gravity profiles across physiological age show a tendency to decrease in magnitude. The graphs show that, past the juvenile region, physiological age has little influence on specific gravity profile. On the contrary, disk position along the stem maintains its impacts on

specific gravity profile along the bole with a tendency for the profile to be consistently lower with increasing height.

Considering the latewood and earlywood specific gravity, one observes the usual pattern (see Figures 4.9, 4.10) except those from rings at the stump level and rings from the juvenile area. Rings at the stump level have prominently higher earlywood specific gravity profile than rings from disks high up on the tree bole – with a tendency to decrease with disk height. Latewood specific gravity profile for rings from the juvenile zone is considerably lower than profiles for the older years. It is not clear why average earlywood specific gravity profile for disk at stump height is substantially higher than profiles for disks from higher up. Nevertheless, overall these results are consistent with the findings of Megraw (1985) for the loblolly pine trees he studied.

These evidences suggest that ring specific gravity variation is explained not only by the proportion of earlywood - latewood, but by changes in the earlywood and latewood specific gravity values as well. Larocque and Marshall (1995) also report the significance of changes in earlywood and latewood specific gravity values to changes in average ring specific gravity values in red pine trees. Unlike the conclusion reached by Larocque and Marshall (1995), results from this study suggest that changes in earlywood and latewood specific gravity values have secondary influence on ring specific gravity values.

4.4 Discussion and conclusions

4.4.1 Discussion

Many studies focusing on the effects of fast growth particularly wide spacing and thinning have been conducted on loblolly pine as well as other species (Clark and Saucier 1989; Petty *et al.* 1990; Barbour *et al.* 1992; Larocque and Marshall 1995). The majority of the studies concluded that growth rate and specific gravity are poorly correlated. Results from the present study, while largely concurring with this basic conclusion, provide an opportunity to assert the claim from a stronger sampling vantage point and broader perspective.

Specific gravity data in many studies were collected on a disk by disk basis which ignores the within disk variation due to physiological age differences among growth rings. In instances where detailed specific gravity data were collected, they tended to be at one point on the stem usually at breast height (see Larocque and Marshall 1995). Such a sampling framework enables examining specific gravity variation due to differing physiological age and treatment effects at one point, but ignores inherent vertical variation in specific gravity.

Petty *et al.* (1990) sampled groups of rings at different disk heights in their studies on Sitka and Norway spruces. Similarly, Barbour *et al.* (1992) took several disks along the stems of red spruce trees in their sample and determined ring-by-ring specific gravity. While potentially addressing the vertical and radial variation, these studies failed to consider regional variation as they were restricted to one location. Unless sampling is designed to capture the major sources of variation by distributing samples over the range of climatic or physiographic regions known to exist within a species range, an important source of variation may be ignored.

Chapter four: Thinning effects on ring specific gravity and ring specific gravity prediction model

Some studies (Talbert and Jett 1981; Megraw 1985; Clark and Saucier 1989) have indicated specific gravity variation in loblolly pine trees due to variation in physiography. The current study with the wide range of factors considered provided an opportunity to also detect the effect of physiography on specific gravity variation. Trees from the Coastal Plains have shown a tendency to have higher specific gravity than trees from the Piedmont and other areas. Zobel *et al.* came to similar conclusion in 1972 (Megraw 1985). Within the Coastal Plains, trees from the Gulf Coastal Plain have a tendency to have higher specific gravity than trees from the Atlantic Coastal Plain.

In his summary on thinning effects, Megraw (1985) suggested thinning can have negative or positive effect on ring specific gravity depending on intensity and whether or not moisture is a limiting factor. The thinning intensity used in this study was not very high and there is no indication that moisture was a limiting factor at the time of thinning to have had significant influence on the proportion of latewood to earlywood.

Moreover, contrary to some studies (see for instance Larocque and Marshall 1995), stand density had limited influence on ring specific gravity of trees studied. This is probably partly due to the limited range in density encountered in the thinning study. In a related context, site index and average dominant height were found to have little effect on ring specific gravity. Further, tree size such as DBH and total tree height did not significantly impact ring specific gravity. However, the ratio of DBH to total tree height, a surrogate for stem taper, significantly explained variation in specific gravity in some of the prediction models considered.

The role of crown in wood formation pattern is well known. The amount and type of annual wood increments as well as its distribution along the stem and branches are influenced by physiological activity of the crown (Kozlowski 1971). Wood formed in the crown, particularly near the terminal shoot, constitutes the juvenile core with the typical

Chapter four: Thinning effects on ring specific gravity and ring specific gravity prediction model

low specific gravity. This is because radial growth in the spring begins first at the top of the tree and proceeds gradually downward (Megraw 1985).

The ratio of crown length to total tree height, crown ratio, markedly influences annual wood along the stem. Crown ratio can thus be considered an important determinant of ring specific gravity variation. However, as observed in Figure 4.7c, crown ratio is correlated with ring specific gravity rather weakly and entered the specific gravity prediction model significantly for only a subset of the models considered. Crown ratio is negatively correlated with ring specific gravity.

The precipitation to temperature ratio variable used to approximate climate was significant and is positively correlated with specific gravity. While both average summer precipitation to temperature ratio and August precipitation to August temperature ratio were significant and positively correlated with ring specific gravity, the summer precipitation to temperature ratio was stronger.

In proposing model [4.4] ring width and percent latewood volume are not easily measurable quantities, but two options are available. For standing trees, one has to use predicted values for both ring width and percent latewood volume. As part of the work on ring width undertaken in this study, a prediction model for ring width will be developed. Also, since percent latewood volume can be closely approximated by the proportion of latewood width to total ring width, a model which predicts this quantity will be used to approximate percent latewood volume. As in any model where measured quantities are approximated by predicted values, the performance of the proposed model is expected to deteriorate.

For felled trees, both ring width and proportion of latewood can be measured and a good approximation to percent latewood volume can be obtained. An investigation has shown that good prediction is achievable in this case because the proportion of latewood

Chapter four: Thinning effects on ring specific gravity and ring specific gravity prediction model

and percent latewood volume describe the same quantity measured using two different techniques. Percent latewood volume is the proportion of latewood to total ring as determined by x-ray densitometry; whereas the proportion of latewood to total wood used to develop the proportion of latewood model was based on image analysis technique. Any difference between prediction performance by the proposed model and that obtained from the measured proportion of latewood is due to differences in measurement techniques.

A limited comparison undertaken between the x-ray technique and image analysis technique on ring width measurement showed that the methods, while highly correlated ($r \simeq 0.9$), vary widely. That is estimating ring width using x-ray densitometry often yields values that significantly differ from measurements obtained using image analysis or other optical instruments. Consequently, the use of the estimated percent latewood volume reduces the precision of the prediction model somewhat. Nevertheless, the model proposed performs superior to competing models, particularly those which did not include percent latewood volume as a predictor.

4.4.2 Conclusions

The study indicated that most variation in specific gravity values is due to within tree factors such as ring position with respect to the vertical axis and physiological age. External factors such as stand density, thinning treatment, site factors, and to the extent considered, climatic factors have minor influence.

Following is a summary of conclusions that can be drawn from the results obtained in this study.

i) Operational thinnings commonly used in loblolly pine plantations have limited effects on wood specific gravity. A statistically insignificant, but perceptible decrease in specific gravity can be expected following thinning.

ii) Broad physiographic factors significantly affect ring specific gravity of loblolly pine trees. Loblolly pine trees from the Coastal Plain tend to have higher specific gravity than trees from the Piedmont and other areas. Within the Coastal Plain, trees from the Gulf Coastal Plain have a tendency to have higher specific gravity than trees from the Atlantic Coastal Plain.

iii) Specific gravity values decrease with increasing height above ground and increases with increasing age. Ring specific gravity shows a sharp increase outward from the pith until about physiological age 10 and then flattens out showing little increase with physiological age.

iv) Stand density and site quality have limited influence on ring specific gravity. Nevertheless, a combination of tree size and stand density, expressed as a tree's competitive position, appears to be a good predictor of specific gravity. Trees subject to higher levels of competition tend to have, on the average, higher specific gravity values.

v) Specific gravity is highly correlated with percent latewood volume- the proportion of latewood width to total ring width. Thus, percent latewood volume is the single most important variable in predicting ring specific gravity among variables considered in this study. Following that, ring position both in terms of the distance from the pith and vertical distance play significant role. Finally, to the extent that wide rings are associated with

Chapter four: Thinning effects on ring specific gravity and ring specific gravity prediction model

juvenile wood, ring width contributes substantially to ring specific gravity prediction. In practice as percent latewood volume and ring width are not readily measurable, estimates or predicted values should be used.

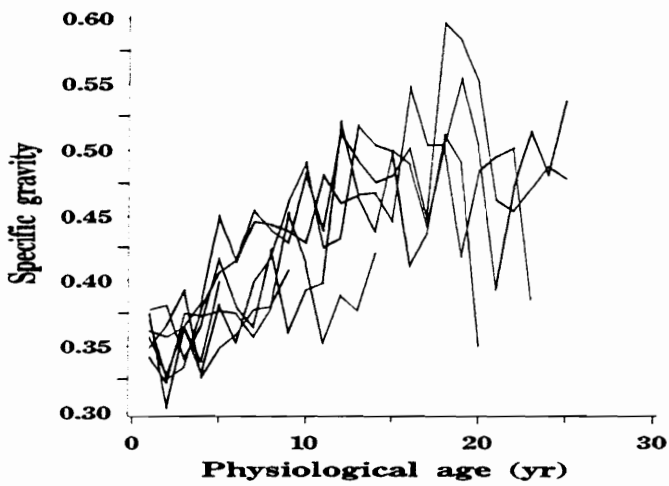
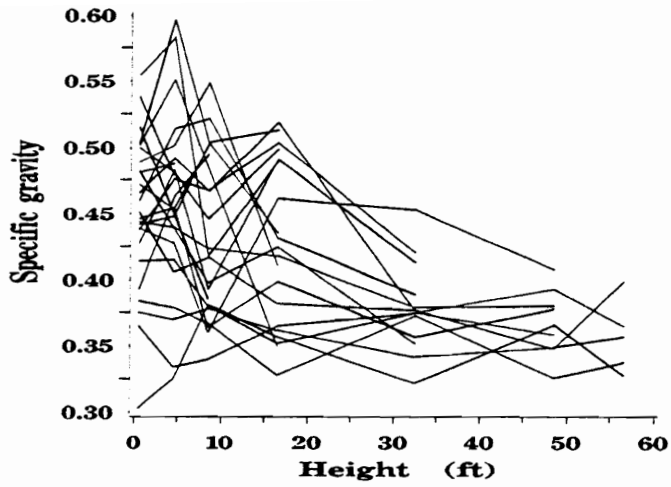


Figure 4.1: Parallel profile plots of ring specific gravity by height and by physiological age for a specific tree.

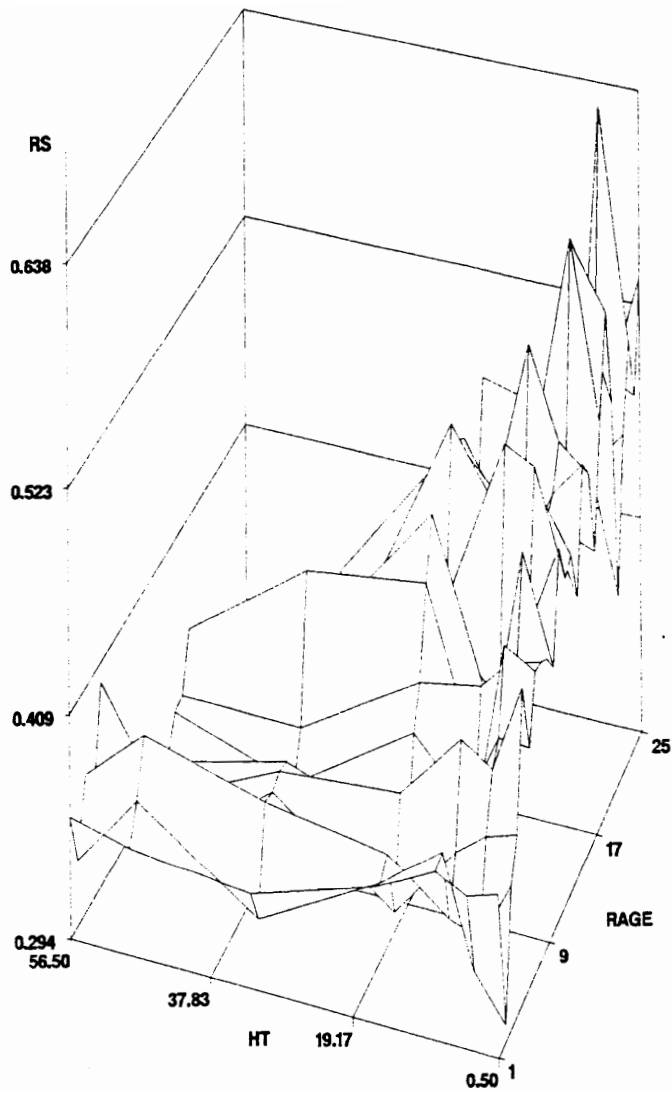


Figure 4.2: A 3D plot of ring specific gravity by height and physiological age for a specific tree (RS=ring specific gravity, RAGE=ring physiological age and Ht=height above ground)

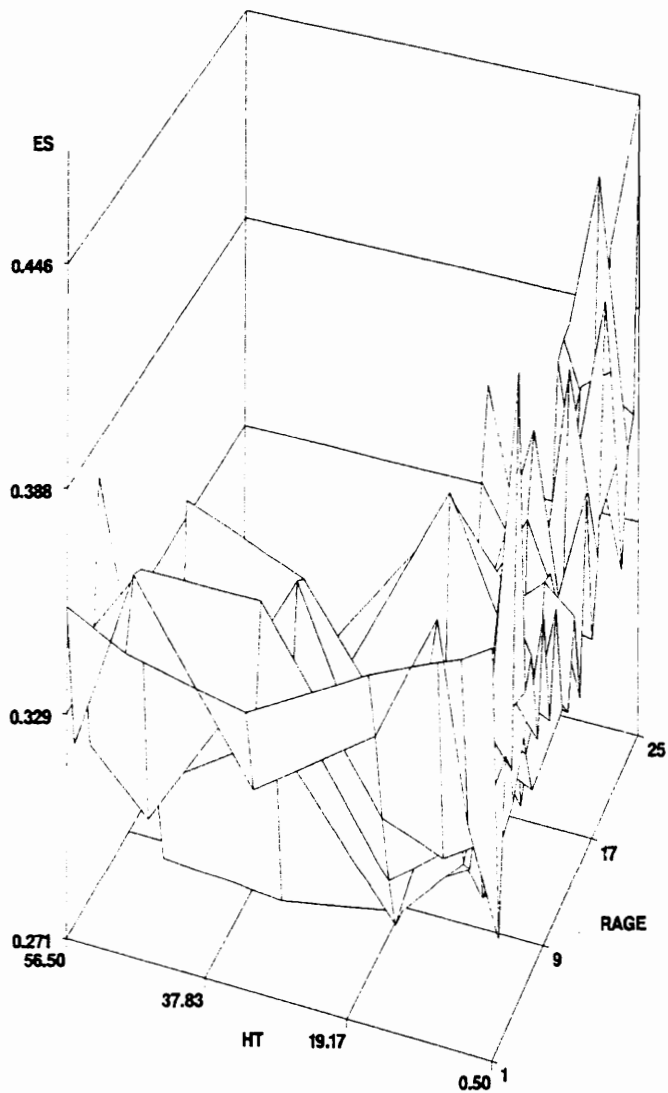


Figure 4.3 :A 3D plot of earlywood specific gravity by height and physiological age for a specific tree (ES= earlywood specific gravity).

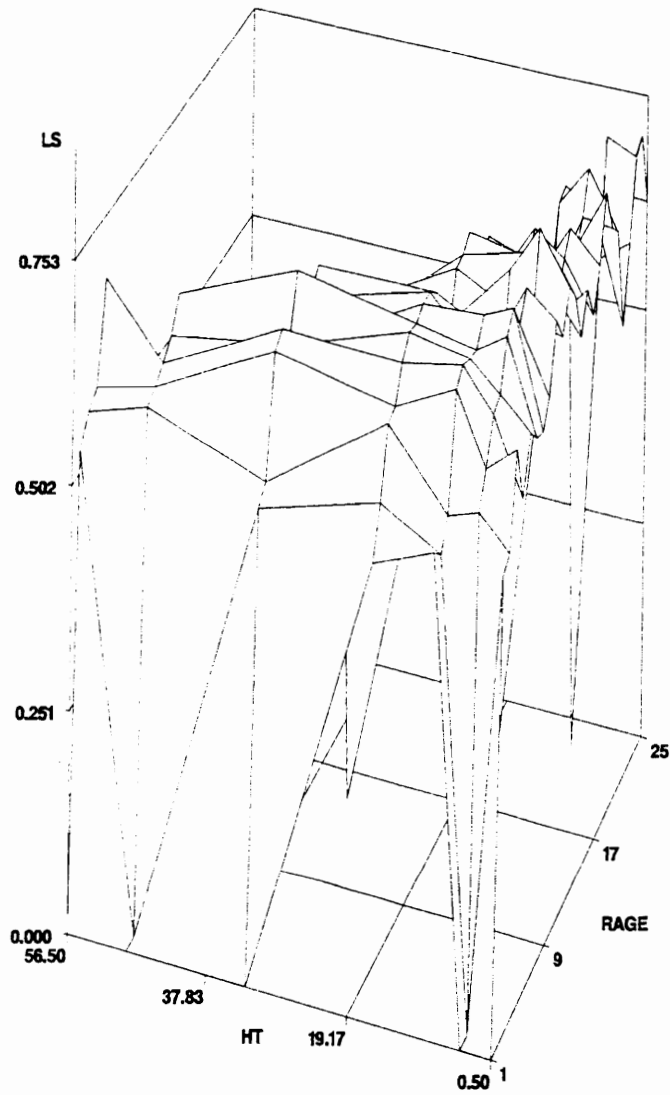
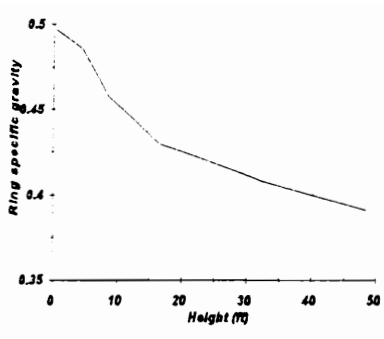
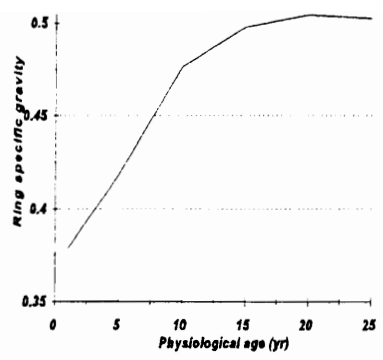


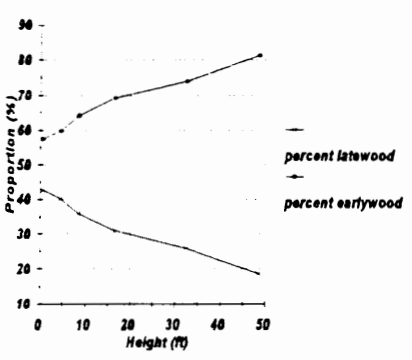
Figure 4.4: A 3D plot of latewood specific gravity by height and physiological age for a specific tree (LS= latewood specific gravity).



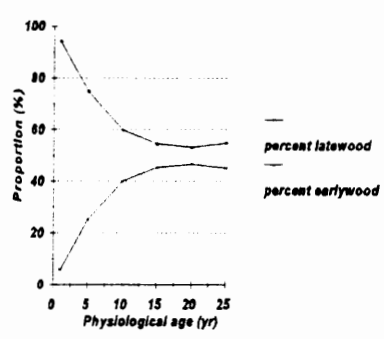
[a]



[b]

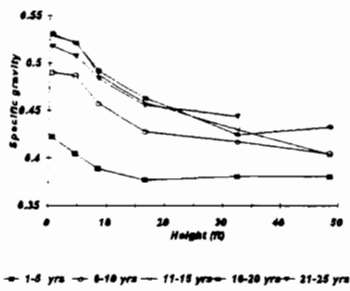


[c]

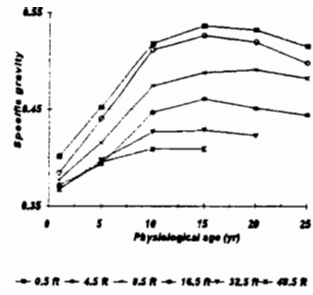


[d]

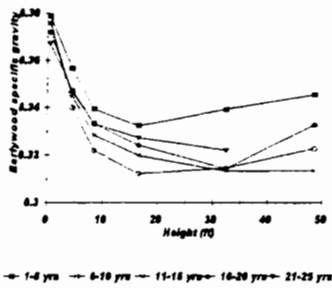
Figure 4.5 : Average ring specific gravity, percent earlywood and percent latewood by height and physiological age.



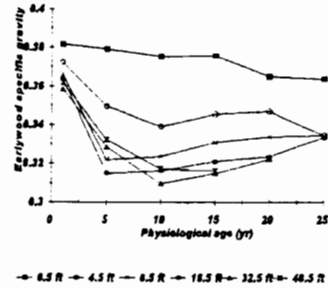
[a]



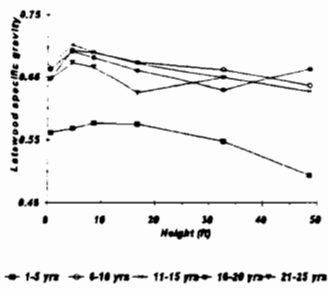
[b]



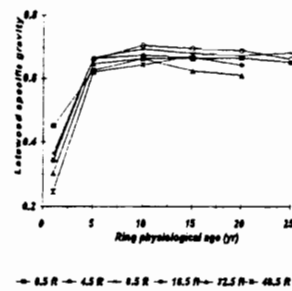
[c]



[d]



[e]



[f]

Figure 4.6 : Average ring , earlywood, and latewood specific gravity for groups of rings by height and physiological age.

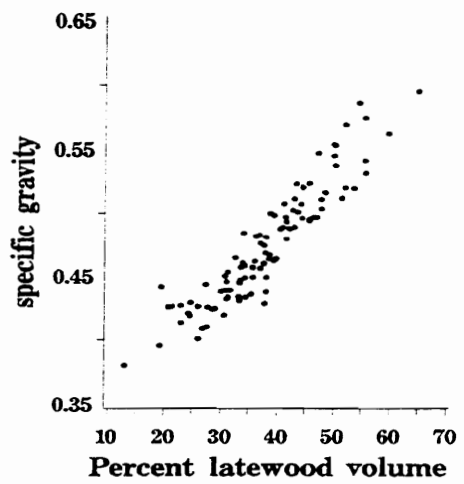
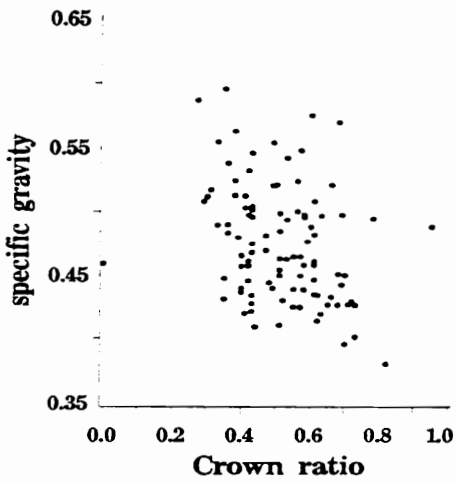
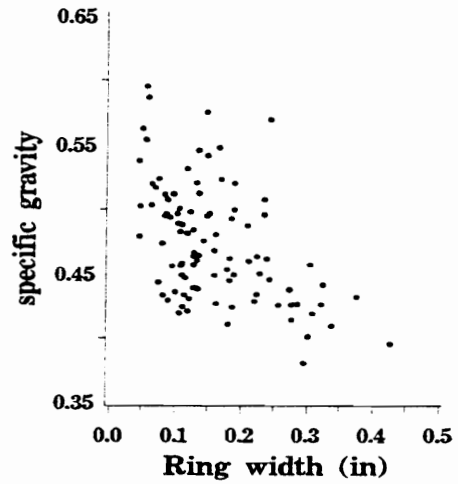
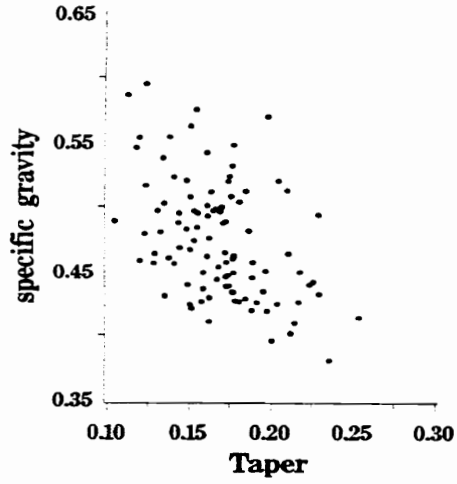


Figure 4.7: Relationships between average specific gravity and various tree level factors.

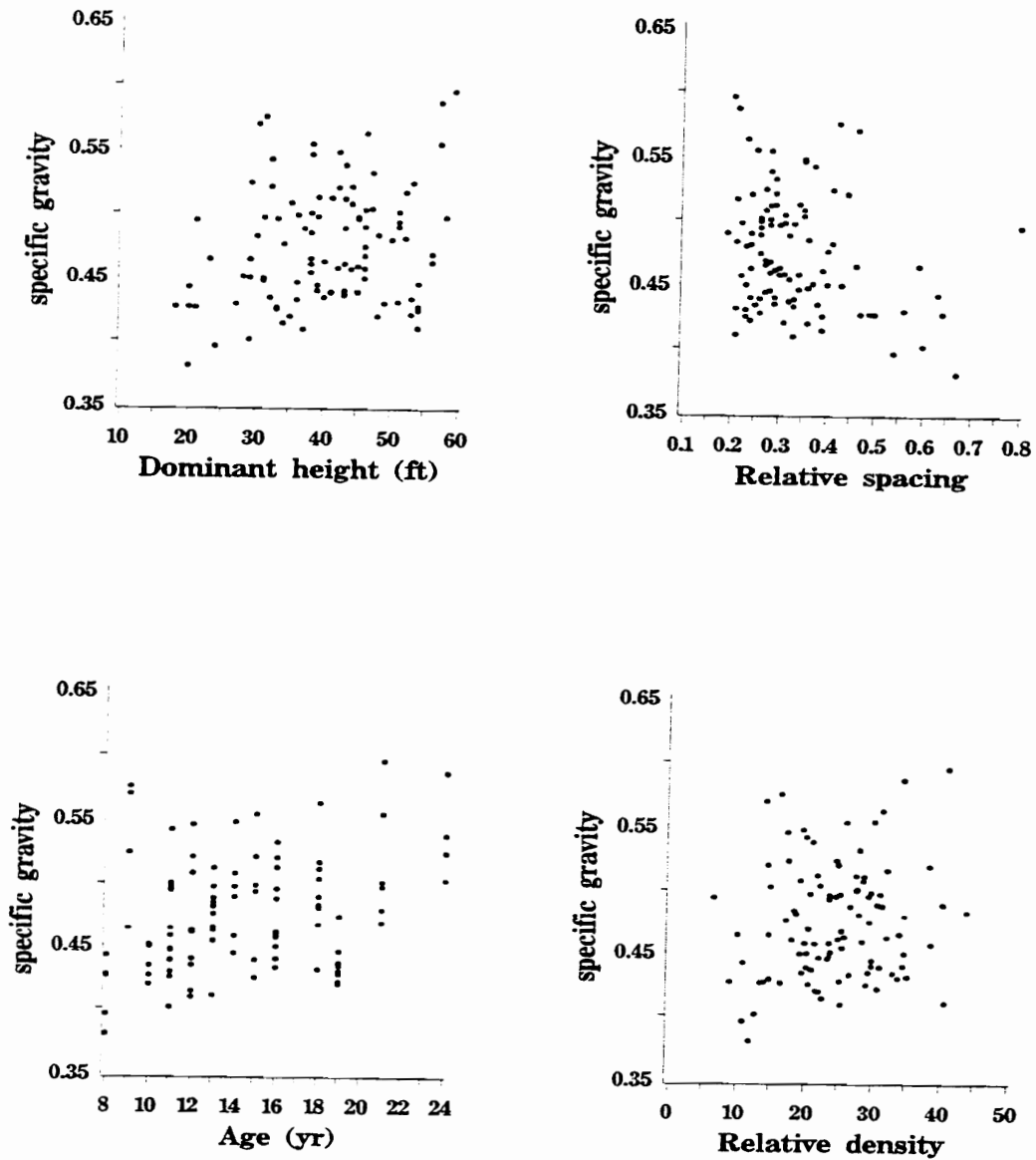
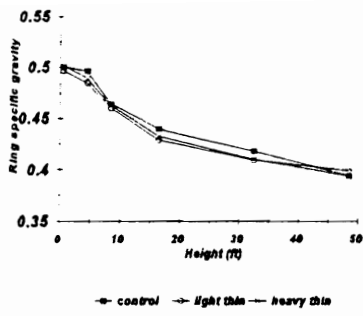
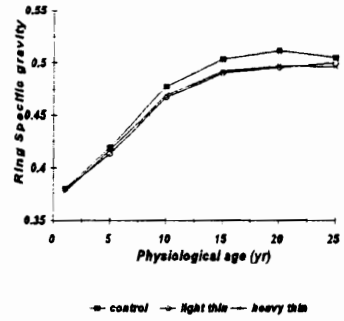


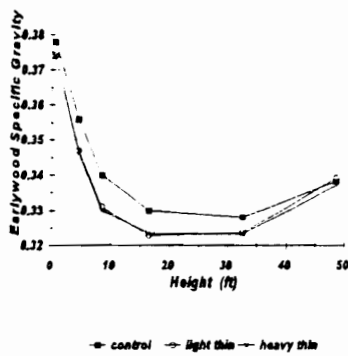
Figure 4.8: Relationships between average specific gravity and various stand level factors.



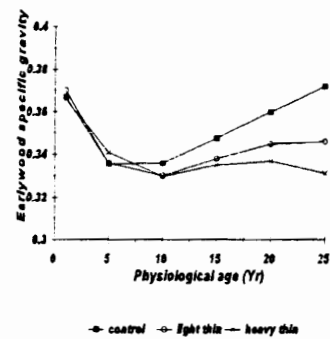
[a]



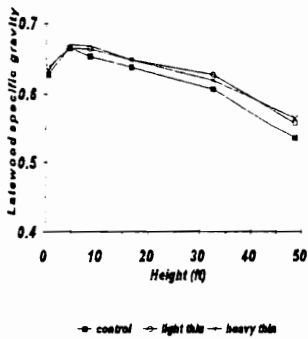
[b]



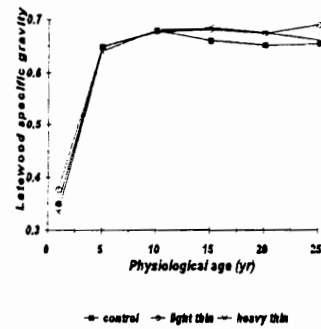
[c]



[d]

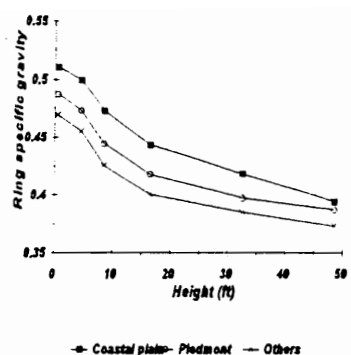


[e]

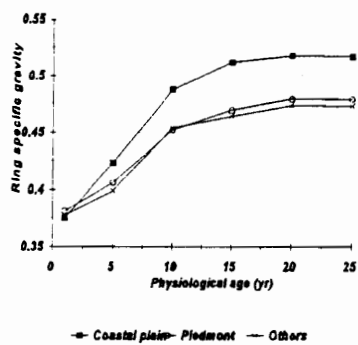


[f]

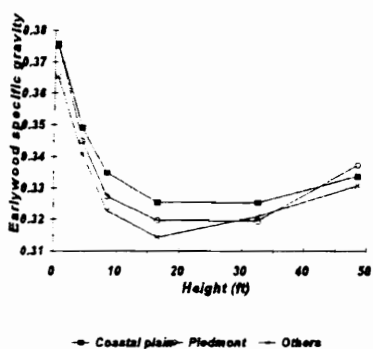
Figure 4.9: Average ring, earlywood and latewood specific gravity by height and physiological age by thinning treatment.



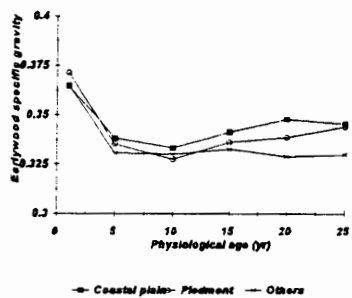
[a]



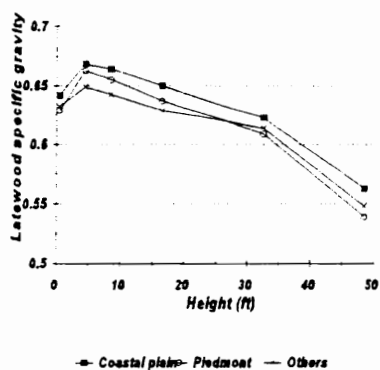
[b]



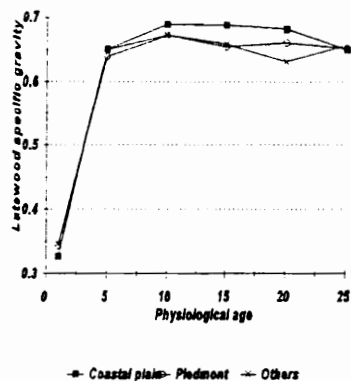
[c]



[d]



[e]



[f]

Figure 4.10: Average ring, earlywood and latewood specific gravity by physiographic region.

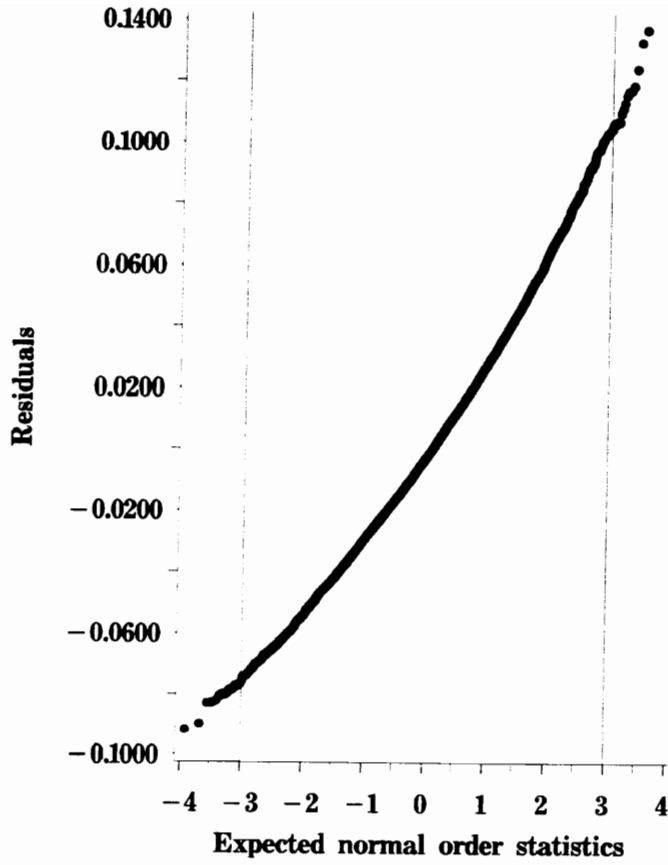


Figure 4.11: A normal probability plot for the specific gravity residuals.

CHAPTER FIVE

5.0 Thinning effects on ring width distribution and prediction models

5.1 Introduction and literature review

5.1.1 Introduction

Loblolly pine plantations commonly receive thinning treatment whose primary purpose is to enhance diameter growth on selected trees. Many studies have been conducted to determine thinning effects on wood production and are commonly based on changes in stem diameter at breast height. Several studies suggest that the pattern of wood deposition along the stem is not uniform, but varies by position along the stem over time (Farrar 1961; Larson 1963 and others). Thus studies based only on changes in breast height diameter do not account for the shift in wood deposition pattern following thinning (Myers 1963; Thomson and Barclay 1984). The primary objective of this study is to investigate thinning effects on the pattern of wood deposition along the stem over time.

Tree diameter at breast height and other measurements are often used to estimate the total wood material in the main bole. It is desirable to be able to predict the layer of woody material deposited along the stem annually so that volume or weight estimates by product classes can be obtained and effects of silvicultural treatments can be directly quantified. A second objective of this study is to develop a model that directly predicts annual wood increment based on tree, stand, site and ring position within a tree.

Chapter five: Thinning effects on ring width distribution and prediction models

In evaluating thinning effects a common concern voiced is its perceived negative effects on wood quality especially on wood density. In the study on specific gravity addressed in this thesis, it has been observed that percent latewood volume, *alias* latewood proportion, is highly correlated with specific gravity. Thinning effects on latewood proportion will be investigated to determine how well it agrees with thinning effects on specific gravity. A latewood proportion prediction model will be developed for use as an input to the proposed specific gravity prediction model.

5.1.2 Literature review

Studies on how ring width varies over tree stem have attracted the attention of investigators for over 100 years. Various researchers have established that ring growth is not uniform along the stem, but varies considerably due to internal and external factors. Among early investigators, Pressler was noted for his observation that ring area growth is related to the quantity of foliage above a point of ring measurement and suggesting that the form of the stem is a function of the crown (Larson 1963).

The observations of Pressler have been corroborated by several investigators. Duff and Nolan (1953, 1957), in studies on red pine (*Pinus resinosa* Ait.), asserted that trees produce a sheath of xylem which varies in thickness and structure at different stem or branch heights and, at a given stem height. They postulated that this growth variation is mainly regulated by the flow of products synthesized in the crown. Earlier, Onaka in 1950 (Larson 1963) came to a similar conclusion when he suggested that the vertical distribution of radial increment is governed by the production and distribution of growth hormone and the flow of nutritive substances. The downward increase of ring growth

within the crown shown earlier by Pressler and verified by subsequent works led to the conclusion that maximum radial growth is reached at or close to the live crown base (Labyak and Schumacher 1954).

Duff and Nolan (1953) hypothesized that cambial growth follows a certain pattern and put forward a theory that three types of sequences could be discerned in ring width growth. The sequences they proposed can be summarized as follows:

Type I Sequence: Strong, regular pattern of gradually rising, maximizing and falling mean, internodal ring width of a single year's growth, with progression from internode to internode down the tree (*i.e.* variation due to height).

Type II Sequence: Strong, regular pattern of gradually rising, and maximizing and falling mean internodal ring width in a single internode with progression from one ring to the next (*i.e.* variation due to ring physiological age).

Type III Sequence: Unpatterned variation of mean, internodal ring width with progression from internode to internode, down the tree at a uniform ring number from the pith.

Other investigators (Mott *et al.* 1957; Stark and Cook 1957; Fayle 1973) concurred with the basic views of Duff and Nolan (1953) as to the existence of growth sequences which show the influence of internal and external factors on the distribution of growth (Fayle and MacDonald 1977), but offered different terminologies which they claimed are more instructive. Mott *et al.*(1957) offered the terms oblique, horizontal and vertical sequences respectively for the Type I, II and III of Duff and Nolan (1953).

Fayle (1973) argued that neither the original definition (Duff and Nolan 1953) nor the alternative suggested by Mott *et al.*(1957) apply to wood in the root and proposed that the terms profile, radial and number be used instead of Type I, Type II and Type III, respectively, sequences of Duff and Nolan (1953).

Chapter five: Thinning effects on ring width distribution and prediction models

Tepper *et al.* (1968) studied radial growth in plantation-grown red pine trees on plots that differed in depth to water table. They noted that Type III sequences are useful for environmental analysis of wood deposition in young trees.

Age, through its relation to crown size in early development of trees, affects ring growth patterns. It has been observed (Smith and Wilsie 1961; Kozlowski 1971; Arbaugh and Peterson 1993) that in young trees with physiologically active branches along most of the main stem, the height of maximum ring thickness occurs low in the stem. As trees mature and the lower branches become less efficient and begin to die, the point of maximum growth shifts upward (Reukema 1961).

The conditions in which trees grow are also known to affect the distribution of ring growth. During years of high rainfall or favorable conditions for growth, the point of maximum xylem increment occurs at a relatively lower level on the stem than when growth conditions are unfavorable (Kozlowski 1971).

An important factor which affects the distribution of growth rings along the stem through its effects on tree crown is stand density (Smith 1980). From the outset, investigators have made distinction between growth patterns of open grown trees and trees grown in stands. Hardtl in 1938 (Larson 1963) noted that as open-grown trees are dominated by crown, their radial growth pattern closely approximates that of the within-crown part of stand grown trees resulting in a more tapered stem form.

Stand grown trees on the other hand, mostly have shorter crowns and are dominated by branch-free bole with less ring growth variation and consequently decreased taper. Among trees grown in stands, thrifty dominants experience conditions similar to open-grown trees. In those trees ring width increases from the apex down to a point of maximum close to the crown base; while in the lower part of the crown as well as along most of the bole, ring width decreases. At the base of the tree, ring width increases again

Chapter five: Thinning effects on ring width distribution and prediction models

reaching a second maximum near the ground line. Trees grown under more crowded conditions, however, tend to have the maximum ring width near the tip of the tree and show less variation in thickness from apex to the base (Farrar 1961).

Farrar (1961) summarized variation in the form of a growth ring for a hypothetical tree as follows. At a young age, before competition sets in, ring width increases from apex to the tree base. With increasing age and competition, the region of maximum growth moves upward to the part within the crown where branch development is at its maximum. As the tree gets older and competition induces the death of the lower branches, the point of maximum growth moves up towards the apex.

Various investigators have observed that silvicultural treatments, at least in the short term, have profound effects on ring growth distribution of trees. In particular, thinning and pruning appear to have opposing effects for red pine (Bickerstaff 1946).

Thinning, an important silvicultural practice largely aimed at directing the growth and yield of a forest stand towards selected trees, also directly affects the form and shape of the residual trees (Larson 1963; Arbaugh and Peterson 1993). The release of a tree from competition has the effect of producing a more tapered tree by greater stimulation of xylem production towards the stem base than at upper stem levels (Kozłowski 1971).

Myers (1963), for instance, studied the vertical distribution of annual increment in thinned Ponderosa pine (*Pinus ponderosa* Dougl.) in South Dakota. He observed that before thinning the annual layers were widest at about 80 to 85 percent of tree height and narrowest at 20 to 25 percent. Thinning, he found, essentially reversed the pattern shifting the points of maximum and minimum growth to tree base and 70 percent of tree height respectively. Thomson and Barclay (1984) also observed a similar pattern in their studies on Douglas-fir (*Pseudotsuga menziesii* (Mirb.) Franco) in British Columbia.

Pruning has been commonly employed to obtain knot-free timber. Larson (1963) cited several works which found pruning to serve the purpose of redistributing growth along the tree stem resulting in a more cylindrical stem form. Larson (1965) conducted an experiment in which he found that drastic removal of the live crown induced growth in the upper portion of the stem at the expense of the lower portion. Some investigators (see for instance Buckman and Roe 1958), however, were unable to substantiate the claim that pruning alters stem form.

Species variation, intensity and timing of thinning, site and stand structure are reported to affect the nature and extent of ring growth distribution. It has been suggested that trees tend to be more tapering on poor sites than on good sites, presumably due to low height growth on poor sites (Larson 1963). Variation due to site differences have been observed (Liu and Keister 1978), but the association of increased taper with poor site has been sometimes disputed (Newberry and Burkhart 1986) for loblolly pine.

Other factors also are reported to cause variation in the growth distribution of the annual rings. In particular, agents such as disease and insect defoliators which affect tree crowns have direct impact on growth allocation. Mott *et al.* (1957) working with balsam fir (*Abies balsamea* (L.) Mill.) and tamarack (*Larix laricina* (Du Roi) K. Koch) investigated the effects of defoliation on ring-width and concluded that defoliation resulted in the decrease of the type I and type II sequences. They noted that defoliation resulted in the decrease of growth in the upper part of the stem.

Among environmental factors known to affect ring growth distribution along the bole, wind has been shown to be a major factor (Larson 1963 and 1965; Burton and Smith 1972; Valinger 1992). The general consensus on the effects of wind is that when stands are opened up or trees are artificially subject to wind, the point of maximum growth moves down the stem to the area at or just above the point of anchor.

Chapter five: Thinning effects on ring width distribution and prediction models

5.2 Data and methods

5.2.1 Data

A complete description of the data used in this study is provided in § 3.1. Summaries of the tree and disk data used in model fitting and validation are presented in Tables 5.1 and 5.2, respectively. Average ring width patterns as well as patterns shown by selected trees are depicted graphically. Figure 5.1 shows parallel profile plots depicting ring width variation by height and by physiological age for a specific tree. Three-dimensional views of the entire ring width, earlywood width and latewood width for the same tree are shown in Figures 5.2-5.4, respectively.

Table 5.1: Tree summary statistics for ring width and latewood proportion prediction models fitting and validation data.

Variable	n	Mean	CV	Minimum	Maximum
<u>Fitting</u>					
DBH (in)	94	8.5	23.6	4.3	13.9
BLC (ft)	94	36.7	20.6	17.7	61.3
H (ft)	94	59.2	14.8	33.8	82.5
<u>Validation</u>					
DBH (in)	91	8.5	23.5	3.8	14.2
BLC (ft)	91	36.1	21.5	19.9	56.8
H (ft)	91	58.8	14.7	35.6	87.9

Table 5.2 : Ring summary statistics for ring width and latewood proportion prediction models fitting and validation data

Variable	n	Mean	CV	Minimum	Maximum
<u>Fitting</u>					
RW (in)	21491	0.161	60.1	0.002	0.646
EWW (in)	21491	0.123	74.0	0.001	0.592
LWW (in)	21491	0.037	65.1	0.001	0.292
<u>Validation</u>					
RW (in)	21472	0.156	63.3	0.002	0.756
EWW (in)	21472	0.120	75.8	0.001	0.728
LWW (in)	21472	0.036	65.6	0.000	0.343

5. 2.2 Methods

The ring width data are similar in structure to the data used in the specific gravity study in Chapter 4. Accordingly, the general model specified in [3.2] was used to represent the ring width data. Thus

$$Y_t = X_t'\beta + Z_t'\alpha_t + \epsilon_t \quad [5.1]$$

where

Y_t is the vector of ring width observations for tree t , and other variables are as defined before.

With the dimensions of Y , X , Z and ϵ and the properties of the random effect parameters as defined in § 3.2, and the error terms assumed to be normally distributed with the variance covariance matrix described in [3.8]-[3.12].

To investigate thinning effects on the ring width and latewood proportion and for prediction models, several linear and nonlinear mixed-effects models were considered (Appendix 5.1 and 5.2). Correlation among observations from the same subjects were accounted for by either specifying random effects covariates or through direct covariance modeling.

5.3 Results and analyses

5.3.1 Covariance structure

In searching the best approach to accounting for correlations, it was noticed that the ring width data did not support specifying both D and R within a single model. However, a comparison of models fit using one or the other showed that modeling covariance in R yielded higher AIC values (superior) than including random effects covariates hence it was decided to model covariance directly.

A comparison of some alternative specifications for R showed results that are comparable on the basis of AIC. Further, investigations conducted with the AR(1) specification on the basis of estimated correlation coefficient and the AIC, indicated that the ξ_{ii} are stronger than the ξ_{th} (see § 3.2). Consequently, fitting under the covariance structure stipulated in [3.13] using the AR(1) and continuous time autoregressive covariance structure were considered.

Because of occasional numerical difficulties in fitting models using the continuous time autoregressive structure and since the two structures gave more or less identical results for the structure in [3.13], the AR(1) covariance specification was used in all hypothesis tests and modeling works on the ring width data. The structure stipulated in [3.13] was further simplified by setting the off-diagonal matrices to the null matrices *i.e.* it was decided to set the $\xi_{th} = 0$ such that $Cov(\epsilon_{thi}, \epsilon_{th'i}) = 0$. This was to preserve the pattern in [3.13], at least partly, and to identify which correlation ξ_{th} or ξ_{ii} (within or between rings, respectively) was actually estimated since both are contained in [3.13].

Thus, correlations between observations in a disk were accounted for, whereas the correlation between corresponding rings in different disks were ignored. An empirical evaluation where the AR(1) was specified for all observations within a tree ignoring the pattern displayed in [3.13] and [3.14] showed no loss in the quality of fit with the approach used here as measured by AIC. Consequently, model [5.1] was modified to:

$$Y_t = X_t' \beta + \epsilon_t \quad [5.2]$$

Where,

$$\epsilon_t \sim N(0, R_t)$$

$$Y_t \sim N(X_t' \beta, R_t)$$

$$R_t = BD(\sigma^2 \rho^{|\delta_{t,i}|})$$

BD = block diagonal matrix, and other symbols are as defined earlier.

The use of [5.2] instead of OLS ($R_t = \sigma^2 I$) resulted in an increase in AIC by up to 23%. Furthermore, the LRT test was highly significant indicating the gain over incorrectly using OLS.

5.3.2 Thinning effects

5.3.2.1 Effects on ring width

A number of studies have concluded that thinning has the effect of redistributing growth over the tree bole. Because of this redistribution, it is not adequate to measure thinning effects on diameter growth at one point, at breast height, say, as is customarily done. Moreover many studies (see, for instance, Hilt and Dale 1979) attempt to determine

Chapter five: Thinning effects on ring width distribution and prediction models

thinning effects after a considerable period of time; yet, studies (for instance, Thomson and Barclay 1984) suggest that thinning effects have a tendency to diminish with time as stand density increases.

Therefore, to obtain a better picture, thinning effects should be evaluated continuously along the tree bole. Moreover, studies relying on measurements obtained soon or long after thinning was conducted risk the possibility of missing the effects they were set out to measure or may even lead to erroneous conclusions. The analyses conducted in this study address these issues by evaluating thinning effects at several points along the stem over time.

Table 5.3 presents test results of overall thinning effects on ring width for the combined data. The results indicate that thinning affects ring width significantly. The thinning by region interaction, however, is not significant – implying no regional variation in thinning response. Figure 5.5 shows average total ring width, earlywood and latewood width by height and physiological age by thinning treatment.

One concern was whether before the thinning treatments were applied the plots were similar *i.e.* whether the treatments were applied to homogeneous experimental units since inherent significant variability would render the thinning treatment conclusions questionable. This is a problem because, while attempts were made to select stands exhibiting specific properties to ensure uniformity of the stands to which the treatments are applied, one can not guarantee that uniformity among experimental units was indeed achieved with a high degree of certainty as would be in controlled laboratory experiments. Consequently, a test was undertaken to determine if there were significant differences among the plots by focusing on rings deposited prior to the thinning treatment.

The test results indicated significant difference among plots when the data are pooled, but no significant differences were evident among plots when comparisons were

made at selected heights. Thus, on balance, it was concluded that the plots were sufficiently homogeneous prior to and the significant differences observed in the tests are largely attributable to the thinning treatment.

Table 5.3: A test of thinning effects on ring width for all data combined.

Source	NDF	DDF	Type III F	Pr > F
Region	2	176	106.47	***
Thinning	2	176	28.63	0.0001
Region* Thinning	4	176	1.69	0.1544

Many studies (see for instance Myers 1963; Farrar 1961) suggest that thinning effects vary along the stem due to changes in the pattern of wood deposition, and pooling data as was done in results presented in Table 5.3 may mask important trends. Thus, thinning effects were evaluated at selected heights along the bole. The results (Table 5.4) indicate that thinning significantly affects ring width over most of the heights considered whereas, thinning by region interactions are not significant. Figure 5.6 shows variation in ring width by height and physiological age.

Studies also indicate that thinning effects diminish over time (Thomson and Barclay 1984). Liu *et al.* (1995) suggest that thinning effects on crowns tend to have a quadratic response surface. Accordingly they suggest that, following thinning, some time elapses before its effects are evident. Once thinning effects are manifest they continue to increase until a maximum is achieved from where they diminish close to the pre-treatment level as the length of time since thinning increases. This is a plausible theory, but whether it is supported by the ring width data needed to be evaluated.

Table 5.4: Tests of thinning effects on ring width by selected heights.

Height (ft)	Region	Thinning	Thinning*Region
0.5	***	0.0001 ¹⁾	0.1808
4.5		0.0002	0.5288
8.5		0.0077	0.6303
16.5		0.1922	0.6905
32.5		0.0159	0.8111
48.5		0.0273	0.2556

¹⁾ The numbers in the table are p – values.

To determine whether thinning effects on ring width show the pattern proposed, the data were grouped into three-year age classes and thinning effects were tested by height (Table 5.5). The results indicate that thinning effects are not evident during the first three years after thinning except near the tree bottom – a result that seems to agree with shift in the point of maximum growth following thinning as observed by Myers (1963), Larson (1963) and others. Thinning effects on ring width continued to be significant over the period since thinning; the thinning by region interaction by selected heights, however, remained statistically insignificant (see also Figure 5.7).

Table 5.5: Thinning effects on ring width over measurement periods for selected heights.

Height (ft)	Years since thinning											
	0-3		4 - 6		7-9		10-12					
0.5	* ¹	0.0008 ²	0.3228 ³	*	0.0008	0.4058	*	0.0001	0.1471	*	0.0001	0.3551
4.5		0.0115	0.8280		0.0001	0.4754		0.0001	0.4508		0.0001	0.3329
8.5		0.1121	0.8549		0.0001	0.4395		0.0001	0.1274		0.0001	0.4683
16.5		0.5357	0.8276		0.0035	0.1457		0.0001	0.2020		0.0011	0.2363
32.5		0.1629	0.6017		0.2747	0.5798		0.0582	0.8003		0.0006	0.8970
48.5		0.7930	0.9750		0.3288	0.5753		0.0112	0.0506		0.0745	0.3366

The numbers in the table are p – values: 1) Region 2) Thinning 3) Thinning*Region.

Results in Table 5.5 demonstrate that thinning affects ring width for the entire period of time since thinning 12 years ago. The next logical step was to determine which treatments are significantly different. To achieve this, comparisons among treatment means were undertaken using contrasts between control and thinned plots, and between heavy and light thinning treatments.

Table 5.6 : Contrast tests between control vs thinned and between heavy vs light thinning treatments.

Source	NDF	DDF	F	Pr>F
control vs thinned	1	176	19.76	0.0001
light vs heavy	1	176	0.68	0.4095

A sequential approach similar to the one used in determining thinning effects was employed. For the combined data, the control vs thinned contrast was significant, whereas the light vs heavy thinning contrast was not significant (Table 5.6). Further contrast tests were undertaken for selected heights (those displayed in Table 5.4) with none of the between heavy thin and light thin contrasts being significant. The contrast between thinned and unthinned plots were, however, significant over most parts of the stem. To determine the effects of time since thinning on these contrasts, the tests were conducted on data grouped into 3 year remeasurement periods (see Table 5.7).

Table 5.7: Contrast tests among control vs unthinned, and heavy vs light thinning treatments for selected heights by measurement periods.

Height (ft)	Years since thinning							
	0-3		4 - 6		7-9		10-12	
0.5	0.0076 ^{a)}	0.2558 ^{b)}	0.0010	0.0370	0.0001	0.0524	0.0012	0.2861
4.5	0.0334	0.3502	0.0002	0.0254	0.0001	0.0151	0.0015	0.2440
8.5	0.1586	0.5763	0.0001	0.0097	0.0001	0.0022	0.0007	0.0992
16.5	0.6660	0.9151	0.0047	0.0953	0.0001	0.0008	0.0006	0.0162
32.5	0.0813	0.2525	0.1333	0.2810	0.0290	0.1266	0.0019	0.0776
48.5	* ^{c)}	*	0.4116	0.9043	0.2055	0.8229	0.0933	0.5364

The numbers in the table are p – values: ^{a)} Control vs thinned ^{b)} Heavy thin vs light thin

^{c)} too few data points

The results indicate that during the first three years following thinning the difference between thinned and unthinned stands are significant only at points low in the bole. There is no significant difference between thinning intensities. Thinning effects became evident in most parts of the stems during 4 -12 years after thinning was applied. During the period 4-9 years after thinning, differences between heavily thinned and lightly thinned stands tended to be significant over most of the bole. Ten to twelve years after thinning, differences between heavily thinned and lightly thinned stands tended to be less significant particularly in the lower bole.

The pattern in the test results displayed in Table 5.7 seems quite in agreement with the shift in wood deposition pattern theory outlined in Farrar (1961) and Larson (1963), and reported for ponderosa pine by Myers (1963) and for Douglas-fir (Thomson and Barclay 1984). During the first few years since thinning, few significant differences are observed between thinned and unthinned stands and they occur very low in the bole.

During the last 3 years, while differences between thinned and unthinned stands remain significant, the difference between thinning intensities tend to be less significant with a pattern more or less the reverse of the first three years with significant differences occurring high on the stem. In the interim period, 4-9 years since thinning, significant differences are more widespread for both between thinned and unthinned conditions as well as between thinning intensities.

Towards the tree top, thinning effects and intensity appear to have little influence on ring width. This is probably partly due to few observations in that region, but a biological explanation can also be given. Whether a stand is thinned or not, trees first allocate photosynthate in the actively growing region of the crown. Once the need for growth and photosynthesis has been met in the actively growing region of the crown, materials are transported down the stem for storage and other needs (Kozlowski 1971).

While trees having more resources due to less competition (dominants, say) can transport materials down the stem for diameter growth and other needs, those which are subject to more intense competition use up their resources within the live crown. That means, differences between trees subject to more intense competition and those which are not is likely to be more detectable by wood deposition pattern away from the crown than that within the crown.

As seen in the various tests, on balance, the difference between light and heavy thinning was not significant hence it was decided to combine data from the two thinning levels. On the other hand, thinned plots differed significantly from unthinned plots; consequently the data were split into thinned and unthinned with thinning effect to be accounted for in the subsequent works on ring width prediction modeling .

Using variables that are known to be correlated with ring width such as ring physiological age and relative height, simple linear regression with dummy variables were

Chapter five: Thinning effects on ring width distribution and prediction models

computed. Initially three physiographic regions: Coastal Plain, Piedmont, and Other areas (Highlands) were recognized. The regression results showed that the regions are significantly different indicating separate regression coefficient estimates for the regions.

Further, to determine if significant difference in ring width is evident between the Gulf Coastal Plain and the Atlantic Coastal Plain, data from the Coastal Plain were divided into the two categories and dummy variable regression was undertaken. The results obtained indicated, that the Coastal Plain regions are indistinct in terms of ring width. Thus, the three major physiographic regions: The Coastal Plain, the Piedmont and other areas were recognized in modeling ring width (see also Figure 5.8).

In summary, three physiographic regions and two treatment combinations were recognized; Coastal Plain, Piedmont and the Highlands – thinned or unthinned. Accordingly, in subsequent works on ring width and latewood proportion, models which account for thinning treatment were separately presented for the three physiographic regions.

5.3.2.2 Effects on latewood proportion

The role thinning plays in enhancing diameter growth hence increased quantity of wood production on selected trees is seldom questioned. What is sometimes controversial is the concern that accelerated wood growth results in the deterioration of wood quality by, for instance, lowering specific gravity. Other measures of wood quality such as size, angle and distribution of branches, the topics of which are beyond the scope of this thesis, can also be used to investigate thinning effects on wood quality. The issue of thinning effects on ring specific gravity has been covered in this thesis (see Chapter 4).

Whereas specific gravity is a good indicator of wood quality, it requires specialized instruments to determine and measurements involved can be expensive and time consuming. A useful and practical surrogate for specific gravity is the latewood proportion – the proportion of latewood width to total ring width. The proportion of latewood in a piece of wood or a growth ring to the total (in terms of width) can be measured using an ordinary ruler and can be used to approximate the specific gravity of wood using regression relationships. One can thus evaluate thinning effects on wood quality using thinning effects on latewood proportion as a close surrogate for specific gravity.

In this segment a procedure similar to the one outlined in §5.3.2.2 was used to test thinning effects on latewood proportion. Since direct evaluation of thinning effects on specific gravity has been undertaken in Chapter 4, the tests conducted here serve in evaluating how well the easily measured wood characteristics, latewood proportion, mimics specific gravity. Table 5.8 presents results on thinning effects on latewood proportion.

The results indicate that thinning effects on latewood proportion are not significant. This is entirely consistent with the results obtained in chapter 4 where it was concluded that thinning does not significantly affect the specific gravity of loblolly pine trees (see Tables 4.3-4.5 in Chapter 4). Considering the highly insignificant thinning effects shown here and the results in Chapter 4, detailed analysis by height and years since thinning was deemed unnecessary and are not shown here. Suffice it to say that latewood proportion responses to thinning are similar to specific gravity responses.

Table 5.8: Tests of thinning effects on latewood proportion all data combined.

Source	NDF	DDF	Type III F	Pr > F
Region	2	176	34.52	***
Thinning	2	176	0.03	0.1752
Region* Thinning	4	176	0.96	0.3565

Physiographic region being a blocking factor is a source of variation for latewood proportion, but cannot be tested due to reasons elaborated elsewhere. A dummy variable regression was undertaken to determine which physiographic regions are significantly different. The results indicated that the data for the Atlantic Coastal Plain can be combined with the data from the Gulf Coastal Plain. The Coastal Plains are significantly different from the Piedmont and the Highlands. Thus, as in the case with ring width, three physiographic regions: Coastal Plains, Piedmont and Highlands were recognized for latewood proportion. Subsequent results on latewood proportion are presented accordingly.

5.3.3 Prediction models

5.3.3.1 Total ring width

An important component of this study was developing a ring width prediction model which can be used to predict ring width at any point in the stem. The ability to accurately predict ring width is important in two respects. If ring width can be predicted accurately and precisely, volume in standing trees can be accurately predicted for any age and height class. In addition, a ring width prediction model can serve a useful purpose in

Chapter five: Thinning effects on ring width distribution and prediction models

wood quality assessment in conjunction with or as an input to ring specific gravity prediction model. Figures 5.9 and 5.10 show the relationships between ring width and selected tree and stand factors, respectively.

The general frame work for the ring width prediction model considered was:

$$RW = f(\text{tree , stand, site, ring attributes}) + \text{error} \quad [5.3]$$

RW = ring width .

tree attributes = DBH, total height, crown size, competitive position.

stand attributes = basal area per acre, relative spacing, relative density, number of trees per acre, quadratic mean diameter, thinning treatment .

site attributes = site quality, climate, physiography.

ring attributes = physiological age, relative vertical position within a tree.

The list of factors affecting ring width is long and many of the factors tend to be redundant. The goal of the study was to obtain a model that can be used to accurately predict ring width at any position on the stem with parsimony and ease of application in that the predictor variables should be relatively easy to measure or determine. Preliminary graphical studies and the coefficient of variation indicated that ring width is highly variable (see Figure 5.1, Table 5.2), thus obtaining a model that is sufficiently precise, simple and parsimonious was a major challenge.

Average ring width by height and physiological age show a relatively clear trend. In particular, the ring width by physiological age trend is quite obvious with ring width decreasing with age. Average ring width has a tendency to decrease until about the area of breast height and then increase with height, but the trend is not as strong as that for

Chapter five: Thinning effects on ring width distribution and prediction models

physiological age (see Figure 5.1). When individual tree rings are considered rather than the average, ring width shows extreme variability.

The primary approach taken in this study was to consider models that entertain factors that have been shown or believed to affect ring width distribution along the stem. In addition to stand, site and tree attributes, ring position was considered an important determinant of ring width. Thus, a number of linear and nonlinear models involving the various factors affecting ring width distribution along the stem were considered. A sample of the models considered is presented in Appendix A5.1. The goal was to select a model with desirable properties in fit and prediction *i.e.* large R_p^2 small MB and MSE, etc.

As can be observed in Table A5.1 of Appendix A5.1, the models generally fit the data rather poorly. In particular, R_p^2 values are low across models and none of the variable transformation efforts resulted in substantial improvements. The results indicate that only limited precision can be attained with direct prediction of ring width. With respect to estimated bias, however, the values are low implying that on the average many of the models give unbiased prediction.

Based on the model selection criteria used, model [5.4] appeared the best overall model. A close competitor was the nonlinear model [5.4g] with the lowest MB and values in MSE, R_p^2 and AIC close to that of [5.4]. Nevertheless, considering all factors, [5.4] appeared most appropriate among the models considered.

$$RW = \beta_0 + \beta_1 RHT + \beta_2 RA + \beta_3 RHT * RA + \beta_4 TAP + \beta_5 CI + \beta_6 SI + \epsilon \tag{5.4}$$

where

RW is ring width in inches.

RHT is relative height.

RA is relative physiological age *i.e.* $RA = \frac{\text{ring physiological age}}{\text{disk physiological age}}$

TAP is a surrogate for stem taper $\left(\frac{DBH}{H} \right)$.

CI is stand level competition index $\left(\frac{QD(\text{in})}{DBH(\text{in})} \right)$.

SI is site index (Burkhart *et al.* 1987)

ϵ is errors as stipulated in [5.2].

β_i $i = 0, \dots, 6$ regression coefficients.

As seen in § 5.3.2.1 thinning significantly affects ring width. Thus, it was necessary to account for thinning treatment effects to improve ring width prediction. A number of alternative thinning variable expressions that express thinning as a continuous variable were evaluated. In particular a thinning variable expressions of the form proposed by Liu *et al.* (1995) which incorporate thinning intensity and time since thinning were considered. Among those considered the following modification of the Liu *et al.* (1995) thinning variable appeared reasonable and is proposed. The thinning variable gives a value of zero for unthinned stands and values which change over time for thinned stands.

Thus the following model is proposed for use in the prediction of ring width at any position in a tree bole from thinned and unthinned stands.

$$RW = \beta_0 + \beta_1 RHT + \beta_2 RA + \beta_3 RHT * RA + \beta_4 TAP + \beta_5 CI + \beta_6 SI + \beta_7 THIN + \epsilon \quad [5.5]$$

where

THIN is a thinning variable calculated as :

$$THIN = \left(\frac{BA_a}{BA_b} \right)^{\frac{(A_s - A_t) - (A_s - A_t)^2}{A_s^2}} - 1$$

BA_a is stand basal area (per acre) after thinning.

BA_b is stand basal area prior to thinning.

A_s is stand age at the time of evaluation.

A_t is stand age at the time of thinning ,and

other variables are as defined before.

Table 5.9 shows quality of fit statistics for model [5.5] for the fit and validation data. Coefficient estimates, their standard errors and other parameter estimates are displayed in Table 5.10.

Table 5.9 : Quality of fit and prediction statistics for the ring width prediction model double cross-validated on the fitting and validation data.

Data	SEE	MB	MSE	R _p ²	AIC
Fitting	0.0711	-0.0081	0.0050	0.499	31265
Validation	0.0708	0.0013	0.0049	0.506	31917

The results indicate that average ring width decreases with height and physiological age. Moreover, ring width increases with higher taper, and decreases with increasing competition and site index. The decreases in ring width with height and site index are counterintuitive, but they can be attributed to the optimization procedure; the other results are in agreement with general expectations.

Table 5.10: Coefficient estimates, asymptotic standard errors (italicized) and associated parameter estimates for the ring width prediction model.

Regions	<i>Coefficient estimates</i>								AIC	
	β_0	β_1	β_2	β_3	β_4	β_5	β_6	β_7	$\hat{\rho}$	$\hat{\sigma}^2$
Combined	0.048003 <i>0.010335</i>	-0.063720 <i>0.004937</i>	-0.217704 <i>0.003602</i>	0.185789 <i>0.007514</i>	0.959463 <i>0.035627</i>	0.002091 <i>0.000074</i>	-0.030143 <i>0.004447</i>	0.010740 <i>0.002303</i>	63211 ¹⁾ 0.673 ²⁾	0.005
Coastal Plain	0.039419 <i>0.014827</i>	-0.063764 <i>0.006765</i>	-0.221025 <i>0.004926</i>	0.193267 <i>0.010250</i>	1.004098 <i>0.051803</i>	0.002004 <i>0.000094</i>	-0.023751 <i>0.005808</i>	0.011717 <i>0.002575</i>	35931 0.681	0.005
Piedmont	0.130230 <i>0.022097</i>	-0.059002 <i>0.008290</i>	-0.220632 <i>0.006120</i>	0.155390 <i>0.012760</i>	0.695876 <i>0.079720</i>	0.002008 <i>0.000164</i>	-0.065769 <i>0.010103</i>	0.002066* <i>0.005166</i>	19807 0.681	0.004
Others	-0.065801* <i>0.040062</i>	-0.070474 <i>0.013205</i>	-0.198546 <i>0.009379</i>	0.195654 <i>0.020554</i>	0.893250 <i>0.079283</i>	0.004606 <i>0.000549</i>	-0.048900 <i>0.014721</i>	0.159642 <i>0.075794</i>	7800 0.604	0.006

* non significant ¹⁾ AIC value and ²⁾ Estimated correlation coefficient ($\hat{\rho}$).

5.3.3.2 Latewood proportion

The proportion of latewood in an annual growth ring is an important attribute as it is directly related to ring specific gravity (see §5.3.2.2). For instance, the patterns seen in Figures 5.11 and 5.12 are similar to those depicted in average ring specific gravity (Figures 4.9a, 4.9b, 4.10a, 4.10b). Similarly, a test of thinning effects on latewood proportion was not significant, again as was in ring specific gravity. Thus, based on tree, stand and site attributes outlined in §5.3.3.1, a prediction model for latewood proportion of the following form is proposed.

$$LW = f(\text{tree, stand, site, ring position}) + \text{error} \quad [5.6]$$

where

$$LW = \frac{\text{latewood width (in)}}{\text{total ring width (in)}}, \text{ and other variables are as defined earlier.}$$

A number of models were fit to the latewood proportion data. A sample of the models considered and a summary of their performance are presented in Table A5.2 in Appendix A5.2.

The models examined showed comparable performance. Whereas the prediction of latewood proportion was somewhat better than that of ring width prediction, the precision of the models was still rather weak. Increasing the number of variables did not correspondingly increase precision, some measures such as the AIC actually declined due to the penalty incurred by including variables which contribute little to the likelihood. Of the models considered, models [5.7], [5.7d], and the nonlinear model [5.7e] performed better than the other models by explaining over 50% of the total variation. Overall, however, [5.7] was the best model in fitting and prediction performance and is proposed for use in the prediction of latewood proportion.

$$LW = \beta_0 + \beta_1 ERHT + \beta_2 RA + \beta_3 (RA)^2 + \beta_4 CI + \epsilon \quad [5.7]$$

where

LW latewood proportion

$ERHT$ is $Exp(-RHT)$ and other symbols are as defined before.

Table 5.11 shows quality of fit and prediction statistics for model [5.7] for the fit and validation data. Coefficient estimates, standard errors and various parameter estimates are shown in Table 5.12.

As latewood proportion is directly related to ring width, the variability in ring width directly carries over making the development of a model which can be used to precisely predict latewood proportion rather difficult. Considering the levels of details in

Chapter five: Thinning effects on ring width distribution and prediction models

measurement of the individual growth rings and other stand and tree attributes measured, there probably is little room for any dramatic improvement. Nonetheless, the model proposed provides prediction of reasonable precision where direct measurement of the quantity is infeasible.

Table 5.11 : Quality of fit and prediction statistics for the latewood proportion model double cross-validated on the fitting and validation data.

Data	SĒE	MB	MSE	R _p ²	AIC
Fitting	0.0996	-0.00136	0.01004	0.593	21761
Validation	0.1048	-0.00057	0.01000	0.595	20898

As expected, latewood proportion increases with ring physiological age and with increasing competition, but decreases with height. This is a pattern much in agreement with ring specific gravity and confirms that latewood proportion is a good surrogate for specific gravity.

Table 5.12: Coefficient estimates, asymptotic standard errors (italicized) and associated parameter estimates for the proposed latewood proportion prediction model.

Regions	<i>Coefficient estimates</i>					AIC	σ^2	$\hat{\rho}$
	$\hat{\beta}_0$	$\hat{\beta}_1$	$\hat{\beta}_2$	$\hat{\beta}_3$	$\hat{\beta}_4$			
Combined	-0.346800 <i>0.005525</i>	0.400587 <i>0.004729</i>	0.841083 <i>0.009579</i>	-0.510958 <i>0.008680</i>	0.071183 <i>0.003428</i>	42660	0.010	0.495
Coastal Plain	-0.357517 <i>0.007279</i>	0.426136 <i>0.006516</i>	0.928707 <i>0.012842</i>	-0.570496 <i>0.011609</i>	0.058273 <i>0.004200</i>	24894	0.011	0.522
Piedmont	-0.333250 <i>0.008516</i>	0.376411 <i>0.006630</i>	0.782201 <i>0.014833</i>	-0.485079 <i>0.013616</i>	0.081186 <i>0.005877</i>	12802	0.008	0.339
Others	-0.316850 <i>0.013184</i>	0.357724 <i>0.009388</i>	0.597459 <i>0.021297</i>	-0.308970 <i>0.019233</i>	0.078687 <i>0.009594</i>	5793	0.008	0.311

Graphical analyses of ring width and latewood proportion were undertaken to obtain insight into their patterns. The literature on ring width states that tree ring widths vary from bottom to the tree top. The study on ring width variation, to a large extent, tended to conform to existing theories.

With respect to the vertical axis (Type I of Duff and Nolan 1953); as one proceeds up the stem from the tree base, ring width decreases with a minimum close to the breast height area from where it gradually increases until about the base of live crown. From about the base of the live crown until the tree top, a sharp increase in ring width is apparent. Earlywood ring width basically shows the same pattern, with the decrease in the lower bole being lower in magnitude than that for ring width and a stronger increase as one proceeds towards the tree top. Latewood width is widest at the tree base sharply declining until about the ten feet mark and then gradually decreasing towards the tree top (Figure 5.8 a,c,e).

The decrease in ring width in the horizontal axis with increasing tree diameter (Type II of Duff and Nolan 1953) is rather obvious and as expected. Average ring width

shows a temporary increase until about age 3-5 from where on it steadily decreases with increasing age. Earlywood width shows a pattern similar to that of the whole ring width except for magnitude. Latewood variation in the horizontal axis shows approximately parabolic response pattern; sharply increasing in width until about age five and then showing a gradual increase to about age ten from where it steadily decreases. The decrease in latewood with increasing physiological age (diameter) is much less than that of the total ring width (Figure 5.8 b, d, f).

With the pattern observed in total ring width and latewood width a clear connection between ring width and specific gravity can be made by examining the latewood proportion of an annual ring. In the vertical axis, we have observed that the total ring width increases with increasing height whereas latewood decreases. As a result latewood proportion decreases with height showing a pattern similar to vertical specific gravity variation (see Figures 4.5a and 5.12a). Similarly, as age increases ring width decreases in general. Due to the fast increase in latewood width initially and only a gradual decrease from about age ten, latewood proportion showed a fast increase to about age ten and a much more gradual increase thereafter – a pattern much similar to specific gravity variation with age (see Figures 4.5b and 5.12b).

5.4 Discussion and conclusions

5.4.1 Discussion

Many studies (Duff and Nolan 1953, 1957; Myers 1963) based their conclusions on limited samples either in size or distribution. This study with its scope and extent enabled us to evaluate some of the wood deposition pattern theories based on a large scale study. Thinning effects on ring width in general was as expected, with stands which received thinning treatment having larger ring width. Thinning effects do not seem to be immediate as seen by the less significant difference among the thinning treatments for the first three years since thinning.

Significant differences among the thinning treatments first occurred near the tree bottom, apparently confirming the shift in maximum growth down the bole for the stands that were thinned. The effects of thinning showed a tendency to persist over the period of time considered in this study; it would be interesting to examine the pattern thinning response takes with increasing time since thinned stands are expected to go back to the pre-thinning condition.

When one further breaks down growth rings into earlywood and latewood, thinning affects both directly. That is thinning does not increase earlywood at the expense of latewood, but both seem to be affected proportionally resulting in a more or less constant proportion of latewood width to total ring width. This result is significant in assessing effects of thinning on wood density. If the proportion of latewood width to total ring width is preserved, as they seem to be in this study (see Figure 5.12), it can be concluded that thinning does not adversely affect wood quality by significantly decreasing

Chapter five: Thinning effects on ring width distribution and prediction models

its density. This is consistent with our findings in the specific gravity study, where it was concluded that thinning at the level considered, has little adverse effect on specific gravity (Chapter 4).

Many stand characteristics particularly density measures (relative spacing, relative density and quadratic mean diameter) do not appear to have significant effects on ring width. Ring widths decrease as stand ages increase since age directly relates to diameter and the width of wood deposited annually decreases with increasing diameter. Various tree attributes showed strong relation with ring width. Crown ratio, DBH and (DBH/H), a surrogate for taper, showed strong positive correlation with ring width. Increasing crown ratio, dominance and increasing taper are all theoretically associated with increased ring width as was also confirmed in this study. As expected, increased competition as measured by stand level competition index, is negatively correlated with ring width.

In developing ring width prediction model, the various tree and stand factors as well as relative position within a tree were used as predictors. While most of the variables considered significantly entered the tested models, they only explained about half of the total variation. This is believed to be, despite the relatively well defined pattern in average ring width distribution, due to considerable variability in individual ring widths. As a result, obtaining a ring width prediction model with sufficient precision, relative for instance to diameter prediction models, was a challenging problem.

Variation observed in latewood proportion was essentially the reverse of that of ring width. Latewood proportion decreases with height, crown ratio, taper, and site index. However, latewood proportion increases with physiological age and competition. The patterns observed here serve in indicating the general tendency and are all within expectation.

The latewood proportion prediction model proposed here is useful as an input to the specific gravity prediction model (Chapter 4). Again due to large variation in individual rings, a large proportion of the total variability remained unexplained. Factors which tend to be common to a group of rings tend to have little explanatory value. This suggests that much of the source of variation in ring width is internal to the tree.

It is possible that some unmeasured biological factors inherent to the rings (or trees) are responsible for a great proportion of the variability in ring width, but unless these factors are readily measured their utility is limited in practice. What was attempted here was to model a biological process which has a tendency to vary considerably. Despite the limited precision we were able to achieve, the model proposed can be used to predict ring width and proportion of latewood.

The problem faced with obtaining a model which precisely predicts individual growth ring implies that if predictions were to be made for a group of rings, unacceptable levels of errors may be accumulated. As an alternative to using models that directly predict ring width, one can approach the problem by modeling cumulative ring width or diameter – which is monotonic hence more stable than individual growth rings. Accordingly, to determine if diameter is better predicted than ring width, diameters were generated and the predictor variables used here [see 5.4] were used to predict diameter.

The variables explained over 80 % of the total variation, a substantial improvement over what was obtained for ring width, confirming that diameter is indeed better predicted than ring width. Since stem profile modeling gives a better fit yet, and is commonly used for predicting upper stem diameters, stem profile modeling is used instead and is the topic of the next chapter (Chapter 6). It should be pointed out that studies that seek to develop models predicting growth generally perform poorer than those that are designed for

predicting cumulative growth (*a la* yield), but it does not necessarily mean that the latter are better.

Thinning effects on ring width were shown to be highly significant. As a consequence, while the need for accounting for thinning effects in ring width prediction models was understandable, obtaining an appropriate thinning variable proved to be rather difficult. The source of the problem appears to be that thinning effects on ring width must be viewed in two dimensions. Yet, including various functions of height did not yield a viable thinning variable. Consequently, a simple thinning variable that at least accounts for thinning intensity and time since thinning is proposed.

5.4.2 Conclusions

As a silvicultural tool used to enhance stand development thinning is often used in loblolly pine plantations. The study reinforces many theoretical results on thinning effects on ring width. From the results obtained in this study the following conclusions can be drawn:

i) Thinning substantially increases ring width over most of the stem of loblolly pine trees from cutover site-prepared plantations. Following thinning, increased ring width first occurs in the lower bole and then proceeds up the stem. While thinning effects on ring width were slow in taking hold, they seemed to last over the study period (12 years) indicating that thinning effects have a tendency to last long relative to intervals between operational thinnings.

ii) The magnitude of increase in ring width is not constant over the entire bole; hence, basing stand response to thinning on diameter at breast height may be misleading. In fact, breast height seems to be associated with the narrowest portion of ring width and hence probably yields a conservative estimate of growth.

iii) It appears that thinning increases the earlywood and latewood components proportionally or nearly so. As a result, while ring width increases following thinning, the proportion of latewood to total ring width remains more or less constant. This, to some extent, refutes the perception that thinning reduces wood quality by lowering specific gravity.

iv) For the thinning intensity levels considered in this study, (the removal of 30% and 50 % of total basal area for lightly thinned and heavily thinned stands, respectively) the difference in ring width between thinning intensities was not statistically significant. Nevertheless, trees in heavily thinned stands tend to have wider rings than those in lightly thinned stands.

v) Stand level factors, particularly stand density measures, showed little relation with individual ring width. It is possible that the variation in the level of these factors, particularly stand density, were not great enough to impart the expected effects on ring width. On the contrary, tree level factors such as crown ratio, dominance (large DBH) and taper are strongly related with ring width.

vi) Despite a well defined pattern in the average ring width both in the vertical and horizontal axis, individual rings showed considerable variation. Since tree level factors

Chapter five: Thinning effects on ring width distribution and prediction models

that were well correlated with ring width failed to explain much of the observed variation, ring width prediction modeling attempted met with limited precision. It appears that some within tree factor(s), possibly genetics, play significant role in determining ring width variation. Yet, growth models such as PTAEDA2 which use breast height diameter increment as an input can substantially improve their predictive capability using the model proposed in this study.

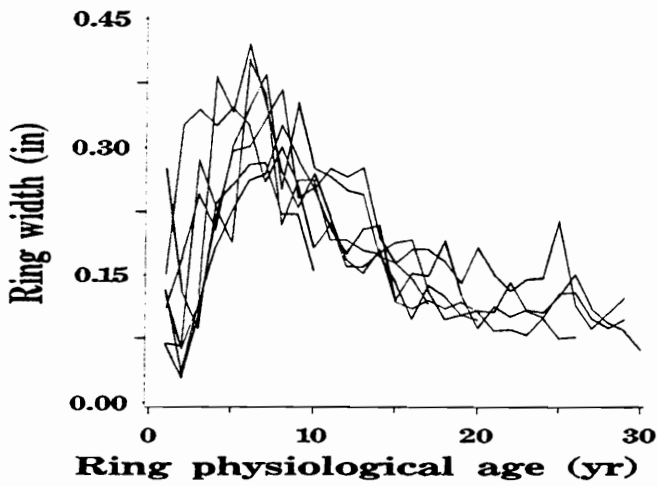
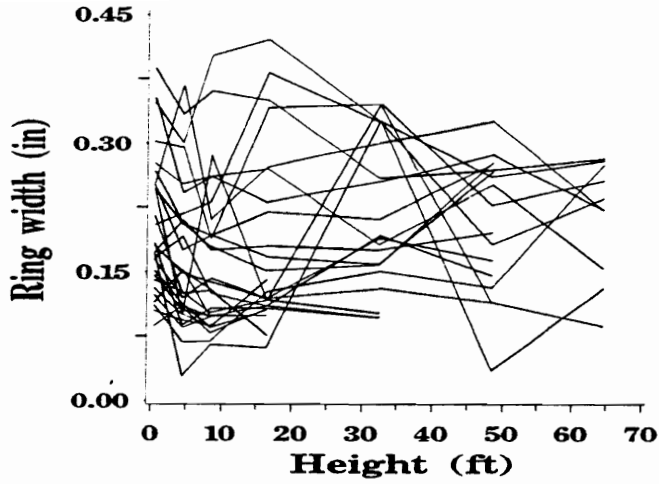


Figure 5.1: Parallel profile plots of ring width by height and by physiological age for a specific tree.

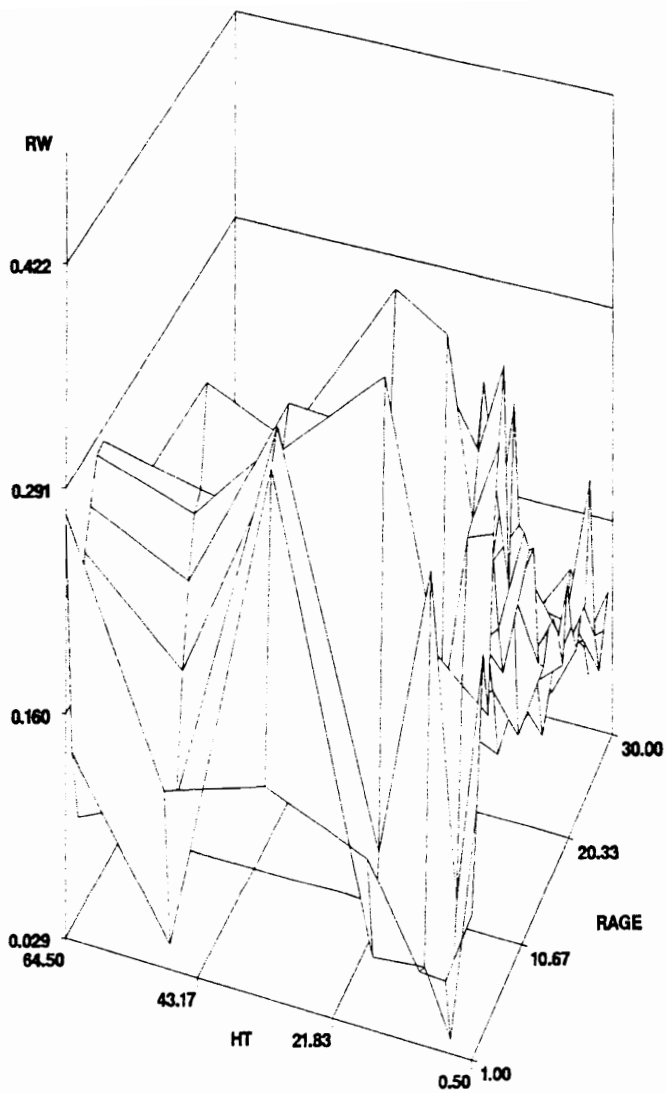


Figure 5.2: A 3D plot of ring width by height and by physiological age for a specific tree (RW= ring width, RAGE=physiological age and HT=height above ground).

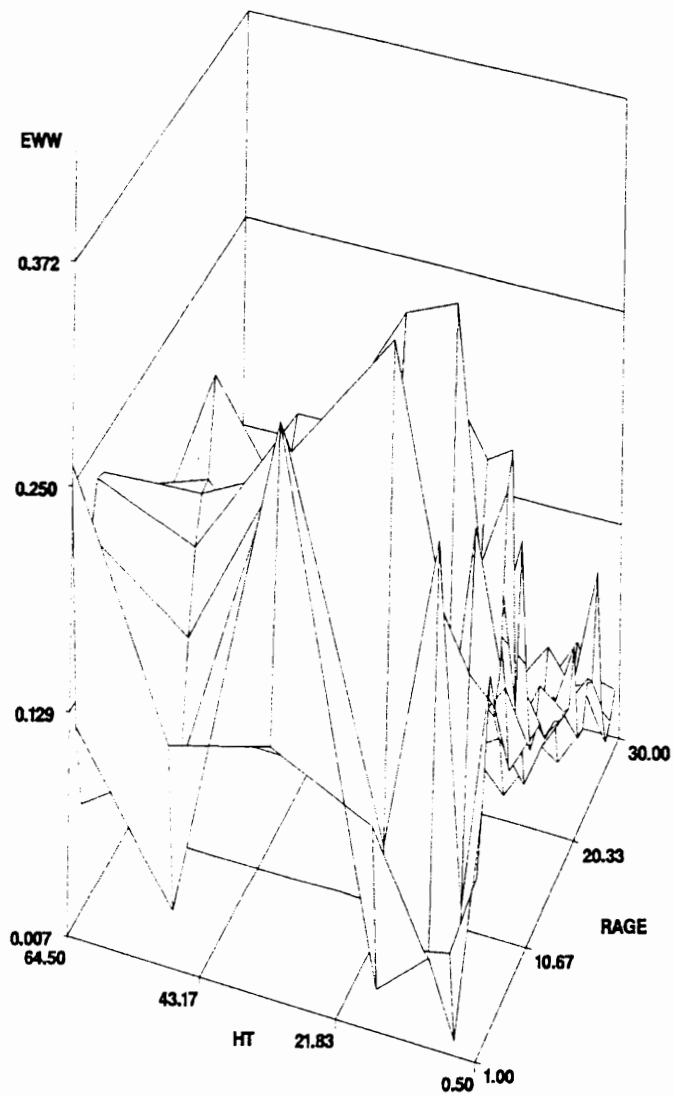


Figure 5.3 :A 3D plot of earlywood width by height and by physiological age for a specific tree (EWW=earlywood width).

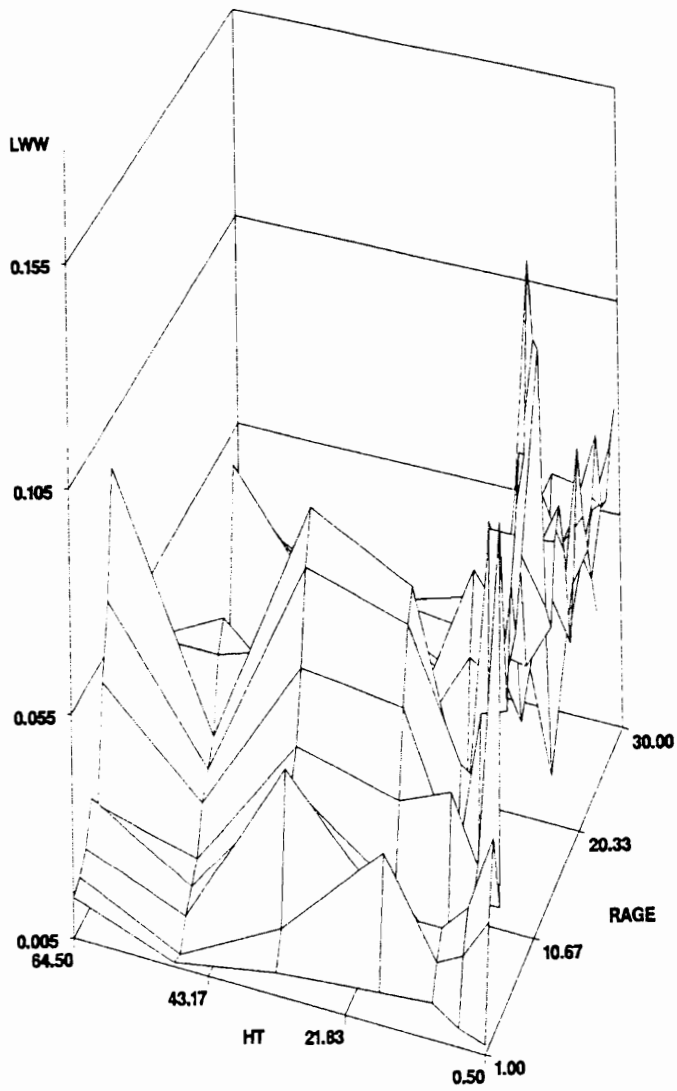
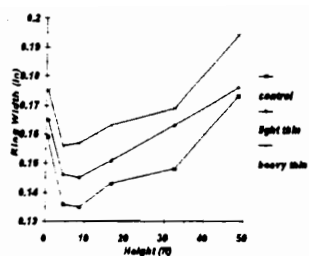
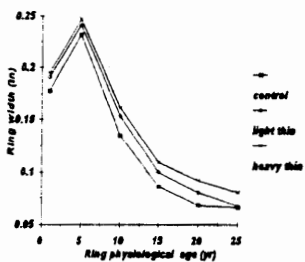


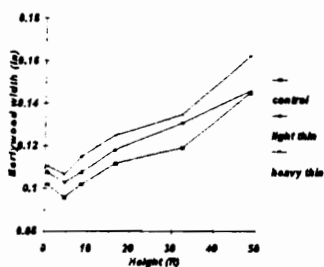
Figure 5.4: A 3D plot of latewood width by height and by physiological age for a specific tree (LWW= latewood width).



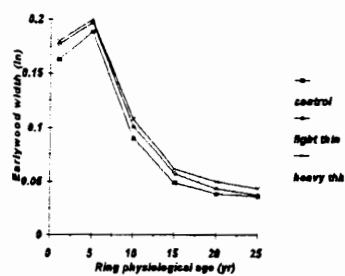
[a]



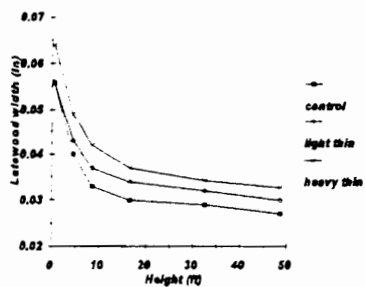
[b]



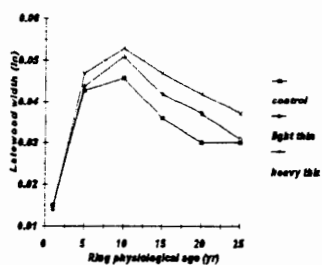
[c]



[d]

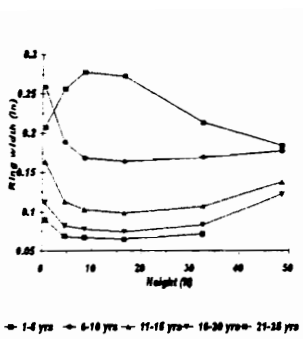


[e]

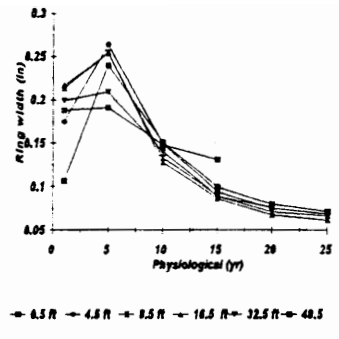


[f]

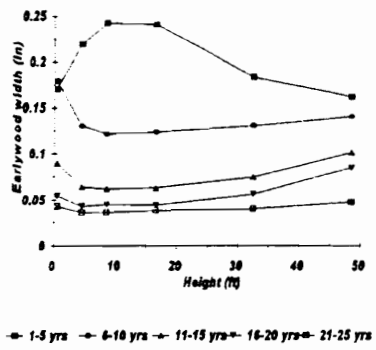
Figure 5.5 : Average ring, earlywood and latewood width by height and physiological age by thinning treatment.



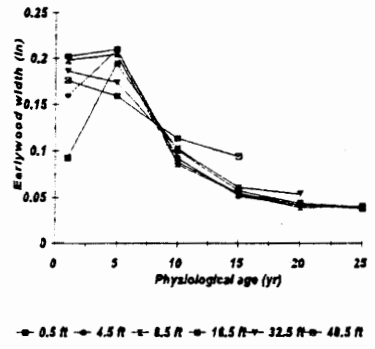
[a]



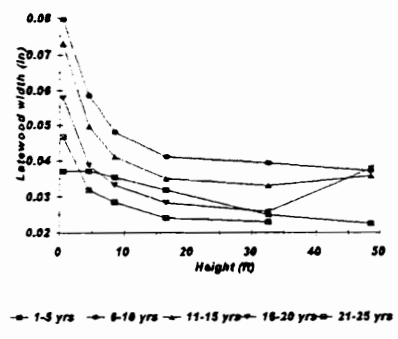
[b]



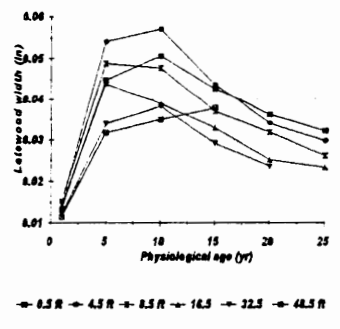
[c]



[d]

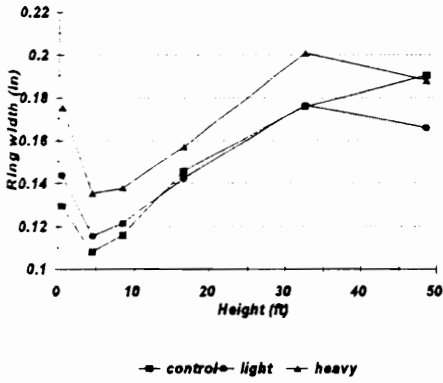


[e]

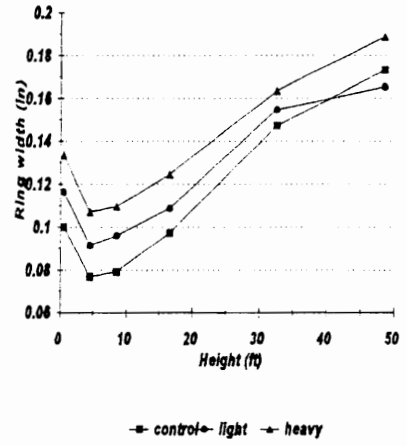


[f]

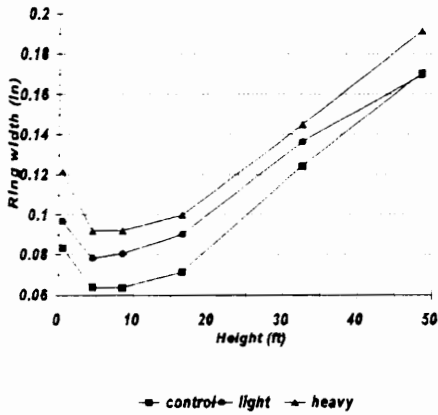
Figure 5.6 : Average ring, earlywood and latewood width by selected height and physiological age classes.



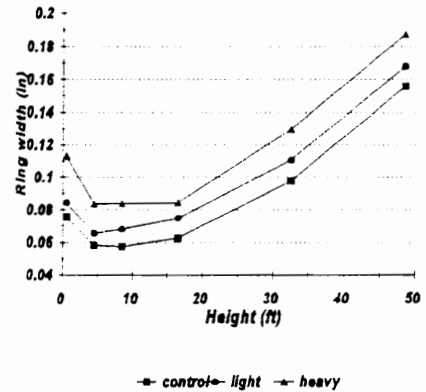
[a]



[b]

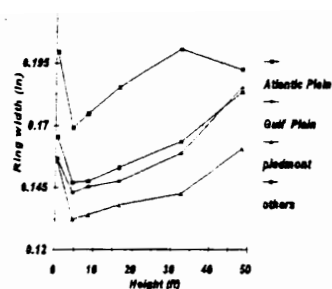


[c]

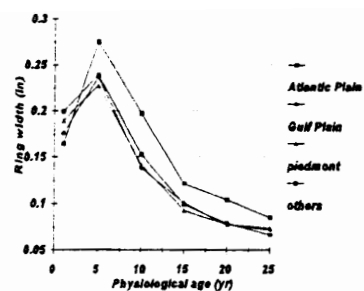


[d]

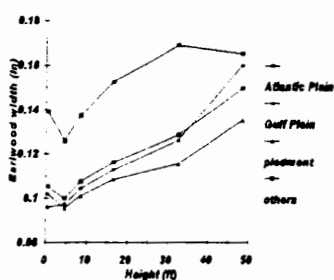
Figure 5.7: Relationships between average ring width and height over time by thinning treatment: [a] first, [b] second, [c] third, and [d] fourth remeasurement.



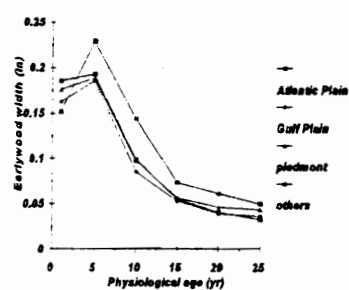
[a]



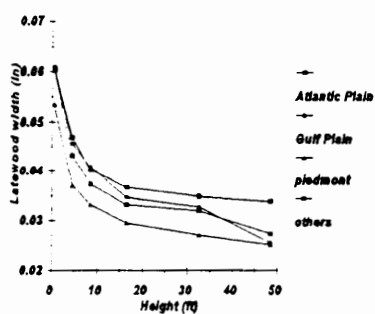
[b]



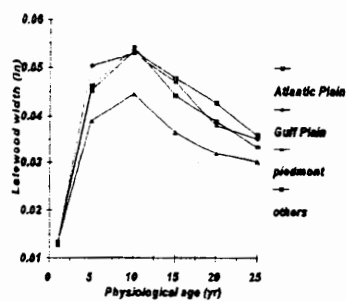
[c]



[d]



[e]



[f]

Figure 5.8: Relationships between average ring, earlywood and latewood width by height and physiological age by physiographic region.

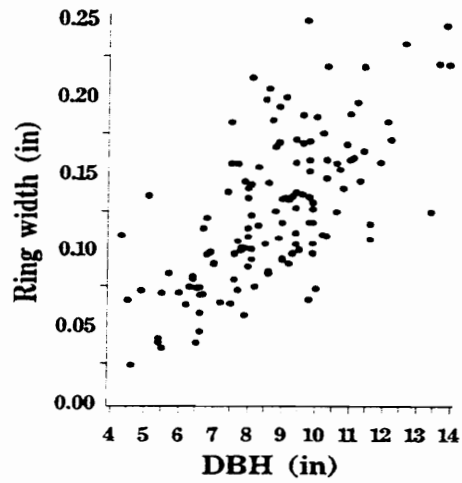
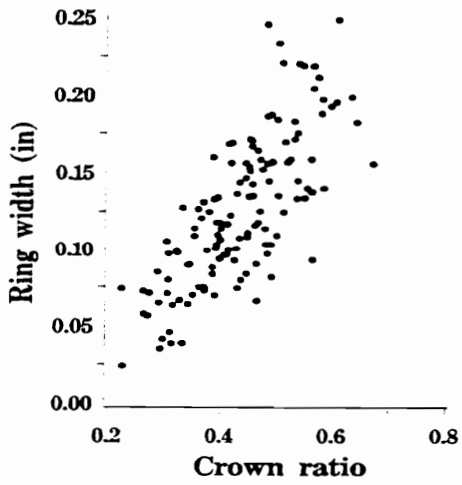
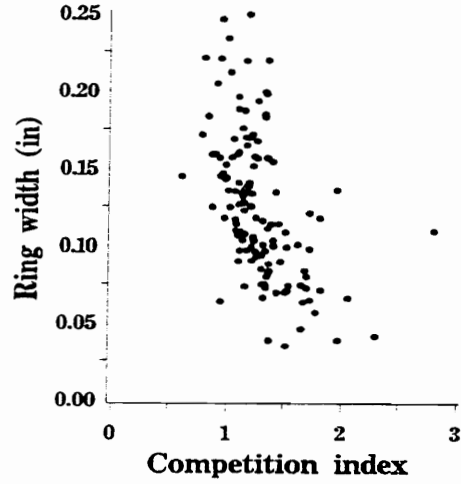
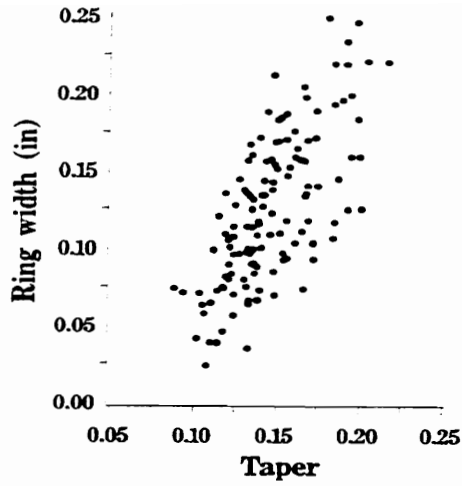


Figure 5.9: Relationships between average ring width and various tree level factors.

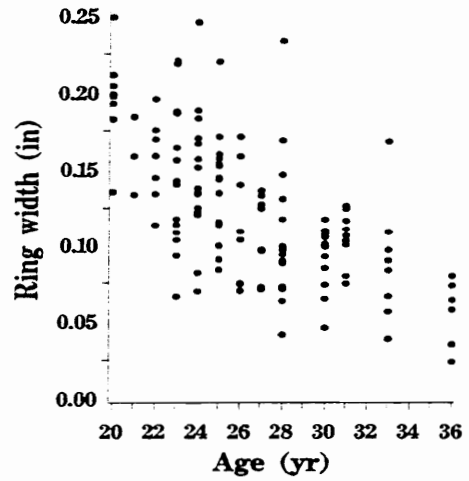
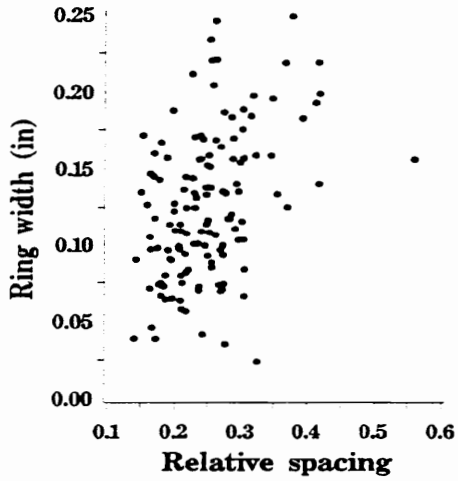
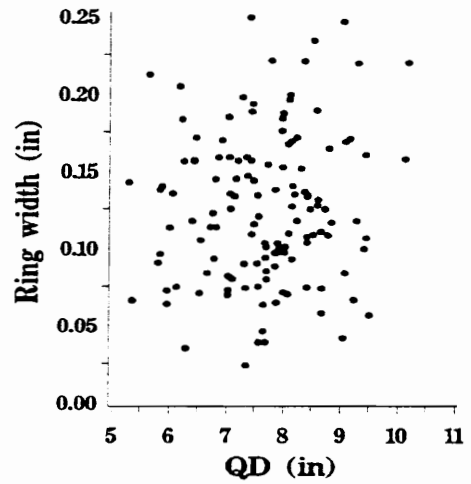
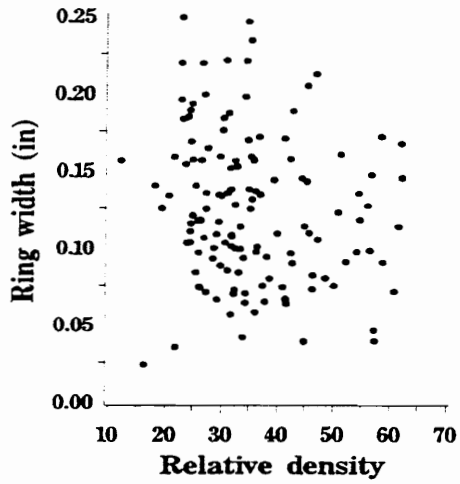


Figure 5.10: Relationships between average ring width and various stand level factors.

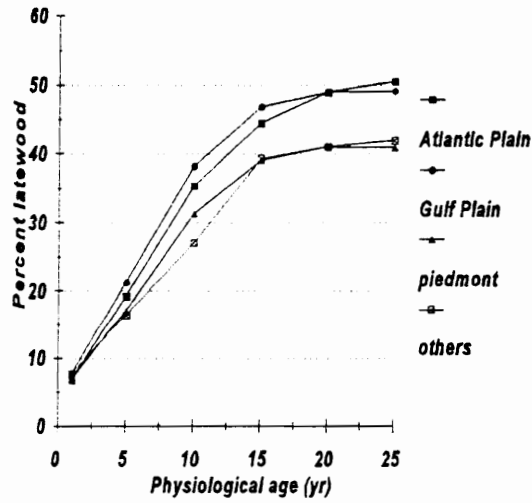
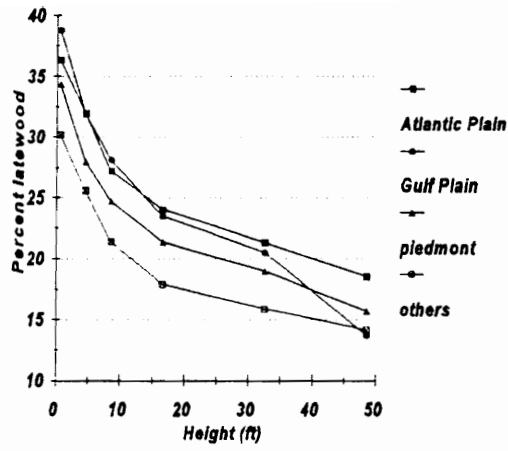
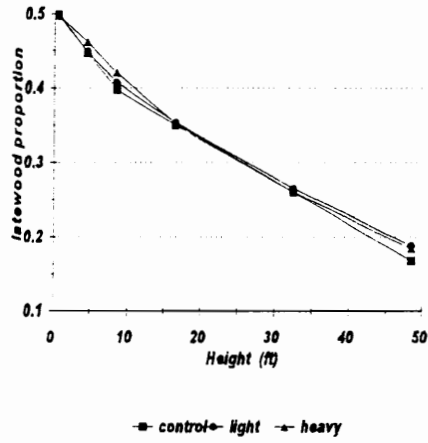
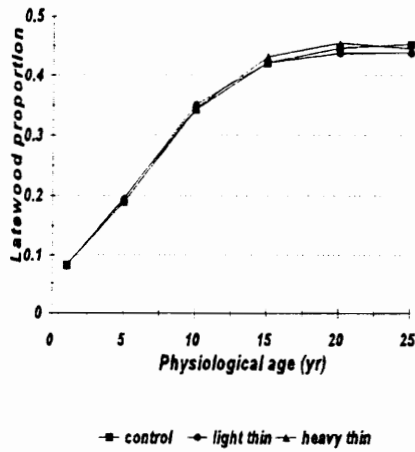


Figure 5.11: Latewood proportion by height and physiological age by physiographic region.



[a]



[b]

Figure 5.12: Latewood proportion by height and physiological age by thinning treatment.

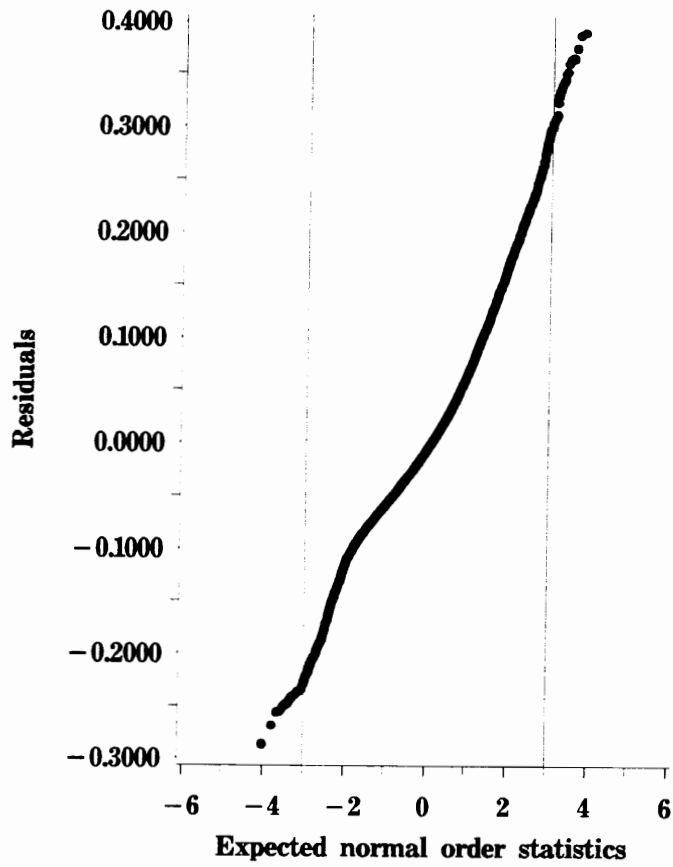


Figure 5.13: A normal probability plot of ring width residuals.

CHAPTER SIX

6.0 Thinning effects on stem form and stem profile model

6.1 Introduction and literature review

6.1.1 Introduction

Many taper¹⁵ models have been proposed for predicting upper stem diameters of loblolly pine trees (see for instance Max and Burkhart 1976; Matney and Sullivan 1980; Newberry and Burkhart 1986 and others). These models have been successfully used to predict upper stem diameters and to determine volume to various merchantability limits. As management intensity in loblolly pine plantations continues to increase, foresters require more precise and accurate volume information. To meet this challenge, it is essential to explore ways of improving existing systems to obtain more precise and accurate predictions of volume in various product classes.

Most stem profile models to date are designed to predict upper stem diameters by explaining the vertical variation in stem form¹⁶ at a specific time (see, for instance, Max and Burkhart 1976; Kozak 1988; Newnham 1992). Since stem form theories suggest that the ring width deposition pattern shifts along the stem based on changes in stand conditions prompting changes in stem form, one expects stem profile models that do not account for such changes to have their performance deteriorate with time. It is, therefore,

¹⁵ Stem profile and taper are used interchangeably in this thesis.

¹⁶ Form and profile are not synonymous, but there is a close relationship between them since form is defined by profile (such as when a geometric solid is generated by rotating a profile around an axis).

appropriate to consider models that account for anticipated changes in stem profile over time.

In the vast majority of existing stem profile modeling works, sample trees selected are from more or less uniform stands; stands that do not necessarily depict the underlying distribution of stem profiles being modeled. Therefore, they tend to be one point snapshots of stem profiles in the life of trees. That is, most existing stem profile models are *static* as they do not account for expected changes in stem profile over time; yet, to accommodate the likely changes over time, stem profile models need to also be *dynamic* as the underlying process.

While attempts have been made to develop dynamic stem profile models in the past (Clyde 1986; Muhairwe 1993) not many successful dynamic profile models exist in practice. Much of the problem in developing such models emanate from the lack of suitable data. Stem analysis data can potentially be used to reconstruct past stem profiles, but past stand history that contributed to the realized stem profile are usually unknown. Muhairwe(1993), for instance, attempted to overcome this problem by combining stem analysis data with stand information from permanent sample plots from another area.

In this study, the sample trees used in stem analysis came from permanent sample plots established for a thinning study. As a result, stand history is available and can be directly related to stem form development. The ring width and tree remeasurment data available for this study present a unique opportunity to reconstruct stem profiles of sample trees and associated stand history since plot establishment. The objectives of the study were to investigate changes in stem form at one point over time as well as along the stem at one point in time due to thinning treatment using the form exponent¹⁷; and to develop

¹⁷ See Appendix A3.1 for derivation.

a stem profile model that seeks to accommodate changes in stem form due to changes in stand density modified by thinning treatment.

6.1.2. Literature review

The literature is replete with works on stem profile modeling (see for instance Sterba 1980). Investigators have long sought to develop stem profile models, which beside predicting upper stem diameters, can be integrated to yield accurate volume estimates. According to Behre (1923), Hojer in 1903 was the first to develop a taper equation that described the diameter of a tree at any point on its stem from measurements on Norway spruce (*Picea abies* (L.) Karst.). Soon after, Jonson in 1910 and Mattsson in 1917 used data from Scots pine (*Pinus sylvestris* L.) and Russian larch (*Larix sibirica* Ledeb.), respectively, to develop taper model similar to Hojer's (Behre 1923). Noting that Hojer's function failed to fit the top and butt swell of the larch (*Larix occidentalis* Nutt.) trees he worked with, Behre (1927) developed a hyperbolic function for describing tree taper.

A number of the early investigators attempted to model stem profiles using simple functions to describe entire tree stem profiles. These models generally failed to fit the bottom and top portions of trees because they lacked the necessary flexibility in these areas. One of the reasons for the limited success of the early profile models was their simplicity due to the computational intensity required in using complex models. With the ushering in of the computer era since the 1960's, numerous more complex entire tree stem profile models have been proposed (see Bruce *et al.* 1968; Kozak *et al.* 1969; Demaerschalk 1973). The failure of single stem profile models to adequately fit the butt portion of trees, depending on species, persisted however.

The primary reason for the failure of single stem profile models, depending on species, to fit entire stem profiles is that segments of a tree bole tend to approximate various geometric solids. Husch *et al.* (1982) suggested that the bottom portion of a tree profile conforms to a neiloid frustrum, the middle to a paraboloid frustrum and the top to a cone. As a consequence, the use of a single equation to describe the often complex profile of a tree stem was questioned.

Investigators suggested that stem profiles may best be modeled in sections. Some researchers (Bennett and Swindel 1972; Amidon 1984; Rustagi and Loveless 1991), noting that the region of poor fit, the butt swell, occurred low in the bole generally below breast height, proposed models that predict diameters above breast height. The approach failed for species which tend to have large buttresses such as many tropical tree species.

Ormerod (1973), appears to be the first to successfully implement fitting tree profile model in sections. He treated the stem as two different conic sections with a common point of inflection at 30% of the total height and suggested that parameters be separately estimated for the two sections. While his work was quite significant, the results obtained tended to vary by species (Reed and Byrne 1985).

A major development in section-wise fitting of taper models to tree stem profile came about with the works of Max and Burkhart (1976) on segmented polynomial taper models. The approach alleviated the fixed join point problem of sub-models such as that of Ormerod's (1973) by allowing the join points to be estimated from data. Moreover, to some extent the number of join points itself is dictated by the data as one can specify a more complex model initially, but eventually adopt a simpler model (fewer join points or simpler functional form) if the data does not support the initial model.

Stem profile models are sometimes integrated to yield estimates of total or sectional volume of tree boles. If volume estimates obtained by integrating taper models

are different from estimates obtained from volume equations, the taper-volume systems are said to be incompatible (Demaerschalk 1972). To alleviate this problem, a number of investigators (Demaerschalk 1972; Matney and Sullivan 1980; Reed and Green 1984 and others) developed compatible stem profile models. Rustagi and Loveless (1991) developed compatible variable form volume and stem profile equations for Douglas-fir trees above breast height.

While fitting stem profiles in sections achieved one of its major breakthroughs with the segmented polynomial stem profile modeling approach, stem form variation in trees remained an obstacle to presenting a universal stem profile model applicable under all circumstances. As Grosenbaugh (1966) observed, tree stems assume an infinite number of shapes with the stem having a number of inflection points making it difficult to present a model that accurately describes the taper of the stem. Consequently, some suggested that rather than specifying any model at all, letting the fit be data driven using smoothing techniques such as cubic splines (see for instance Liu 1980). While such approach may be useful for fitting a given data set, the primary purpose of taper models is prediction which requires some form of model.

Reed and Byrne (1985) approached stem profile modeling by introducing “variable-form” taper functions. Similarly, Kozak (1988) and Newnham (1988, 1992) developed taper functions with varying exponent and variable-form taper functions, respectively. Perez *et al.* (1990), noting that the Kozak (1988) model is highly over parameterized, suggested a more parsimonious version of the variable exponent taper function for *Pinus oocarpa* Schiede in Honduras. These models were designed to account for form change along the bole. Newberry and Burkhart (1986) used Gray's (1956) stem profile model in conjunction with Ormerod's (1973) model to develop a variable form taper model.

A variety of stem profile modeling approaches have been proposed. Alternatives suggested include principal component analysis (Fries and Matern 1966), mixed-effects modeling in polar coordinates (Lappi 1986). Ojansuu and Maltamo (1995) used polar coordinates in analyzing sapwood and heartwood taper in Scots pine (*Pinus sylvestris* L.) trees. Thomas and Parresol (1991) suggested a modeling approach using trigonometric functions. While these approaches may all be based on sound theoretical principles, they do not appear to have had wide applications in practice.

To improve the prediction performance of stem profile models researchers have attempted to incorporate auxiliary information beside the traditional variables such as DBH and relative height. The pattern of wood deposition along the stem is affected by variation in the size of crown (Kozlowski 1971) which in turn is affected, among other things, by tree characteristics and stand conditions-particularly stand density (Larson 1963). For instance, Burkhart and Walton (1985) attempted to specify the join points of segmented polynomial models as functions of crown ratio.

While their attempt did not provide much improvement in the residual sum of squares, Burkhart and Walton (1985) did show that some stem form parameters are related to crown ratio. On the other hand Valenti and Cao (1986) succeeded in expressing the join points of the segmented polynomial model for the loblolly pine trees they studied. Similarly, Newberry and Burkhart (1986) used various tree and stand level variables in their variable form stem profile model.

Since stand conditions, particularly densities, change over time tree stem profile is also expected to change. Most stem profile models in use are based on the conditions of the stand at a particular point. These models, sometimes referred to as *static* models, do not explicitly account for changes in profile over time. Muhairwe (1993) developed dynamic taper model for interior lodgepole pine (*Pinus contorta* Dougl.) by modifying the

variable exponent taper equation proposed by Kozak (1988). He expressed the form exponent as a function of relative height, stand density measures and age – thus potentially accounting for form change over time.

6.2 Data and methods

6.2.1 Data

The data used in evaluating thinning effects on stem form and for developing a stem profile model were derived from the ring width data as described in § 3.1. Table 6.1 presents a descriptive summary of the data. The relationships between average form exponent and various factors are presented graphically. Accordingly, Figure 6.1 shows a parallel profile plot of the form exponent by height and time since thinning for a specific tree. A 3-dimensional view of the form exponent of the same tree is presented in Figure 6.2. Figures 6.3 and 6.4 show the relationships between average form exponent and height over time and average form exponent and time by selected heights, respectively.

Table 6.1: Tree summary statistics for stem profile model fitting and validation data

Variable	n	Mean	CV	Minimum	Maximum
<u>Fitting</u>					
DBH (in)	80	8.4	25.2	4.5	13.5
BLC (ft)	79	36.7	21.1	17.7	61.3
H (ft)	80	57.7	15.7	38.0	76.0
FE	12982	1.65	75.0	0	15.77
<u>Validation</u>					
DBH (in)	78	8.5	22.8	4.4	14.2
BLC (ft)	78	36.1	21.5	19.9	56.8
H (ft)	78	57.8	16.6	37.0	88.0
FE	12350	1.69	78.7	0	19.41

6.2.2 Methods

The data used here, as noted earlier, are a special case of the ring width data. Thus the model and notations used in §3.2 are preserved. Using the mixed-effects model [3.2] we represent the diameter measurements used in this study as:

$$Y_t = X_t' \beta + Z_t' \alpha_t + \epsilon_t \quad [6.1]$$

where

Y_t is a vector of diameter measurements for the t^{th} tree and the other variables are as defined before.

Linear mixed effects models were used to investigate thinning effects on the form exponent. Since stem profile is a nonlinear function of height, nonlinear models were used in stem profile modeling. The possibility of accounting for correlations by direct covariance modeling in R or indirectly by including random effect covariates or both simultaneously were considered.

6.3 Results and analyses

6.3.1 Covariance structure

Specifying random covariates and direct modeling of correlation in R simultaneously was not supported by the data. Thus, both direct covariance modeling and the inclusion of random effects were considered separately. For hypothesis tests on thinning effects, direct covariance modeling was superior since it resulted in a substantially higher AIC values than including random effects covariates. Accounting for correlations by including random effect covariates proved to be superior in modeling stem profiles. In line with the works on the other issues addressed in this thesis, correlations among observations were expected to diminish with spatial or temporal distance.

Since fitting under the continuous autoregressive structure occasionally resulted in numerical difficulties, the AR(1) structure was selected for direct covariance modeling. Regarding correlations among measurements on rings in subsequent growth years and those among measurements on the same growth ring, depicted respectively by ξ_{ti} and ξ_{th} , the former tended to be substantially stronger. Thus, variance-covariance structure with the ξ_{ti} 's in the diagonal matrices, as displayed in [3.13], was used. Also, all off-diagonal matrices were set identically to zero *i.e.* again $Cov(\epsilon_{thi}, \epsilon_{th'i}) = 0$. Accordingly for testing thinning effects on the form exponent, model [6.1] was modified to:

$$Y_t = X_t' \beta + \epsilon_t \quad [6.2]$$

where

$$\epsilon_t \sim N(0, R_t)$$

$$Y_t \sim N(X_t' \beta, R_t)$$

$$R_t = BD(\sigma^2 \rho^{|\delta_{it}|})$$

BD is block diagonal and other symbols are as defined before.

We recall that [6.2] is a special case of [3.2] and [6.1] with $Z_t = 0$. Since the specification appropriately accounts for correlation among observations, a substantial gain was achieved over ignoring correlation as measured by the AIC and the LRT.

6.3.2 Thinning effects on stem form

In our treatment of ring width distribution we have observed that thinning significantly affects ring width. Particularly thinned stands tend to have wider rings than unthinned stands. It was also observed that no significant difference existed between the ring widths of lightly thinned and heavily thinned stands. Due to the close relationship between the ring width data and the derived diameter measurements used in stem profile modeling, the results from tests on thinning effects on ring width can be considered directly applicable to thinning effects on stem form.

Alternatively, thinning effects on stem form can be evaluated via test on its effects on the form exponent. This approach was taken to test thinning effects on stem form because the form exponent directly relates to stem profile and the method provided an opportunity to compare results obtained here with those of tests on thinning effects on ring width.

In testing thinning effects on stem form, we again refer to the distribution of the permanent sample plots in the various physiographic regions at the different locations. The results of a test on thinning effects on the form exponent are presented (see Table 6.2).

Table 6.2 : A test of thinning effects on the form exponent for all data combined.

Source	NDF	DDF	Type III F	Pr >F
Region	2	149	1.79	***
Thinning	2	149	7.62	0.0007
Region*Thinning	4	149	2.76	0.0296

As observed in Table 6.2 thinning effects on the form exponent and the thinning by region interaction are both significant. Now to determine if the significance in thinning treatment effect is due to the difference in the form exponent of trees from thinned stands or if it is due to differences in thinning intensity (light thin vs heavy thin) or both, contrast tests were undertaken. The results indicate that the difference in the form exponent between thinned and control stands is significant, but there is no significant difference between the heavily and lightly thinned stands (see Table 6.3).

Table 6.3 : A contrast test between control vs thinned and between heavy vs light thinning treatments.

Source	NDF	DDF	F	Pr>F
control vs thinned	1	149	7.77	0.0026
light vs heavy	1	149	2.19	0.1408

We have, so far, attempted to determine thinning effects on the form exponent by pooling all data together. However, due to changes in the pattern of wood deposition along the stem, thinning effects on stem form may vary by the vertical position in the stem.

Therefore, tests on thinning effects were undertaken for selected height classes. Table 6.4 presents results of the tests.

Table 6.4 : Tests of thinning effects on the form exponent, and contrast tests between control vs thinned and light vs heavy thinning treatment by height classes.

Height class (ft)	thinning	thinning*region	control vs thinned	light vs heavy
≤ 12.5	0.0343 ¹⁾	0.6047	0.0341	0.2713
>12.5 ≤ 32.5	0.0021	0.0050	0.0389	0.7134
>32.5	0.0025	0.0003	0.0017	0.0443

¹⁾ The numbers in the table are *p*-values.

A more detailed analysis of thinning effects by height and measurement occasions were also conducted. However, the results for most heights were non significant and are not reported here.

In testing thinning effects on stem form, as usual, the *p*-values associated with regions were not reported because region is a blocking factor. A dummy variable regression was conducted to determine differences among physiographic regions. The results indicated that tree form in the Coastal Plain is significantly different from the Piedmont, whereas the difference between the Piedmont and the Highland areas was not significant.

A dummy variable regression conducted to determine if differences in tree stem form existed between the Gulf Coastal Plain and the Atlantic Coastal Plain was not significant. Thus, it was concluded that the data from the Piedmont can be combined with the data from the Highlands and the data from the Atlantic Coastal Plain can be combined with that from the Gulf Coastal Plain for the purpose of stem profile modeling.

6.3.3 Stem profile model

Modeling stem profile to obtain accurate and precise prediction of upper stem diameters was a primary objective of this study. As seen in Figures 6.3 and 6.4, the basic stem form parameter, the form exponent, varies by height and over time. Furthermore, some tree and stand level factors are related to the form exponent (see Figures 6.5 and 6.6). To enable the development of a dynamic model, models which reflect changes in stem form as a result of changes in tree and stand conditions are needed. Thus, we define upper stem diameter, d , say as:

$$d = f(tc_i, sc_i, p) + error \quad [6.3]$$

where

d is diameter at any point along the stem.

tc_i is tree characteristics at time i .

sc_i is stand conditions at time i .

p is position in tree usually expressed as a function of relative

height ; $\frac{h}{H}$, where h is height above ground and H is total tree height.

The taper of a tree can be defined by a simple function such as the one given in [A3.1] (Husch *et al.* 1982). A practical example corresponding to [A3.1] is Ormerod's (1973) model in which $Y = \frac{d}{D_{bh}}$ and $X = \frac{H-h}{H-4.5}$ the parameter r is estimated from the data and approximates the average tree form.

However, as noted earlier, using average tree form does not provide a good upper stem diameter prediction as the main bole of a tree is a composite of geometrical solids

(Husch *et al.* 1982). The question, which can not definitively be answered because of the extreme variability of tree stem, is how many geometric solids does it exactly take to represent a tree bole?

The issue is further complicated as the form exponent should vary not only along the tree stem at one time, but also over time. These variations cause a tree stem profile to vary from one point in time to the next (see Figures 6.7 and 6.8). So, what we have is not a constant form exponent r , but r_{thi} , *i.e.* the form exponent of the t^{th} tree at the h^{th} height at the i^{th} time. By taking Ormerod's (1973) model as the base:

Let

$$Y = \delta X^\omega + \epsilon \quad [6.4]$$

where

$$Y = \frac{d}{D_b} \text{ and } X = \left(\frac{H-h}{H-4.5} \right)$$

H is total tree height,

D is diameter at breast height,

ω and δ are parameters to be estimated.

As can be observed from several existing stem profile models, various functions of relative height tend to account for a very large proportion of the total variation in predicting upper stem diameters. As a consequence, here, we seek to include stand level variables for which measurements have been collected over the thinning study period and are believed to contribute to changes in a stem profile in order to improve the prediction of upper stem diameters.

Much in the same spirit as in Newnham (1988, 1992) and Kozak (1988), a continuous form exponent (ω) is assumed. Further, it is assumed that variation in δ , a

variable often associated with taper, would be accounted for by variation in tree, site and stand characteristics; whereas we assume that variation in α can be accounted for by functions of relative height.

Thus,

$$\delta = f(\text{tree, stand and site characteristics})$$

$$\omega = f(\text{relative height})$$

Among the tree characteristics considered were: crown ratio, the ratio of diameter at breast height to tree height, DBH and tree's competitive position. Stand characteristics considered include stand density measures such as basal area per acre, relative density and relative spacing. Also, the role of stand age as a predictor variable was investigated. Site index was used to approximate the inherent productivity of sites.

Several models that included variables correlated with diameter and used in other taper models were fitted to the data. The results of the fit and prediction performance of a sample of the models considered are presented in Table A6.1 in Appendix 6.1. The models presented showed comparable performance with none of the models showing clear advantage. Consequently, the parsimonious model [6.5] was selected.

$$d_{thi} = D_{ti}^{\beta_1} \left(\frac{D_{ti}}{H_{ti}} \right)^{\beta_2} \left(\frac{SI}{A_s} \right)^{\beta_3} RE_{ti}^{\omega} + \epsilon_{thi} \quad [6.5]$$

where

$$\omega = \alpha_1 X_{ti}^2 + \alpha_2 \ln(X_{ti} + 0.001)$$

d_{thi} is diameter inside bark of the t^{th} tree at the h^{th} height at time i .

D_{ti} is the DBH of the t^{th} tree at time i .

H_{ti} is the total height of the t^{th} tree at time i .

SI is site index (Burkhart *et al.* 1987).

RE_{ti} is defined as $\frac{H_{ti} - h_{t,i}}{H_{ti} - 4.5}$.

X_{thi} is relative height $\left(\frac{h_{t,i}}{H_{t,:}}\right)$.

\ln is natural logarithm.

α, β, γ are regression coefficients.

ϵ_{thi} are errors whose distribution is assumed to be as in [6.2].

Model [6.5] was compared with some existing stem profile models to evaluate its efficacy. The models chosen for comparison were the Max and Burkhart (1976) segmented polynomial model and Kozak's (1988) variable exponent taper model. The Kozak (1988) model and the new model proposed here performed about the same, with the Kozak (1988) model performing slightly better in some respects. The Max and Burkhart (1976) model did not perform quite as well. The results are presented in Table A6.2.1 of Appendix A6.2.

In the effort to develop dynamic stem profile model the basic premise taken was that stem form is affected by stand factors – particularly stand density. However, stand density measures such as quadratic mean diameter, relative spacing, relative density failed to significantly enter the stem profile models considered. Whereas stand level competition index entered some of the models, it was not significant in the final model selected.

In § 6.3.2 it has been established that thinning affects tree stem form and hence profile. Thus it was necessary to account for thinning effects in modeling stem profile. A valid, but cumbersome, approach that can be and often is taken is to fit model [6.5] to the data from thinned plots and unthinned plots separately. Alternatively, particularly in

the case of sparse data, one can account for thinning directly using a thinning variable designed to depict thinning effects.

The thinning variables that were proposed for crown ratio by Short and Burkhart (1992) and Liu *et al.* (1995) were considered to determine if they could be used directly. These thinning variables, however, did not fit the stem profile data suitably, but a variable constructed by a modification of the Liu *et al.* (1995) thinning variable proved to be a useful approximation to thinning effects among the alternatives considered. Accordingly model [6.5] was modified to account for thinning treatment as:

$$d_{thi} = D_{ti}^{\beta_1} \left(\frac{D_i}{H_i} \right)^{\beta_2} \left(\frac{SI}{A_s} \right)^{\beta_3} RE_{ti}^{\omega} \gamma_1 T_{thi} + \epsilon_{thi} \quad [6.6]$$

where

$$T_{thi} = \left(\frac{BA_a}{BA_b} \right)^{\gamma_2 X_{thi}} \left(\frac{(A_s - A_t) - (A_s - A_t)^2}{A_s^2} \right)$$

A_s is stand age at time i .

A_t stand age at the time of thinning.

BA_a is stand basal area after thinning.

BA_b is stand basal area before thinning.

and other symbols are as defined before.

Table 6.5 presents the quality of fit and prediction performance of the modified model [6.6].

Table 6.5: Quality of fit and prediction statistics for the stem profile model
double cross-validated on the fitting and validation data.

Data	SEE	MB	MSE	R _p ²	AIC
Fitting	0.5185	0.0342	0.1987	0.961	-4149
Validation	0.4204	0.0267	0.3120	0.947	-3002

To account for the expected correlation among observations from the same tree, direct covariance modeling as was done in § 6.3.2 and indirectly accounting for correlation by including random effect covariates were considered. Based on the AIC criterion, the inclusion of random effects appeared more justifiable (substantial increase in the AIC value) than direct covariance modeling. However, including random effect covariates rendered the taper variable $\left(\frac{D_{ti}}{H_{ti}}\right)$ insignificant. Consequently, the variable was dropped and the remaining parameters in model [6.7] were re-estimated .

$$d_{thi} = D_{ti}^{\beta_1} \left(\frac{SI}{A_s}\right)^{\beta_2} RE_{ti}^{\omega} \gamma_{1t} T_{thi} + \epsilon_{thi} \quad [6.7]$$

where

$$\omega = \alpha_{1t} X_{thi}^2 + \alpha_{2t} \ln(X_{thi} + 0.001)$$

$$T_{thi} = \left(\frac{BA_t}{BA_s}\right)^{\gamma_{2t}} X_{thi} \left(\frac{A_s - A_t - (A_s - A_t)^2}{A_s^2}\right)$$

and other variables are as defined before.

Due to the inclusion of the random effect covariates, we assume that the ϵ_t have local independence; *i.e.* $R_t = I_t$. The asymptotic distributional properties of Y_t , ϵ_t , and

the parameters are as outlined in Chapter 3 and § 6.2.3 in this Chapter. Given the random effects parameters, model [6.7] is an individualization of model [6.6] and allows a closer fit to the individual tree data. Modifying the model by including random effects resulted in an increase in the AIC by up to 49 % – indicating a substantial improvement over the OLS fit.

Predictions of upper stem diameters for new trees is undertaken at the expected value of the random effects *i.e.* by using the fixed effects coefficient estimates only. Because the OLS coefficient estimates of the regression parameters are unbiased, the use of [6.7] rather than [6.6] should not be expected to lead to any improvement in the point estimates (in prediction), but addresses biases in confidence intervals and hypothesis tests on the estimated parameters. Table 6.6-6.8 present coefficient estimates and various statistics for the model selected.

Table 6.6: Estimates of regression parameters, covariance parameters standard errors and quality of fit measures for all regions combined.

Parameter	Regression Parameter Estimates	Est. Std. Error of Regression Parameter	Covariance Parameter Estimates	Est. Std Error of Covariance Parameters	AIC and Estimated Variance
β_1	1.010717	0.009357			AIC = -3766 $\hat{\sigma}^2 = 0.0995$
β_2	-0.050023	0.005828			
α_1	0.750420	0.012183	0.02026	0.002462	
α_2	-0.400521	0.014591	0.03073	0.003904	
γ_1	1.027470	0.021551	0.00164	0.000209	
γ_2	-0.388500	0.039417	0.24040	0.031671	

Table 6.7: Estimates of regression parameters, covariance parameters, standard errors and quality of fit measures for the Coastal Plain.

Parameter	Regression Parameter Estimates	Est. Std. Error of Regression Parameter	Covariance Parameter Estimates	Est. Std Error of Covariance Parameters	AIC and Estimated Variance
β_1	1.010717	0.009357			AIC = -2585 $\hat{\sigma}^2 = 0.1147$
β_2	-0.050023	0.005828			
$\hat{\alpha}_1$	0.750420	0.012183	0.01975	0.003205	
$\hat{\alpha}_2$	-0.400521	0.014591	0.02468	0.004239	
γ_1	1.027470	0.021551	0.00131	0.000230	
γ_2	-0.388500	0.039417	0.24030	0.041400	

Table 6.8: Estimates of regression parameters, covariance parameters, standard errors and quality of fit measures for the Piedmont.¹⁸

Parameter	Regression Parameter Estimates	Est. Std. Error of Regression Parameter	Covariance Parameter Estimates	Est. Std Error of Covariance Parameters	AIC and Estimated Variance
β_1	0.995558	0.017179			AIC = -1113 $\hat{\sigma}^2 = 0.0785$
β_2	-0.070054	0.010269			
α_1	0.754955	0.019053	0.02153	0.003965	
α_2	-0.416165	0.025173	0.04071	0.007690	
γ_1	1.068614	0.041362	0.00225	0.000430	
γ_2	-0.400149	0.060270	0.25218	0.051330	

Average form exponent shows a well defined within tree variation. As observed in Figures 6.1-6.3, the form exponent tends to decrease with height sharply at first, but gradually beyond the lower bole. The primary reason for the fast decrease in the form exponent values in the lower bole is because the region is associated with a neiloid form;

¹⁸ Here Piedmont includes the Highlands (Other areas).

in essence sharp difference between the rate of change in relative diameter and the rate of change in relative height. The middle portion where changes in the form exponent is gradual is associated with the more paraboloid form.

The form exponent changes at one point in the stem over time. Changes in the form exponent from one time period to the next is to be expected since changes in relative diameter is likely to be different from changes in relative height from one time period to the next. The form exponent generally increases with increasing time since thinning. Here also, the heavily thinned stands show a tendency to have larger form exponent than the lightly thinned stands and the control stands (see Figure 6.4).

The relationships between average form exponent and average tree and stand level factors are depicted in Figures 6.5 and 6.6. The form exponent increases with DBH, total tree height and crown ratio, but decreases as competition level increases. This seems to agree rather well with the concept that trees with large diameter are more tapered (larger form exponent) and trees subject to high competition are less tapered (small form exponent). The relationship between the form exponent and stand level factors is not well defined. To a minor extent, however, the form exponent appears to increase with quadratic mean diameter and relative density, but decrease with relative spacing and stand age.

Variations in the form exponent among thinning treatments also are evident. The heavily thinned stands, in general, have larger form exponents in the lower bole area than the lightly thinned and control stands. Considering the fact that diameter growth shifts to the lower bole, at least temporarily, for thinned stands it seems that the lower bole areas of trees from the heavily thinned stands have a tendency to show a more neiloid form. As one proceeds up the stem, however, the distinction among thinning treatments tends to be rather fuzzy.

6.4 Discussion and Conclusions

6.4.1 Discussion

The principal objectives of the study in this chapter were effectively addressed through tests on the form exponent and stem profile modeling. The results tended to show that thinning at the level applied to the loblolly pine plantations had significant effects on stem form. Similar tests were also undertaken using diameter as the dependent variable. The results obtained essentially confirmed the findings with the form exponent. Consequently, the form exponent proved to be a useful tool in assessing thinning effects on stem form.

Several theories suggest that variation in the pattern of wood deposition along a tree stem is largely dictated by stand density (Larson 1963; Myers 1963). Many studies in the past have considered improving prediction of stem profiles by including auxiliary variables (see Burkhart and Walton 1985; Byrne 1993; Muhairwe 1993 and others) essentially with limited success. The possibility of improving stem profile prediction by including stand level factors to account for possible changes in the stem form attempted in this study also met with a limited success since the stand density measures failed to enter a model which effectively predicts upper stem diameter.

Most existing stem profile models describe variation in tree form and taper by functions of relative height. The results of this study also showed that the within tree factors particularly functions of relative height explain over 90 % of the variations in tree stem profiles. While the lack of significant stand density measures in the stem profile models may appear odd, it is noteworthy that most of the effects of stand density measures

are manifested by tree level factors *i.e.* by diameters at the various heights. It has to be remembered that the thinning variable included in the model selected also accounts for some changes in stand densities.

The weak correlation between stand level variables and tree stem profile causes one to ponder whether the approach taken by some investigators, such as Fries and Matern (1966) and others, of using principal components analysis is not the way to go. However, it is not difficult to note that such approaches are of little practical utility since the significance of the first, second, etc. principal component do not translate into easily measurable variables to be used in prediction. Because of the interdependence between the tree level factors and stand level factors (density in particular) little gain in predictive ability was achieved. However, the exercise here enabled us to address the issue of bias in the standard error of estimates which is largely ignored in traditional stem profile modeling.

Regarding the thinning variable, attempts made to effectively model the wood deposition pattern expected following thinning was not very successful. The hypothesis that the maximum wood deposition shifts to close to the tree base following thinning and then shifts up the stem as stand density increases requires a complicated model which itself is a function of several variables (position in the tree, thinning level, time since thinning and stand condition, etc.) basically on a continuous scale. Even if technically such a model can be constructed, it still has to be incorporated with a basic stem profile model that describes an average tree profile; calling for a very cumbersome model whose parameters can at best be estimated poorly.

Unlike laboratory experiments where factors can be controlled, field studies such as the one considered here tend to be observational where factors can only be partly controlled. Alternatively stated, the realized response cannot be partitioned and assigned

to the various factors. Therefore modeling response as a function of the factors in accordance with existing theories becomes a problem. Consequently a simpler thinning variable that does take into account time since thinning and, to some extent, position along the stem is adopted to represent thinning effects on stem form.

As pointed out earlier, due to the extreme variation in ring width, obtaining adequately precise ring prediction model was a problem. Since cumulative values (here diameter at one time point) is monotonic, stem profiles tend to be smoother and less variable than individual ring growth – akin to the relationship between growth and yield (see also Figures 6.9 and 6.10). Thus, by approaching the problem from the stem profile modeling perspective, considerable gain over the direct prediction of ring width has been achieved.

6.4.2 Conclusions

This study has provided an opportunity to evaluate thinning effects on stem form from a different perspective. The data available in this study enabled us to examine the efficacy of using height diameter measurements from several occasions to model tree stem profiles. It is believed that the study has extended our understanding of thinning effects on tree stem form variation. The following conclusions can be made based on the results obtained.

i) Thinning, at the level considered, significantly affects the stem forms of loblolly pine trees in plantations on cutover, site-prepared areas. Thinned stands have a tendency to have larger form exponent values than unthinned stand particularly in the lower bole area.

ii) Differences in stem form due to differences in thinning intensity (removal of approximately 30 % and 50% of the total basal area) were not significant. Consequently, in deciding on which of the two levels to choose, other factors should be considered.

iii) A large proportion of the total variation in stem profile is explained by tree level variables (DBH, total tree height, etc.). As most stand level influences are directly reflected by these tree level variables, including stand level variables such as stand density measures contribute little to improving prediction of upper stem diameters.

iv) The form exponent is a good measure for evaluating thinning effects on stem form. Though no formal comparisons were made, the form exponent determined from several pairs of height diameter measurements should yield better indication of effects of silvicultural treatments on stem form than measures which use two or less pairs of height diameter measurements such as form quotients .

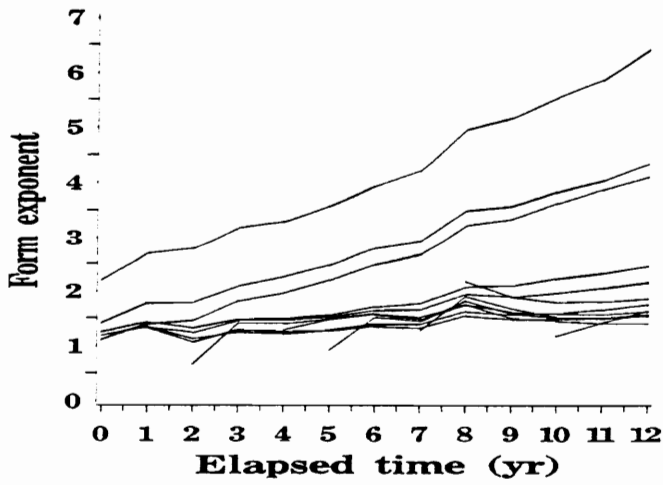
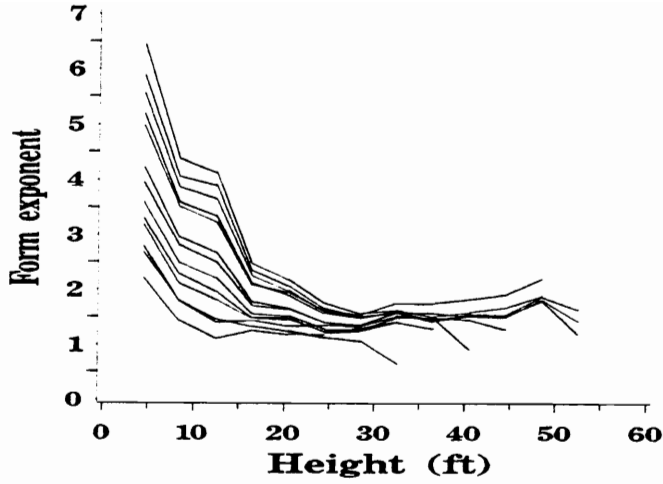


Figure 6.1: Parallel profile plots of the form exponent by height and time since thinning for a specific tree.

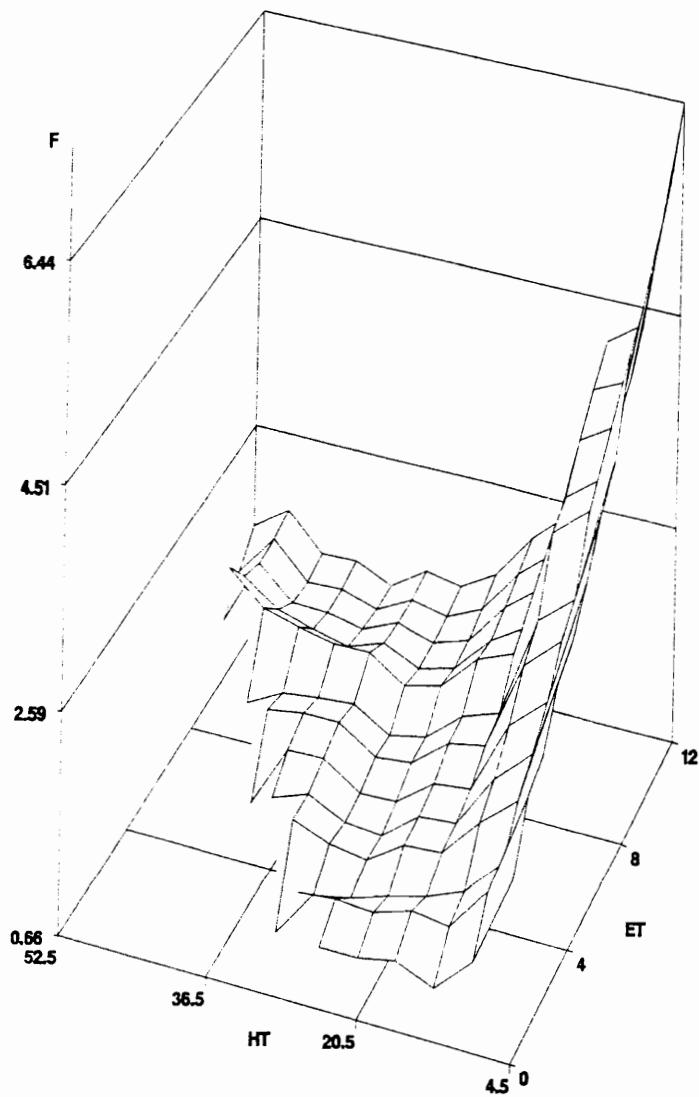
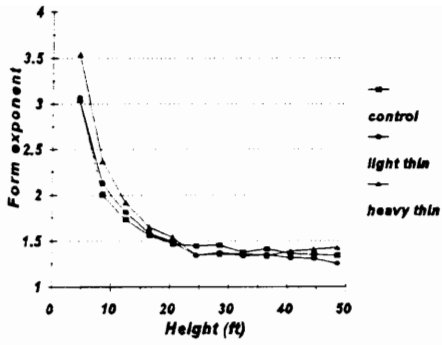
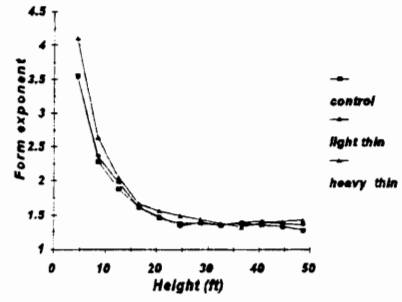


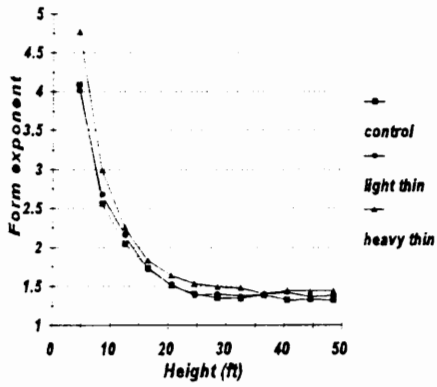
Figure 6.2: A 3D plot of the form exponent by height and time since thinning for a specific tree (F= form exponent, ET= Elapsed time and HT=height above ground).



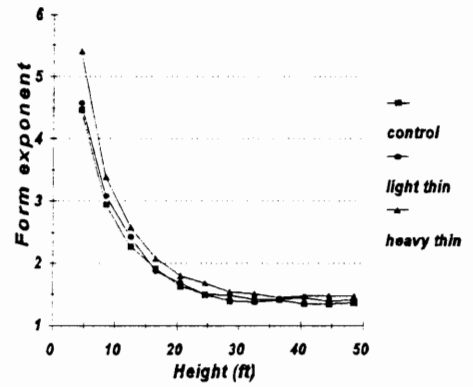
[a]



[b]

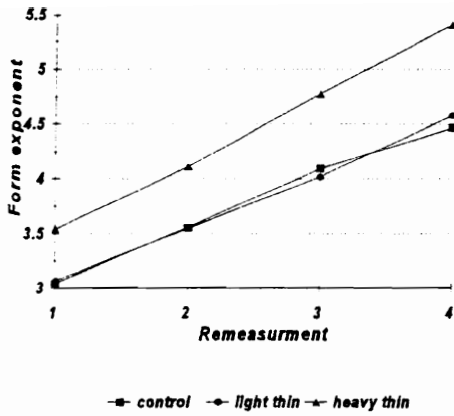


[c]

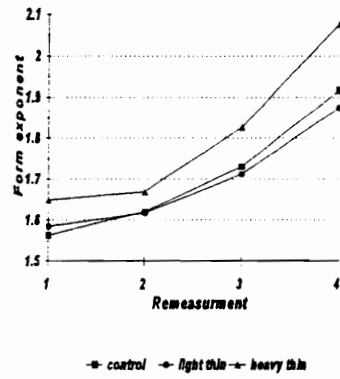


[d]

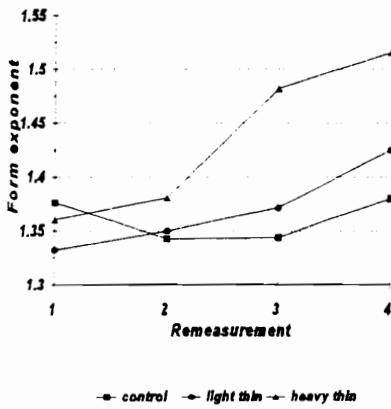
Figure 6.3: Relationships between average form exponent and height by thinning treatment over time: [a] first, [b] second, [c] third, and [d] fourth remeasurement.



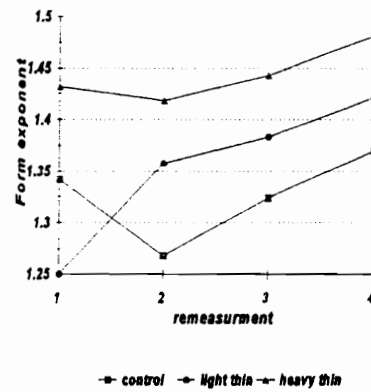
[a]



[b]



[c]



[d]

Figure 6.4: Relationships between average form exponent and remeasurement occasion by thinning treatment at selected heights:
 [a] 0.5 ft [b] 16.5 ft [c] 32.5 ft [d] 48.5 ft

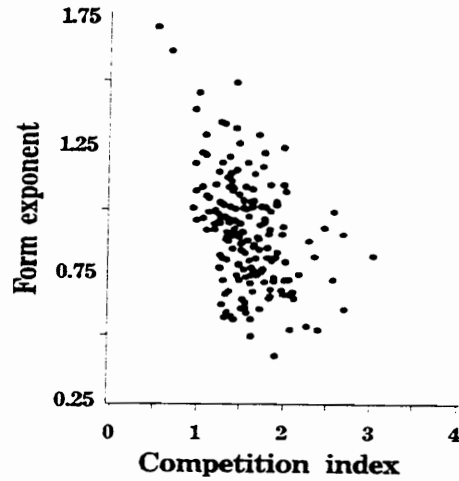
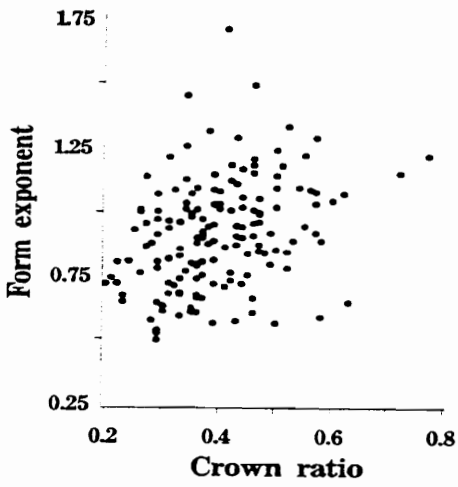
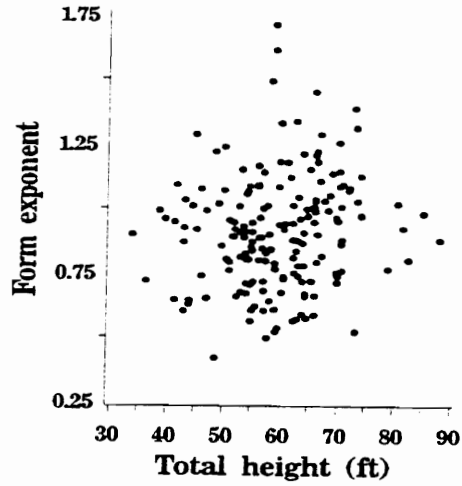
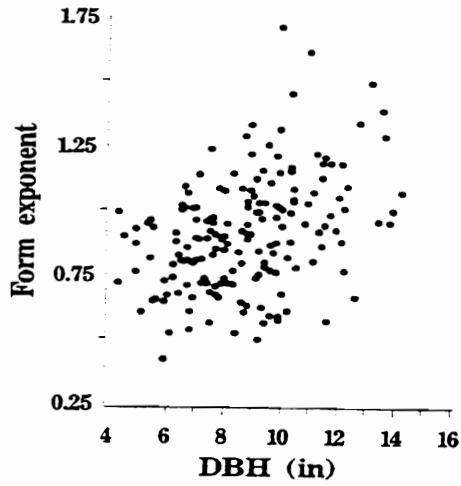


Figure 6.5: Relationships between average form exponent and various tree level factors.

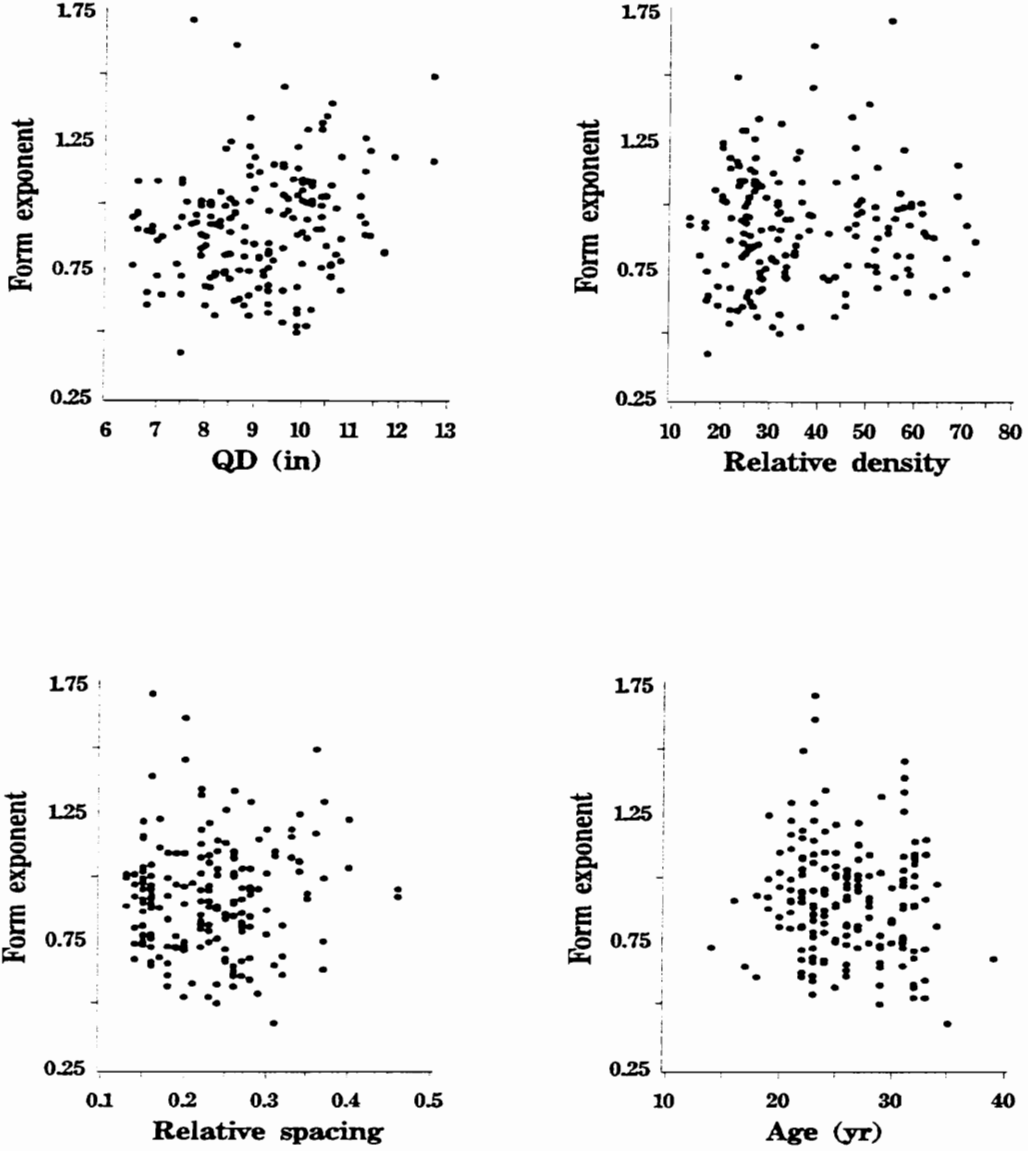
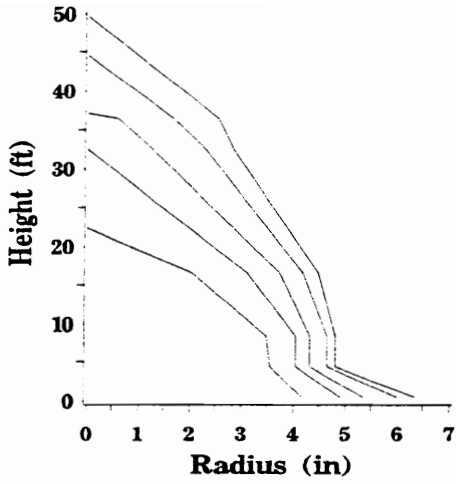
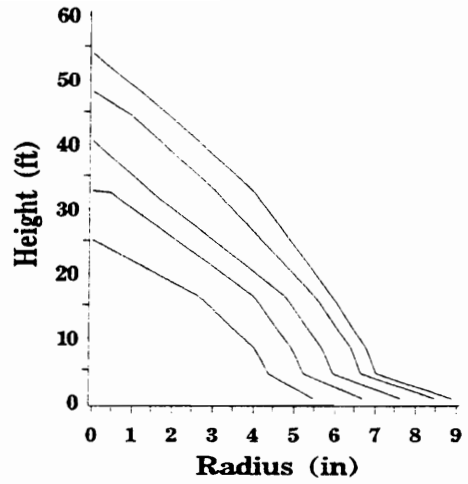


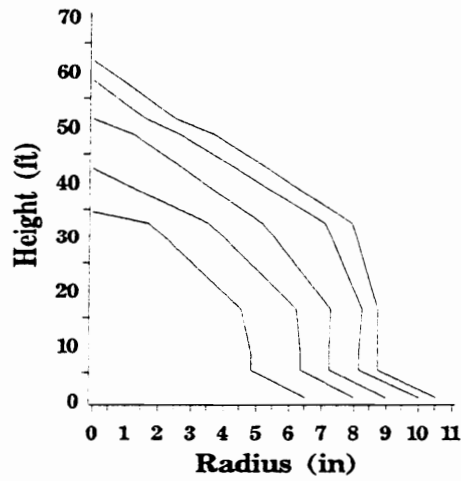
Figure 6.6: Relationships between average form exponent and various stand level factors.



[a]



[b]



[c]

Figure 6.7: Absolute tree stem profile over measurement occasions for specific trees from [a] control, [b] light thinned, and [c] heavy thinned stands.

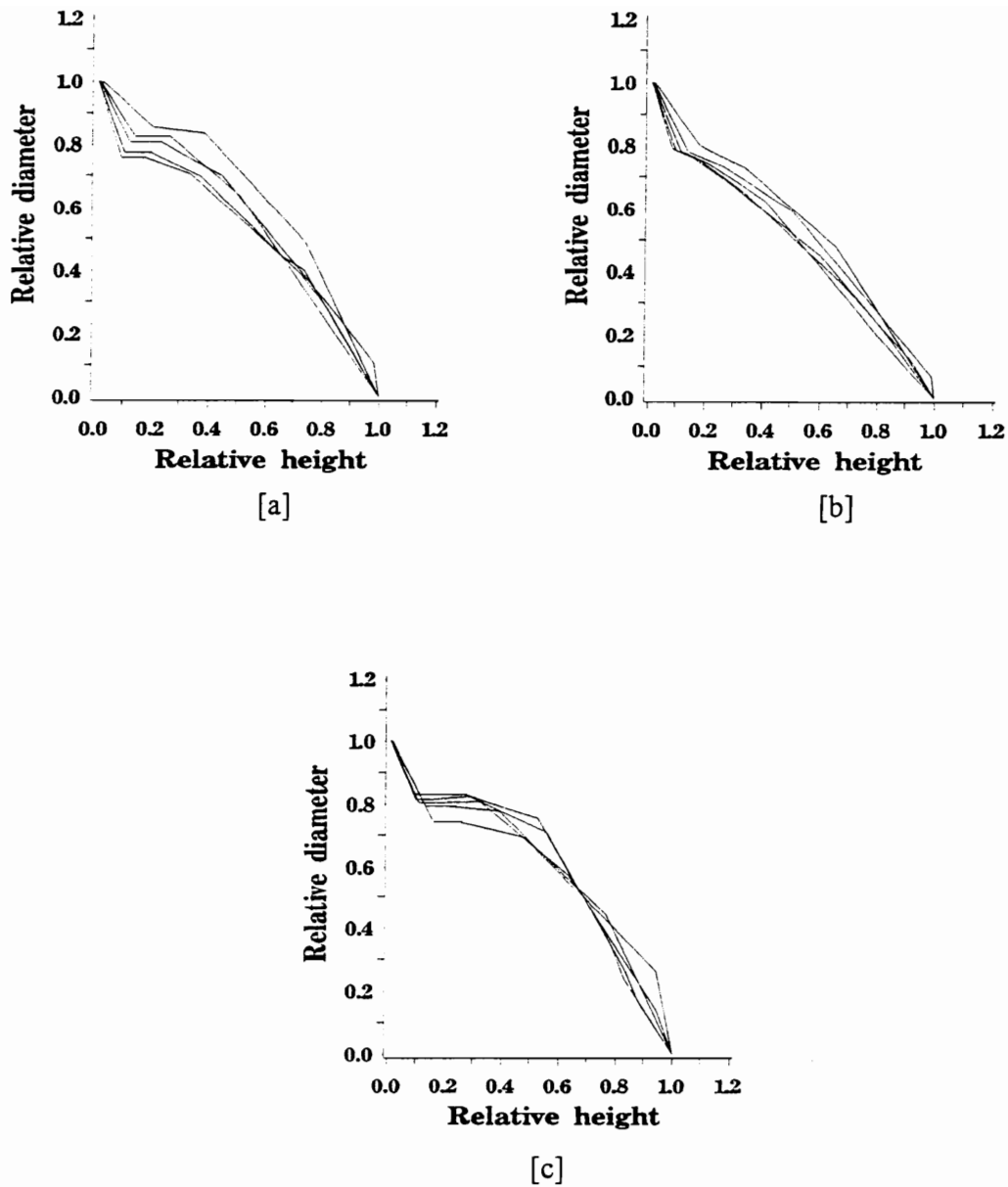


Figure 6.8: Relative tree stem profile over measurement occasions for specific trees from [a] control, [b] light thinned, and [c] heavy thinned stands.

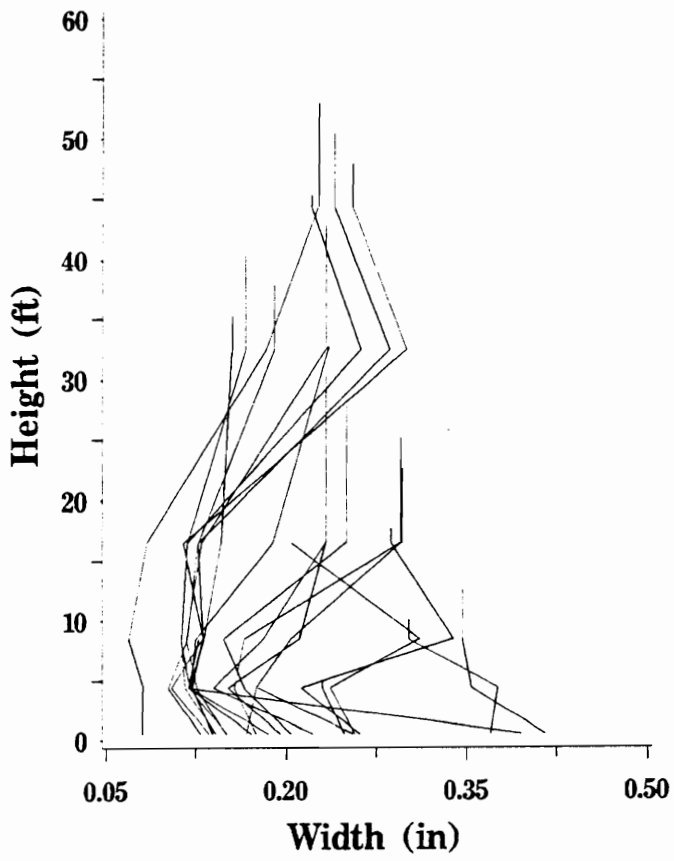


Figure 6.9: A vertical profile of individual growth rings for a specific tree.

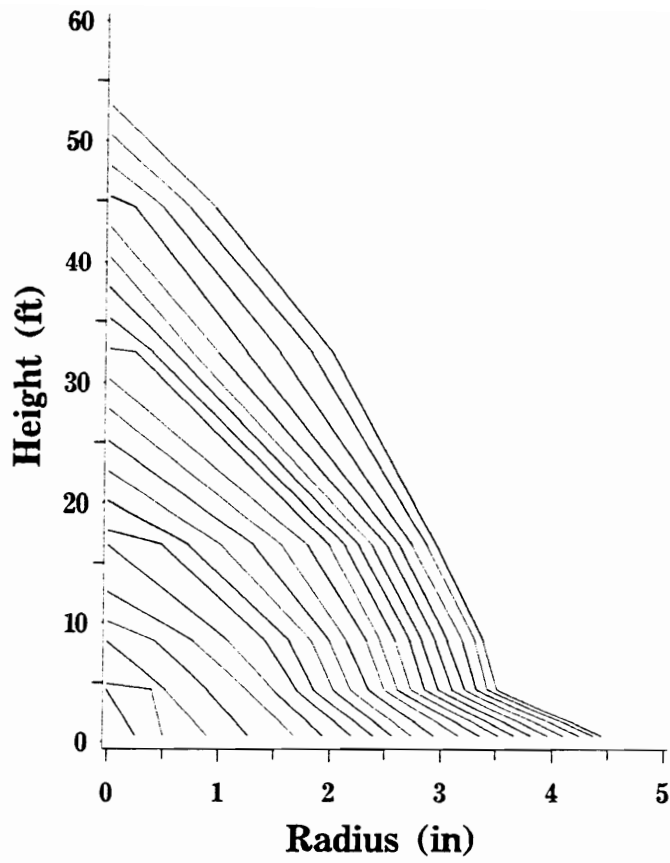


Figure 6.10: A vertical profile of cumulative growth for the tree depicted in Figure [6.9]

CHAPTER SEVEN

7.0 Summary and recommendations

7.1 Summary

A search for ways of increasing forest production is a process which continues to evolve. Silvicultural treatments are applied to forest stands in an effort to increase production or to improve product quality. Since treatment effects are seldom totally understood or quantified, efforts to get full understanding of treatment effects constitute a continuous process.

Besides tree improvement through selection and breeding, foresters still rely on cultural practices such as vegetation control, fertilization and thinning to maximize/optimize forest production. In particular, the age old silvicultural practice, thinning, remains an important form of stand manipulation and is a key to successful tree husbandry. As a result, thinning continues to command considerable research interest among the scientific community and the industry .

Thinning effects on wood quantity and quality are topics which have received wide interest among silviculturists and wood utilization scientists for a long time. While numerous studies have been conducted on thinning effects and volumes of research results exist, the studies are seldom coordinated and the results tend to be scattered throughout the literature. Thus the forester entrusted with growing trees and supplying the mills generally focuses on maximizing volume production, whereas the interests of those at the utilization end of the spectrum tends to be geared towards wood quality. Due to the lack

of coordination between the producer and the marketer then, optimum utilization of resources may not be achieved. This study has attempted to bridge some of that gap.

In this study various aspects of thinning effects on loblolly pine trees in plantations on cutover site-prepared areas were examined. Wood quality is an attribute which can not be precisely defined because it is dependent on the use intended for the piece of wood being considered. However, certain wood characteristics, such as wood specific gravity tend to be universal and are commonly used to evaluate wood quality.

It is often a concern that thinning, conducted to increase diameter growth on selected trees, may reduce specific gravity making the product unsuitable for some uses. This study undertaken on thinning effects on wood specific gravity has attempted to address many of the concerns from different perspectives. While there has been some variation in the conclusions reached by scientists depending on factors such as species, age, geographic location, and other factors, our findings tended to confirm the hypothesis that thinning does not significantly reduce the specific gravity of loblolly pine tree rings.

Thinning effects in inducing diameter growth is well known. Despite existing theories on wood deposition patterns, many studies base their conclusions on changes in breast height diameters or utmost two diameter measurements. This study examined thinning effects on wood deposition pattern along the stem over time. It has been found that thinning does significantly increase ring width over most of the tree bole over time.

A related issue is thinning effects on stem form. Various investigators have addressed thinning effects on stem form using different measures of tree form. The form exponent proved to be a useful measure to assess thinning effects on stem form in this study. Thinned stands showed a tendency to have larger form exponents particularly in the lower bole. This, to a great extent, was as expected because trees experiencing a more

open condition should have large form exponents in the lower bole area as they tend to have a neiloid form.

As observed earlier, the lack of connection between studies conducted on thinning effects on growth rate and studies of wood quality makes it difficult to devise an optimum treatment regime. This study established a direct connection between thinning effects on the rate of growth and a measure of wood quality via investigations on thinning effects on the proportion of latewood in a growth ring. Since specific gravity was found to be highly correlated with the proportion of latewood, thinning effects on latewood proportion were expected to show close similarity with thinning effects on specific gravity. This indeed turned out to be the case.

Tests on latewood proportion showed that thinning does not significantly affect the proportion of latewood. That means thinning induces an increase in the latewood component that is roughly proportional to increase in the earlywood component, thus maintaining approximately a constant latewood proportion. The upshot is that, since the proportion of latewood does not change even if growth is accelerated, thinning does not have a significant effect on specific gravity.

Prediction models of various forms have been calibrated to estimate wood characteristics of interest. The models were designed to predict the quantities of interest based on tree, stand and site factors. As repeatedly observed, tree level factors tended to explain more variations than stand level factors. In particular, stand level factors such as stand density measures which were expected to explain much of the variation in ring specific gravity, ring width, and tree stem form tended to play a minor role. The apparent anomaly is probably because the tree level factors are partly manifestations of stand level factors. This is a problem inherent to observational studies, which the thinning study

largely is, where factors can not be fully controlled to enable partitioning of treatment effects into the various factors.

An important merit of the data utilized in this thesis was the availability of several measurements over a period of time or at several locations on the same subject. In such data, stronger inferences are possible in some respects because a subject serves as its own control thus minimizing the effects of inherent, but unaccounted for, differences between experimental units (subjects). The likely correlation among within subject observations has been successfully accounted for using mixed effects analysis technique and direct covariance modeling.

Test results showed significant improvement over techniques in which correlation among observation are ignored. Beside the standard tests, it was observed that the significance levels (as judged by the p-values) of variables included in models tended to substantially change when a covariance structure depicting correlation among observations was specified compared to the usual assumption of independence. As observed in the main text of the thesis, the magnitude of bias incurred due to using OLS instead of accounting for correlation is indiscernible, but the significant changes in p-values can be partly attributed to bias in the standard error of estimates.

An important issue that must be considered in studies such as the ones considered here is the scope. Thinning studies tend to be of limited scope because of high establishment and maintenance costs. Thus, even if valid inferences are drawn and correct conclusions are made, the inability to include important sources of variation reduces the inference space.

Clearly, no single study can be expected to include every factor that may have influence on the phenomena of interest. Yet, the thinning study from which the data used in this thesis were obtained has a wide scope in that it essentially covers the entire

loblolly pine range, consists of longitudinal data, has a sample size that is large, and enables the examination of thinning effects along the tree stem over time while accounting for possible regional variation. It is hoped that the results obtained and conclusions drawn in this study will significantly contribute to our understanding of thinning effects on loblolly pine trees in plantations on cutover, site-prepared areas.

7.2 Recommendations

Whereas attempts were made to thoroughly investigate thinning effects on the various attributes of the loblolly pine trees studied, we are still limited by the data, the method of analysis, and many other unforeseen factors. Consequently, further investigations are required to gain a better understanding of thinning treatment effects. Among points that need further consideration are:

i) The thinning plots have received second thinning recently and the thinning study will eventually terminate. A follow up to the present study would help in assessing not only extended thinning effects on various attributes of the loblolly pine trees, but also the response to thinning treatment as stands age.

In addition, it has been pointed out that trees representing the control plots for destructive sampling were selected among trees in the buffer zone. This is because the thinning study is not terminated and the control trees cannot be destructively sampled. Selection of alternative trees was undertaken carefully, but one cannot totally discount a difference in micro site variation between the plot location and the buffer zone, a source of variation that may have been overlooked. Thus, the anticipated follow up study should

verify if results obtained using the actual trees, felled at study termination, coincides with results obtained here.

ii) As mentioned elsewhere, thinning effects on wood quality are manifested in several ways. The conclusions drawn in this study regarding thinning effects on specific gravity gave us a good indication that wood quality as measured by specific gravity does not significantly deteriorate following thinning. A further study should be undertaken to evaluate thinning effects on the mechanical and chemical properties of wood.

iii) Species variation sometimes is credited with differences in response to thinning. The trends observed in the study may vary depending on species. While the trends observed and conclusions drawn in this study largely corroborate many past studies particularly on loblolly pine, studies with other species, in which the major factors are appropriately controlled would help in determining if further generalizations are warranted.

iv) In attempting to incorporate thinning effects in modeling ring width and stem profile, it was noted that simple functions had to be used partly because of the number of parameters that had to be estimated in these models. However, it seems appropriate to look into ways of modeling thinning response over time by itself to determine if indeed the hypothesis on shifts in wood deposition pattern can be mathematically represented.

v) In mixed effects modeling prediction of new values is based on the fixed effects parameter estimates. Since the fixed effects parameter estimates are asymptotically BLUE, they should predict as good as the OLS parameter estimates. Further studies are needed

to determine the behavior of fixed effect parameter estimates in predicting future values. Limited empirical evaluations have shown, for the mixed effect parameter estimates, a tendency to perform poorer than their OLS counterparts. A carefully designed study which seeks to evaluate whether minimizing the bias in standard error estimates comes at a cost in prediction performance is appropriate.

Literature cited

- Alig, R. L., H. A. Knight, and R. A. Birdsey. 1986. Recent area changes in southern forest ownership and cover types. USDA For. Serv., South. Exp. Stat. Res. Pap. SE-260: 10p.
- Amidon, E. L. 1984. A general taper functional form to predict bole volume for five mixed-conifer species in California. For. Sci. **30**: 166-171.
- Arbaugh, M. J., and D. L. Peterson. 1993. Stemwood production patterns in ponderosa pine: Effects of stand dynamics and other factors. USDA For. Serv. Res. Pap. PSW- RP-217. 11p.
- Arner, S. L., and D.W. Seegrist. 1979. A computer program for the maximum likelihood estimator of the general multivariate linear model with correlated errors. USDA For. Serv. Gen. Tech. Rep. NE-51. 10p.
- Arner, S. L., and D.W. Seegrist. 1980. "MISSING". A computer program for the maximum likelihood estimates of the parameters of the multi variate linear model with incomplete measurements. USDA for. Serv. Gen. Tech. Rep. NE-56. 19 p.
- Barbour, R. J., R. E. Bailey, and J. A. Cook. 1992. Evaluation of relative density, diameter growth, and stem form in a red spruce (*Picea rubens*) stand 15 years after precommercial thinning. Can. J. For. Res. **22**: 229-238.
- Behre, E. C. 1923. Preliminary notes on studies of tree form. J. For. **21**: 507-511.
- Behre, E. C. 1927. Form-class taper tables and volume tables and their application. J. Agr. Res. **35**: 673-744.
- Belsley, D. A., E. Kuh, and R. E. Welsch. 1980. *Regression diagnostics: Identifying influential data and sources of collinearity*. John Wiley & Sons, New York. 292 p.
- Bendtsen, B. A. 1978. Properties of wood from improved and intensively managed trees. For. Prod. J. **28** (10): 61-72.
- Bennett, F. A., and B. F. Swindel. 1972. Taper curves for planted slash pine. USDA For. Serv. Res. Note. SE-179. 4 p.
- Bickerstaff, A. 1946. Effect of thinning and pruning upon the form of red pine. Can., Dept. Mines and Resou., For. Serv. Silv. Res. Note 81. 26 p.

- Biging, G. S. 1985. Improved estimates of site index curves using varying-parameter model. *For. Sci.* **31**: 248-257.
- Bruce, D., R.O. Curtis, and C. Vancoevering. 1968. Development of a system of taper and volume tables for red alder. *For. Sci.* **14**: 339-350.
- Buckman, R. E. and E. I. Roe. 1958. Effects of pruning on the form growth of a red pine plantation. USDA For. Serv. Lake States For. Expt. Sta. Tech. Note 533. 2 p.
- Burkhart, H. E., and J. R. Beckwith III. 1970. Specific gravity prediction and dry-weight yield estimation. *Tappi* **53**: 603-604.
- Burkhart, H. E., and S. B. Walton. 1985. 1985. Incorporating crown ratio into taper equations for loblolly pine trees. *For. Sci.* **31**: 478-484.
- Burkhart, H. E., D. C. Cloeren, and R. L. Amateis. 1985. Yield relationships in unthinned loblolly pine plantations on cutover, site-prepared lands. *South. J. Appl. For.* **9**: 84-91.
- Burkhart, H. E., K. D. Farrar, R. L. Amateis, and R. F. Daniels. 1987. Simulation of individual tree growth and stand development in loblolly pine tree plantations on cutover, site-prepared areas. Virginia Polytechnic Institute and State University, School of Forestry and Wildlife Resources, Publ. FWS-1-87.
- Burton, J. D., and D. M. Smith. 1972. Guying to prevent wind sway influences loblolly pine growth and wood properties. USDA For. Serv. Res. Pap. SO-80. 8 p.
- Burton, J. D., and E. Shoulders. 1974. Fast-grown, dense loblolly pine saw logs: a reality. *J. For.* **72** (10): 637-641.
- Byrne, J. C. 1993. Incorporating additional tree and environmental variables in a lodgepole pine stem profile model. *West. J. Appl. For.* **8** (3): 86-90.
- Choong, E. T., P. J. Fogg, and E. Shoulders. 1989. Effect of cultural treatment and wood type on some physical properties of longleaf and slash pine wood. *Wood and Fiber Sci.* **21**(2): 193-206.
- Clark, A. III, and J. R. Saucier. 1989. Influence of initial planting density, geographic location, and species on juvenile wood formation in southern pine. *For. Prod. J.* **39**(7/8): 42-48.

- Clyde, M. A. 1986. Variation in stem diameter increment and its effects on taper in conifers. Unpublished M. Sc. Thesis, University of Alberta. 85 p. (Cited by Muhairwe 1993)
- Cregg, B. M., P. M. Dougherty, and T. C. Hennessey. 1988. Growth and wood quality of young loblolly pine trees in relation to stand density and climatic factors. *Can. J. For. Res.* **18**: 851-858.
- Davidian, M., and A. R. Gallant. 1993. The nonlinear mixed effects model with a smooth random effects density. *Biometrics* **80**(3): 475-488.
- Davidian, M., and D. M. Giltinan. 1993. Some general estimation methods for nonlinear mixed-effects models. *J. Biopharm. Stat.* **3**: 23-25.
- Davidian, M., and D. M. Giltinan. 1995. *Nonlinear models for repeated measurements data*. Chapman & Hall. 359 p.
- Davis, A.W., and P. W. West. 1981. Remarks on “generalized least squares estimation of yield functions” by I.S. Ferguson and J. W. Leech. *For. Sci.* **27**: 233-239.
- Demaerschalk, J. P. 1972. Converting volume equations to compatible taper equations. *For. Sci.* **18**: 241-245.
- Demaerschalk, J. P. 1973. Integrated systems for estimation of tree taper and volume. *Can. J. For. Res.* **3**: 90-94.
- Diggle, P. J. 1988. An approach to the analysis of repeated measurements. *Biometrics* **44**: 959-971.
- Diggle, P. G., K. Liang, and S. L. Zeger. 1994. *Analysis of longitudinal data*. Clarendon Press, Oxford. 253 p.
- Doruska, P. F., and H. E. Burkhart. 1994. Modeling the diameter and locational distribution of branches within the crowns of loblolly pine trees in unthinned plantations. *Can. J. For. Res.* **24**: 2362-2376.
- Duff, G. H., and N. J. Nolan. 1953. Growth and morphogenesis in the Canadian forest species. I. The controls of cambial and apical activity in *Pinus resinosa* Ait. *Can. J. Bot.* **31**: 471-513.
- Duff, G. H., and N. J. Nolan. 1957. Growth and morphogenesis in the Canadian forest species. II. Specific increments and their relation to the quality and activity of growth in *Pinus resinosa* Ait. *Can. J. Bot.* **35**: 527-572.

- Erickson, H. D., and G. M. G. Lambert. 1958. Effects of fertilization and thinning on chemical composition, growth and specific gravity of McTaggart Douglas-fir. *For. Sci.* **4**: 307-315.
- Ezell, A. W., and P. E. Schilling. 1980. A note on within-tree variation of specific gravity in sweetgum (*Liquidambar styraciflua* L.). *Wood and Fiber* **12**(2): 80-87.
- Farrar, J. L. 1961. Longitudinal variation in the thickness of the annual ring. *For. Chron.* **37**: 323-30.
- Fayle, D. C. F. 1973. Patterns of annual xylem increment integrated by contour presentation. *Can. J. For. Res.* **3**: 105-111.
- Fayle, D. C. F., and G. B. MacDonald. 1977. Growth and development of sugar maple as revealed by stem analysis. *Can. J. For. Res.* **7**: 526-536.
- Ferguson, I. S., and J. W. Leech. 1978. Generalized least squares estimation of yield functions. *For. Sci.* **24**: 27-42.
- Fomby, T. B., R. C. Hill and S. R. Johnson. 1984. *Advanced econometric methods*. Springer-Verlag, New York. 624 p.
- Fries, J., and B. Matern. 1966. On the use of multivariate methods for the construction of tree taper curves. Advisory Group of Forest Statisticians of the IUFRO. Sect. 25, Stockholm conference, Sept. 27 to Oct. 1, 1965. Paper No. 9. p.1-33.
- Fuller, W. A. and G. E. Battese. 1974. Estimation of linear models with crossed-error structure. *J. Econometrics* **2** : 67-78.
- Gray, H. R. 1956. The form and taper of forest tree stems. Oxford, Imp. For. Inst. Paper No. 32. 79 p.
- Gregoire, T. G. 1987. Generalized error structure for forestry yield models. *For. Sci.* **33**: 423-444.
- Gregoire, T. G. 1992. The error rate of tests for regression coincidence and parallelism under unknown multiplicative heteroskedasticity. *Biom. J.* **34** (2): 193-208.
- Gregoire, T. G., and M. E. Dyer. 1989. Model fitting under patterned heterogeneity of variance. *For. Sci.* **35**: 105-125.

- Gregoire, T. G., and O. Schabenberger. 1996. A nonlinear mixed -effects model to predict cumulative bole volume of standing trees. *J. App. Stat.* **23**: 257-271.
- Gregoire, T. G., O. Schabenberger, and J. P. Barrett. 1995. Linear modeling of irregularly spaced, unbalanced, longitudinal data from permanent plot measurements. *Can. J. For. Res.* **25**: 137-156.
- Grosenbaugh, L. R. 1966. Tree form: definition, interpolation, extrapolation. *For. Chron.* **42**: 443-456.
- Harville , D. A. 1976. Extension of the Gauss-Markov theorem to include the estimation of random effects. *Annals of Statistics* **4**: 384-395.
- Harville, D. A. 1990. BLUP (best linear unbiased prediction), and beyond. *Advances in statistical methods for genetic improvement of livestock*, Gianola, D. and Hammond, K. (eds). New York: Springer-Verlag, 239-276.
- Hasenauer, H., H. E. Burkhart, and H. Sterba. 1994. Variation in potential volume yield of loblolly pine plantations. *For. Sci.* **40**: 162-176.
- Haygreen, J. G., and J. L. Bowyer. 1996. *Forest products and wood science*. ed 3. Iowa State Univ. Press, Ames, Iowa. 484 p.
- Heger, L. 1974. Longitudinal variation of specific gravity in stems of black spruce, balsam fir, and lodgepole pine [*Picea mariana*, *Abies balsamea*, *Pinus contorta*]. *Can. J. For. Res.* **4**: 321-326.
- Hilt, D. E., and M. E. Dale. 1979. Stem form changes in upland oaks after thinning. USDA For. Serv. Res. Pap. NE-433. 7 p.
- Hinkelmann, K., and O. Kempthorne. 1994. *Design and analysis of experiments Volume I: Introduction to experimental design*. John Wiley & Sons, New York. 495 p.
- Hirst, K., G. O. Zerbe, D. W. Boyle, and R. B. Wilkening .1991. On nonlinear random effects models for repeated measurements. *Comm. Stat. Simul.* **20** :463-478.
- Husch, B., C. I. Miller, and T. W. Beers. 1982. *Forest mensuration*. ed 3. John Wiley & Sons, New York. 402 p.
- Jackson, L. W. R. 1968. Effect of thinning on growth and specific gravity of loblolly and slash pine. Res. Pap. Ga. For. Res. Coun. No. 50. 6 p.

- Jennrich, R. I., and M. D. Schluchter. 1986. Unbalanced repeated-measures models with structured covariance matrices. *Biometrics* **42**: 805-820.
- Judge, G. G., R. C. Hill, W. E. Griffiths, H. Lutkepohl and T. Lee. 1988. *Introduction to the theory and practice of Econometrics*. ed 2. John Wiley & Sons, New York. 1024 p.
- Kmenta, J. 1986. *Elements of econometrics*. ed 2. The Macmillan Publishing Co., New York. 786 p.
- Koch, P. 1972. *Utilization of the southern pine trees*, Vol. I. USDA For. Ser. , Agric. Handbook 420. 734 p.
- Kozak, A., D. D. Munro, and J. H. G. Smith. 1969. Taper functions and their applications in forest inventory. *For. Chron.* **45**: 278-283.
- Kozak, A. 1988. A variable - exponent taper equation. *Can. J. For. Res.* **18** : 1363-1368.
- Kozlowski, T. T. 1971. *Growth and development of trees*. Vol. II. Academic Press, New York. 514 p.
- Labyak, L. F. and F. X. Schumacher. 1954. The contribution of its branches to the main-stem growth of loblolly pine. *J. For.* **52**: 333-337.
- Laird, N. M. and J. H. Ware. 1982. Random-effects models for longitudinal data. *Biometrics* **38**: 963-974.
- Lappi, J. 1986. Mixed linear models for analyzing and predicting stem form variation of Scots pine. *Communicationes Instituti Forestalis Fenniae* **134**: 1-69.
- Lappi, J., and R. L. Bailey. 1988. A height prediction model with random stand and tree parameters: An alternative to traditional site index methods. *For. Sci.* **34**: 907-927.
- Larocque, G. R., and P. L. Marshall. 1995. Wood relative density development in red pine (*Pinus resinosa* Ait.) stands as affected by different initial spacings. *For. Sci.* **41**: 709-728.
- Larson, P.R. 1963. Stem form development of forest trees. *For. Sci. Monogr.* **5**. 42 p.
- Larson, P. 1965. Stem form of young larix as influenced by wind and pruning. *For. Sci.* **11**: 413-424.

- Lenhart, J. D. , K. H. Shinn, and B. E. Cutter. 1977. Specific gravity at various positions along the stem of loblolly pine (*Pinus taeda* L.) trees. For. Prod . J. **27** (9): 43-44.
- Liang, K., and S. L. Zeger. 1986. Longitudinal data analysis using generalized linear models. Biometrika **73** : 13-22.
- Lindstrom, M. J., and D. M. Bates. 1988. Newton-Raphson and EM algorithms for linear mixed-effects models for repeated-measures data. J. Am. Stat. Assoc. **83**: 1014-1022.
- Lindstrom, M. J., and D. M. Bates. 1990. Nonlinear mixed effects models for repeated measures data. Biometrics **46** : 673-687.
- Liu, C. J. 1980. Log volume estimation with spline approximation. For. Sci. **26**: 361-369.
- Liu, C.J., and T.D. Keister. 1978. Southern pine stem form defined through principal component analysis. Can. J. For. Res. **8**: 188-197.
- Liu, J., H. E. Burkhart, and R.L. Amateis. 1995. Projecting crown measures for loblolly pine trees using a generalized thinning response function. For. Sci. **41**: 43-53.
- Louis, T. A. 1988. General methods for analyzing repeated measures. Stat. in Med. **7**: 29-45.
- Matney, T. G., and A. D. Sullivan. 1980. Inside and outside bark taper equations for old field plantation loblolly pine trees in the Central Gulf Coastal Plain. Mississippi Agr. and For. Exp. Sta. Tech. Bull. 101. 25 p.
- Max, T. A., and H. E. Burkhart. 1976. Segmented polynomial regression applied to taper equations. For. Sci. **22**: 283-289.
- Megraw, R. A. 1985. *Wood quality factors in loblolly pine. The influence of tree age, position in tree, and cultural practice on wood specific gravity, fiber length and fibril angle*. TAPPI Press, Atlanta. 88 p.
- Myers, C. A. 1963. Vertical distribution of annual increment in thinned ponderosa pine. For. Sci. **9**: 394-404.
- Monserud, R. A. 1986. Time series analyses of tree ring chronologies. For. Sci. **32**: 349-372.

- Morgan, B., S. Pantula, and M. Gumpertz. 1995. Testing whether coefficients are random in a linear random coefficient regression model. *In Proceedings of the 1995 American Statistical Association, Biometrics Section, August 13-17, 1995, Orlando, Florida, USA.*
- Mott, D. G., L. D. Narin, and J. A. Cook. 1957. Radial growth in trees and effects of insect defoliation. *For. Sci.* **3**: 286-303.
- Muhairwe, C. K. 1993. Examination and modeling of tree form and taper over time for interior lodgepole pine. Ph. D. thesis (unpublished), For. Resou., Manag., the University of British Columbia, Vancouver, Canada. 179 p.
- Myers, R. H. 1990. *Classical and modern regression with applications*. ed. 2. Duxbury press, Belmont, CA. 488 p.
- Newberry, J. D., and H. E. Burkhart. 1986. Variable - form stem profile models for loblolly pine. *Can. J. For. Res.* **16**: 109-114.
- Newnham, R. M. 1988. A variable-form taper function. *Petawawa Nat. For. Inst., For. Can. Information Rep. PI-X-83.* 33 p. (Cited by Newnham 1992)
- Newnham, R. M. 1992. Variable-form taper functions for four Alberta tree species. *Can. J. For. Res.* **22**: 210-223.
- Ojansuu, R., and M. Maltamo. 1995. Sapwood and heartwood taper in Scots pine. *Can J. For. Res.* **25**: 1928-1943.
- Olson, J. R., and D. G. Arganbright. 1977. The uniformity factor — a proposed method for expressing variations in specific gravity. *Wood and Fiber* **9**(3): 202-210.
- Ormerod, D. W. 1973. A simple bole model. *For. Chron.* **49**: 136-138.
- Paul, B. H. 1957. Growth and specific gravity responses in a thinned red pine plantation. *J. For.* **55**: 510-512.
- Perez, D. N., H. E. Burkhart, and C. T. Stiff. 1990. A variable-form taper function for *Pinus oocarpa* Scheide in central Honduras. *For. Sci.* **36**: 186-191.
- Petty, J. A., D. C. Macmillan, and C. M. Steward. 1990. Variation of density and growth ring width in stems of Sitka and Norway spruce. *Forestry* **63**: 39-49.
- Racine-Poon, A. 1985. A Bayesian approach to nonlinear random effects models. *Biometrics* **41**: 1015-1023.

- Reed, D. D., and J. C. Byrne. 1985. A simple, variable form volume estimation system. *For. Chron.* **61**: 87-90.
- Reed, D. D., and E. J. Green. 1984. Compatible stem taper and volume ratio equations. *For. Sci.* **30**: 977-990.
- Reukema, D. 1961. Crown development and its effect on stem growth of six Douglas-firs. *J. For.* **59**: 370-371.
- Robinson, G. K. 1991. That BLUP is a good thing: The estimation of random effects (with discussion). *Stat. Sci.* **6**: 15-51.
- Rustagi, K. P., and R. S. Loveless, Jr. 1991. Compatible variable-form volume and stem-profile equations for Douglas-fir. *Can. J. For. Res.* **21**: 143-151.
- Rutter, C. M., and R. M. Elashoff. 1994. Analysis of longitudinal data: random coefficient regression modeling. *Stat. in Med.* **13** : 1211-1231.
- SAS Institute Inc. 1992. *SAS/STAT Software: Changes and Enhancements, Release 6.07* SAS Technical Report P-229, SAS Institute Inc., Cary, NC.
- Schabenberger, O., and T. G. Gregoire. 1996. Population-averaged and subject-specific approaches for clustered categorical data. *J. Stat. Comp. Simul.* **54**: 231-253.
- Searle, S. R., G. Casella, and C. E. McCulloch. 1992. *Variance components*. John Wiley & Sons, New York. 501 p.
- Sheiner, L. B., and S. L. Beal. 1980. Evaluation of methods for estimating population pharmacokinetic parameters. I. Michelis-Menton model: Routine clinical pharmacokinetic data. *J. Pharmacokinetics and Biopharm.* **8**:553-571.
- Shepard, R. K., and J. E. Shottafer. 1990. Effect of early release on specific gravity and wood yield of black spruce. *For. Prod. J.* **40**(1): 18-29.
- Short, E. A. III, and H. E. Burkhart. 1992. Predicting crown-height increment for thinned and unthinned loblolly pine plantations. *For. Sci.* **38**: 594-610.
- Smith, D. M. 1986. *The practice of silviculture*. Ed. 8. John Wiley & Sons, New York. 687 p.

- Smith, D. M. and M. C. Wilsie. 1961. Some anatomical responses of loblolly pine to soil-water deficiencies. *Tappi* **44**:179-184.
- Smith, J. H. G. 1980. Influences of spacing on radial growth and percentage latewood of Douglas-fir, western hemlock, and western red cedar. *Can. J. For. Res.* **10**: 169-175.
- Stark, R. W., and J. A. Cook. 1957. The effects of defoliation by the lodgepole needle miner. *For. Sci.* **3**: 377-395.
- Sterba, H. 1980. Stem curves-a review of the literature. *For. Abs.* **41**: 141-145.
- Stram, D. O., and J. W. Lee. 1994. Variance components testing in longitudinal mixed effects model. *Biometrics.* **50** : 1171-1177.
- Stiratelli, R., N. Laird, and J. H. Ware. 1984. Random-effects models for serial observations with binary response. *Biometrics* **40** : 961-971.
- Sullivan, A. D., and J. L. Clutter. 1972. A simultaneous growth and yield model for loblolly pine. *For. Sci.* **18**: 76-86.
- Sullivan, A. D., and M. R. Reynolds, Jr. 1976. Regression problems from repeated measurements. *For. Sci.* **22**: 382-385.
- Swindel, B. F. 1968. On the bias of some least-squares estimators in a general linear model. *Biometrika.* **55**: 313-316.
- Szymanski, M. B., and C. G. Tauer. 1991. Loblolly pine provenance variation in age of transition from juvenile to mature wood specific gravity. *For. Sci.* **37** : 160-174.
- Talbert, J. T., and J. B. Jett. 1981. Regional specific gravity values for plantation grown loblolly pine in the southern United States. *For. Sci.* **27**: 801-807.
- Taylor, F. W., and J. D. Burton. 1982. Growth ring characteristics, specific gravity, and fiber length of rapidly grown loblolly pine. *Wood and Fiber.* **14**(3): 204-210.
- Tepper, H. B., H. E. Wilcox, and F. A. Valentine. 1968. The effect of fertilization and depth to ground water on wood deposition in red pine. *For. Sci.* **14**:2-6.
- Thomas, C. E., and B. R. Parresol. 1991. Simple, flexible trigonometric taper equations. *Can. J. For. Res.* **21**: 1132-1137.

- Thomson, A. J. and H. J. Barclay. 1984. Effects of thinning and urea fertilization on the distribution of area increment along the bole of Douglas-fir at Shawnigan Lake, British Columbia. *Can. J. For. Res.* **14**: 879-884.
- USDA Forest Service. 1988. *The South's fourth forest: alternatives for the future*. Forest Resource Report No. 24, Washington, D C, 512 p.
- Valenti, M. A., and Q. V. Cao. 1986. Use of crown ratio to improve loblolly pine taper equations. *Can. J. For. Res.* **16**: 1141-1145.
- Valinger, E. 1992. Effects of wind sway on stem form and crown development of Scots pine (*Pinus sylvestris* L.). *Aust. For.* **55**: 15-21.
- Vonesh, E. F., and R. L. Carter. 1992. Mixed-effects nonlinear regression for unbalanced repeated measures. *Biometrics* **48**:1-17.
- Walker, S. A. 1981. Modeling the effects of management on dry weight production in loblolly pine plantations. M. S. Thesis. VPI & SU, Blacksburg, Va. 99 p.
- Ware, J. H. 1985. Linear models for the analysis of longitudinal studies. *Am. Stat.* **39**(2): 95-101.
- Wiemann, M. C., and G. B. Williamson. 1989. Radial gradients in the specific gravity of wood in some tropical and temperate trees. *For. Sci.* **35**: 197-210.
- West, P. W., D. A. Ratkowsky, and A. W. Davis. 1984. Problems of hypothesis testing of regressions with multiple measurements from individual sampling units. *For. Ecol. Manag.* **7**: 207-224.
- Wolfinger, R. 1992. *A tutorial on mixed models*. SAS Technical Report TS-260 .SAS Institute Inc., Cary, North Carolina. 42 p.
- Wolfinger, R. 1993. Laplace's approximation for nonlinear mixed models. *Biometrika.* **8** : 791-795.
- Zeger, S. L., K. Liang , and P. S. Albert. 1988. Models for longitudinal data: a generalized estimating equation approach. *Biometrics* **44**: 1049-1060.

Appendix

Appendix A3.1

The form exponent was chosen to examine thinning effects on stem form. The values of the form exponent were calculated for using the procedures described below.

We note that any solid of revolution can be generated by rotating a curve of the form :

$$Y = K \sqrt{X^r} \quad [\text{A3.1}]$$

around the X axis Husch *et al.* (1982). Where Y is radius X is height or length and K is some constant relating the rate of change in radius with height (length) and r is the form exponent. As the form exponent changes, different solids are generated. Thus, when r is 1 a paraboloid is obtained; when r is 2 a cone; when r is 3 a neiloid. As alluded to elsewhere, tree form is much more complex and is composed of a mixture of more than one solid of revolution.

For a tree stem, the variables in [A3.1] are: Y is a function of diameter, $\frac{d}{2}$, say; where d is diameter at any point on the stem, K is an expression of taper, $\frac{R_b}{\sqrt{H^r}}$, where R_b is radius at tree base and H is total tree height, and X is a function of tree height, usually $H - h$ where h is height above ground to a point on the stem. Since in forestry we commonly deal with diameter rather than radius, both sides of [A3.1] are multiplied by 2 to yield values in terms of diameter.

Thus :

$$d = \frac{D_b}{\sqrt{H^r}} \sqrt{(H - h)^r} = D_b \left(\frac{x}{H}\right)^{\frac{r}{2}}$$

where

$$D_b = 2 * R_b$$

and rearranging yields:

$$\frac{d}{D_b} = \left(\frac{x}{H}\right)^r \quad [\text{A3.2}]$$

Because trees are not simple solids their form cannot be described by a simple form exponent as the common solids of revolution do. Instead, one has to determine the form exponent value that closely approximates the form of a section of the tree bole at any point on the bole from [A3.2]. Thus, solving for r in [A3.2] obtains :

$$r = \frac{2 * \ln(W)}{\ln(Z)} \quad [\text{A3.3}]$$

where

W is $\frac{d}{D_b}$, Z is $\frac{x}{H}$, \ln is natural logarithm.

The form exponent was calculated at several heights along the stem by measurement occasion. Form exponent is undefined both at the top and bottom of trees.

Appendix A4.1

The following models are among the models considered for predicting ring specific gravity of loblolly pine trees on cutover, site-prepared plantations. The models include tree, stand, site and environmental variables or their surrogates as predictors. The results presented in Table A4.1.1 indicate that factors inherent to a tree alone can effectively be used to predict ring specific gravity.

$$RS = \beta_0 + \beta_1 LA + \beta_2 RHT + \epsilon \quad [4.4a]$$

$$RS = \beta_0 + \beta_1 LA + \beta_2 RHT + \beta_3 CI + \epsilon \quad [4.4b]$$

$$RS = \beta_0 + \beta_1 LA + \beta_2 RHT + \beta_3 CI + \beta_4 ENV + \epsilon \quad [4.4c]$$

$$RS = \beta_0 + \beta_1 LA + \beta_2 RHT + \beta_3 CR + \beta_4 CI + \beta_5 SI + \epsilon \quad [4.4d]$$

$$RS = \beta_0 + \beta_1 LA + \beta_2 RHT + \beta_3 PLV + \beta_4 RW + \beta_5 CI + \epsilon \quad [4.4]$$

$$RS = 1 - \beta_1 \text{Exp}(-X) + \epsilon \quad [4.4e]$$

where

$$X = \beta_2 LA + \beta_3 RHT + \beta_4 PLV + \beta_5 RW + \beta_6 CI$$

RS is ring specific gravity.

LA is the natural logarithm of ring physiological age.

RHT is relative height ($\frac{h}{H}$).

H is total tree height (ft).

h is height above ground (ft).

CI is competition index ($\frac{QD(\text{in})}{DBH(\text{in})}$).

QD is stand quadratic mean diameter.

CR is the ratio of live crown length to total tree height.

PLV is percent latewood volume.

ENV is a surrogate for environmental factors defined as

$$\frac{\text{summer precipitation (inches)}}{\text{July plus August mean maximum temperature (}^\circ\text{F)}} \times 10$$

SI is site index base age 25 (Burkhart *et al.* 1987),

RW is ring width (in.).

$\beta_i, i=1,2,\dots$ are regression coefficients.

Table A4.1: A comparison of the performance of alternative specific gravity models

Model	SEE	MB	MSE	R_p^2	AIC
[4.4a]	0.0622	0.0048	0.0037	0.368	22356
[4.4b]	0.0613	0.0043	0.0036	0.385	22398
[4.4c]	0.0584	0.0038	0.0034	0.440	21966
[4.4d]	0.0612	-0.0011	0.0036	0.386	22392
[4.4]	0.0295	0.0028	0.0009	0.853	30978
[4.4e]	0.0314	0.0028	0.0010	0.836	30448

Appendix A5.1

A number of models based on site, stand and tree level variables were considered for predicting ring width. Because of the extreme variability in ring width, a substantial portion of the variation in ring width remained unexplained. A sample of the models considered and their fit and prediction performances are presented .

$$RW = \beta_0 + \beta_1 RHT + \beta_2 RA + \epsilon \quad [5.5a]$$

$$RW = \beta_0 + \beta_1 RHT + \beta_2 RA + \beta_3 CI + \epsilon \quad [5.5b]$$

$$RW = \beta_0 + \beta_1 RHT + \beta_2 RA + \beta_3 CI + \beta_4 SI + \epsilon \quad [5.5c]$$

$$RW = \beta_0 + \beta_1 RHT + \beta_2 RA + \beta_3 TAP + \beta_4 CI + \beta_5 SI + \epsilon \quad [5.5d]$$

$$RW = \beta_0 + \beta_1 RHT + \beta_2 RA + \beta_3 RHT*RA + \beta_4 TAP + \beta_5 CI + \beta_6 SI + \epsilon \quad [5.5]$$

$$RW = \beta_0 + \beta_1 RHT + \beta_2 RA + \beta_3 TAP + \beta_4 ENV + \epsilon \quad [5.5e]$$

$$RW = \beta_0 + \beta_1 RHT + \beta_2 RA + \beta_3 CI + \beta_4 CR + \beta_5 TAP + \epsilon \quad [5.5f]$$

$$RW = \beta_1 TAP * Exp(-X) + \epsilon \quad [5.5g]$$

where

$$X = \beta_2 RHT + \beta_3 RA + \beta_4 SI + \beta_5 RHT*RA$$

and

RHT is relative height ($\frac{\text{height above ground (ft)}}{\text{total tree height (ft)}}$).

RA is relative age $\left(\frac{\text{ring physiological age (yr)}}{\text{disk physiological age (yr)}} \right)$.

SI is site index base age 25 (Burkhardt *et al.* 1987).

TAP is a surrogate for taper $\left(\frac{DBH \text{ (in)}}{\text{total tree height (ft)}} \right)$, and other variables are as defined earlier (see Appendix A4.1)

Table A5.1 : A comparison of the performance of alternative models for ring width prediction

Model	S $\bar{E}E$	MB	MSE	R $_p^2$	AIC
[5.5a]	0.0871	0.00046	0.00739	0.274	21098
[5.5b]	0.0830	-0.00048	0.00661	0.351	21217
[5.5c]	0.0806	-0.00119	0.00623	0.388	21282
[5.5d]	0.0786	-0.00019	0.00590	0.421	21346
[5.5]	0.0764	-0.00054	0.00563	0.446	21442
[5.5e]	0.0811	-0.00012	0.00627	0.402	20795
[5.5f]	0.0810	0.00499	0.00642	0.389	20518
[5.5g]	0.0787	0.00009	0.00591	0.418	21314

Appendix A5.2

Different models for use in the prediction of latewood proportion were evaluated. Again, the high variability observed in ring width was also evident in latewood proportion. Consequently, latewood proportion could not be predicted with very high precision. Among models considered are:

$$LW = \beta_0 + \beta_1 ERHT + \beta_2 RA + \epsilon \quad [5.7a]$$

$$LW = \beta_0 + \beta_1 ERHT + \beta_2 RA + \beta_3 CI + \epsilon \quad [5.7b]$$

$$LW = \beta_0 + \beta_1 ERHT + \beta_2 RA + \beta_3 (RA)^2 + \beta_4 CI + \epsilon \quad [5.7]$$

$$LW = \beta_0 + \beta_1 ERHT + \beta_2 RA + \beta_3 CI + \beta_4 SI + \epsilon \quad [5.7c]$$

$$LW = \beta_0 + \beta_1 ERHT + \beta_2 RA + \beta_3 (RA)^2 + \beta_4 CI + \beta_5 CR + \epsilon \quad [5.7d]$$

$$LW = 1 - \beta_1 Exp(-X) + \epsilon \quad [5.7e]$$

where

$$X = \beta_2 RHT + \beta_3 RAT + \beta_4 RHT * RAT + \beta_5 SI + \beta_6 TAP$$

$ERHT$ is $exp(-RHT)$, and

other variables are as defined before.

Table A5.2 : A comparison of the performance of alternative models for predicting latewood proportion.

Model	SEE	MB	MSE	R _p ²	AIC
[5.7a]	0.1211	-0.01047	0.01591	0.470	12367
[5.7b]	0.1203	-0.00951	0.01571	0.477	12398
[5.7]	0.1105	-0.00246	0.01394	0.535	13030
[5.7c]	0.1202	-0.00941	0.01568	0.478	12395
[5.7d]	0.1095	-0.01579	0.05200	0.510	12650
[5.7e]	0.1157	-0.00631	0.01471	0.508	12662

Appendix 6.1

In order to select an appropriate model for predicting upper stem diameter, a number of models were tested. To select a suitable model, several models which included the variables believed to affect tree stem profile were evaluated. A sample of the models considered is presented.

$$d = D^{\beta_1} CI^{\beta_2} RLS^{\beta_3} RE \{ \alpha_1 X^2 + \alpha_2 \ln(X+0.001) + \alpha_3 \exp(X) + \alpha_4 \sqrt{X} \} + \epsilon \quad [6.5a]$$

$$d = D^{\beta_1} RE \{ \alpha_1 X^2 + \alpha_2 \ln(X+0.001) + \alpha_3 \exp(X) + \alpha_4 \sqrt{X} \} + \epsilon \quad [6.5b]$$

$$d = D^{\beta_1} CI^{\beta_2} \left(\frac{SI}{A} \right)^{\beta_3} RE \{ \alpha_1 X^2 + \alpha_2 \ln(X+0.001) + \alpha_3 \exp(X) + \alpha_4 \sqrt{X} \} + \epsilon \quad [6.5c]$$

$$d = D^{\beta_1} \left(\frac{D_s}{H} \right)^{\beta_2} RLS^{\beta_3} RE \{ \alpha_1 X^2 + \alpha_2 \ln(X+0.001) + \alpha_3 \exp(X) + \alpha_4 \sqrt{X} \} + \epsilon \quad [6.5d]$$

$$d = D^{\beta_1} \left(\frac{D_s}{H} \right)^{\beta_2} \left(\frac{SI}{A_s} \right)^{\beta_3} RE \{ \alpha_1 X^2 + \alpha_2 \ln(X+0.001) + \alpha_3 \exp(X) + \alpha_4 \sqrt{X} \} + \epsilon \quad [6.5e]$$

$$d = D^{\beta_1} CR^{\beta_2} \left(\frac{SI}{A_s} \right)^{\beta_3} RE \{ \alpha_1 X^2 + \alpha_2 \ln(X+0.001) \} + \epsilon \quad [6.5f]$$

$$d = D^{\beta_1} \left(\frac{D}{H} \right)^{\beta_2} \left(\frac{SI}{A_s} \right)^{\beta_3} RE \{ \alpha_1 X^2 + \alpha_2 \ln(X+0.001) \} + \epsilon \quad [6.5]$$

where

d is diameter inside bark at height h (in.) .

D is DBH (in.) .

RE is defined as $\frac{H-h}{H-4.5}$.

X is relative height $\left(\frac{h}{H} \right)$.

A_s is stand age.

RLS is relative spacing.

\ln is natural logarithm.

β_i, α_j regression parameters and other symbols are as defined before.

Table A6.1: A comparison of the performance of alternative stem profile models.

Model	SEE	MB	MSE	R_p^2	AIC
[6.5a]	0.5146	0.0465	0.1997	0.961	-4113
[6.5b]	0.5270	0.0136	0.2061	0.959	-4201
[6.5c]	0.5154	0.0486	0.2023	0.960	-4124
[6.5d]	0.5191	0.0423	0.1917	0.962	-4153
[6.5e]	0.5152	0.0415	0.1963	0.961	-4121
[6.5f]	0.5202	0.0877	0.2466	0.952	-4145
[6.5]	0.5181	0.0342	0.1987	0.961	-4149

Appendix A6.2

To evaluate the efficacy of the new model the Max and Burkhart (1976) model [6.8] and Kozak's (1988) variable-exponent taper model [6.9] were selected. These models and model [6.6] were fit to the fitting data and validated against the data set aside for validation (see Table A6.2).

$$y^2 = \beta_1 Z_1 + \beta_2 Z_2 + \beta_3(\alpha_1 - x)^2 I_1 + \beta_4(\alpha_2 - x)^2 I_2 + \epsilon \quad [6.8]$$

Max and Burkhart (1976).

where

$$y = \frac{d}{DBH}, \quad x = \frac{h}{H}, \quad Z_1 = x - 1; \quad Z_2 = x^2 - 1$$

$$I_1 = \begin{cases} 1 & \text{if } \alpha_1 \geq x \\ 0 & \text{elsewhere} \end{cases}, \quad I_2 = \begin{cases} 1 & \text{if } \alpha_2 \geq x \\ 0 & \text{elsewhere} \end{cases}$$

β_i and α_j , $i = 1, \dots, 4$; $j = 1, 2$ are regression parameters.

$$d = \beta_0 D^{\beta_1} \beta_2 D^{\beta_3} R_k^{\{\beta_3 X^2 + \beta_4 \ln(X + 0.001) + \beta_5 \sqrt{X} + \beta_6 \exp(X) + \beta_7 \left(\frac{D}{H}\right)\}} + \epsilon \quad [6.9]$$

Kozak (1988)

where

$$R_k \text{ is defined as } \frac{1 - \sqrt{h/H}}{1 - \sqrt{p}}$$

$$p \text{ is } \frac{HI}{H}$$

HI height of inflection point from the ground (for the purpose of this study, $p = 0.25$ was used).

other variables are as defined before.

Table A6.2 :A comparison of the performance of the proposed stem profile model with selected existing taper models.

Model	SEE	MB	MSE	R_p^2
[6.5]	0.5173	0.0343	0.3297	0.963
[6.8]	0.5435	-0.2349	0.4311	0.952
[6.9]	0.5126	0.0919	0.3275	0.964

Vita

The author was born in Lalo Kile town, Wollega region, in western Ethiopia. He attended public and missionary schools in the region until he completed high school. He then joined the forestry program at Wondo Genet Forestry Institute from where he received an Associate Degree in 1979. The author proceeded with his higher education in the US in 1984 and received Bachelor of Science and Master of Science degrees in Forestry from Washington State University in Pullman, Washington in 1986 and 1987, respectively. After that, he went back to Ethiopia and served within the Ministry of Agriculture and Natural Resources until July 1993. The author joined Virginia Polytechnic Institute and State University in August 1993 as a candidate for a Doctor of Philosophy in Forest Biometrics. He received a Master of Science in Statistics in 1995.

A handwritten signature in black ink, consisting of several loops and a long vertical stroke, positioned below the main text block.